Hydrodynamics and loadings of tsunami waves with different fluid characteristics: Newtonian & non-Newtonian

by

Mohamad Razman Bin MOhd Sahimy

16685

Interim report/ extended proposal/ progress report/ dissertation submitted in partial fulfilment of

the requirements for the

Bachelor of Engineering (Hons)

(Civil and Environmental Engineering)

SEPTEMBER 2016

Universiti Teknologi PETRONAS,

32610, Bandar Seri Iskandar,

Perak Darul Ridzuan

CERTIFICATION OF APPROVAL

Hydrodynamics and loadings of tsunami waves with different fluid characteristics: Newtonian & non-Newtonian

by

Mohamad Razman Bin Mohd Sahimy
16685

A project dissertation submitted to the
Civil and Environmental Engineering Programme
Universiti Teknologi PETRONAS
in partial fulfilment of the requirement for the
BACHELOR OF ENGINEERING (Hons)
(CIVIL AND ENVIRONMENTAL ENGINEERING)

Approved by,

_____

(Name of Main Supervisor)

UNIVERSITI TEKNOLOGI PETRONAS
BANDAR SERI ISKANDAR, PERAK
September 2016

CERTIFICATION OF ORIGINALITY

This is to certify that I am responsible for the work submitted in this project, that the original work is my own except as specified in the references and acknowledgements, and that the original work contained herein have not been undertaken or done by unspecified sources or persons.

_____

MOHAMAD RAZMAN BIN MOHD SAHIMY

ABSTRACT

Tsunamis are impulsively generated waves which may severely damage structures within the coastal zones. Damage may occur to protective structures, port and waterfront facilities, and commercial and residential structures. As a result, major damages occurs from the force of the tsunami, from flooding, or from impacts of waterborne debris. Tsunami waves that propagates shoreward frequently connected with sediment and debris, either the ones existing on the shorelines or carried away by the waves from afar. Therefore, compelling level of suspended sediment may change the rheology of the wave from Newtonian to non-Newtonian fluid. The changes in the type of fluid will affect and modifies the hydrodynamics of the waves. This hypothesis requires validation through more extensive experimentation involving viscosity of the fluid. Another experiment on the different types of fluid can affect the wave loadings against structures will also be involve in order to fully understand and explore the knowledge on the fluid characteristics. Experimental data will be analyzed and presented in various interactive graphical forms. Through this analysis the limitations design guidelines for coastal structures and infrastructure will be identified and more robust design can be revealed. The efficiency of the design improvement will be ascertained through another series of laboratory tests.

ACKNOWLEDGEMENTS

It is a genuine pleasure to express my deep sense of thanks and gratitude to my supervisor, **Dr. Teh Hee Min**, Senior Lecturer in Civil and Environmental Engineering Department. His dedication and keen interest above all his overwhelming attitude to help his students had been solely and mainly responsible for completing my work. His timely advice, meticulous scrutiny, scholarly advice and scientific approach have helped me to a very great extend to accomplish this task.

I would also like to express my deepest gratitude to Aaron Keith Philips, Post-Graduate student for his keen interest on me at every stage of my research. His prompt inspiration, timely suggestions with kindness, enthusiasm and dynamism have enabled me to complete my thesis.

Not to forget, I thank profusely to all the Staffs and Lab technicians for their kind help and co-operation throughout my study period.

I am extremely thankful to all of my family and friends for their endless support regardless the time and distance.

TABLE OF CONTENTS

LIST OF FIGURES

LIST OF TABLES

Chapter 1

INTRODUCTION

1.1 BACKGROUND OF STUDY

The coastal areas have assumed a critical part all through humankind history for trading goods, transportation and businesses purposes. Ports and industries are built at several parts of the coastal areas due to their strategically location. Several human activities such as fishing, swimming, recreational purposes and tourism are very popular near the coastal areas. However, all of these can be easily destroyed by a powerful and destructive forces of ocean waves. Major erosion and destruction are often the results of the oceans waves. Therefore it is crucial that the coastal areas are well protected and actions must be taken to at least reduce the destructive forces of the ocean waves or worst, tsunami. Newton (1642), introduced the existence of Newtonian fluid, who described the flow behavior of fluids with a simple linear relation between shear stress and shear rate. In general, Newtonian fluid is known to be a debris-free type of fluid. Another type of fluid is called Non-Newtonian fluid. A non-Newtonian fluid is a fluid with properties that are different in any way from those of Newtonian fluids. Most commonly, the viscosity (the measure of a fluid's ability to resist gradual deformation by shear or tensile stresses) of non-Newtonian fluids is dependent on shear rate or shear stress. In short, a Newtonian fluid, the relation between the shear stress and the shear rate is linear, passing through the origin, the constant of proportionality being the coefficient of viscosity. In a non-Newtonian fluid, the relation between the shear stress and the shear rate is different and can even be time-dependent (Time Dependent Viscosity). Therefore, a constant coefficient of viscosity cannot be defined.

In order to prevent or reduce the destructive forces of tsunami waves, one must reduce the severity of tsunami waves and dissipating the disastrous amount of energy associated with them. In this case, the nature of real tidal waves that spreads from nearshore and up to the most extreme immersion limits conveys different sorts of residue and flotsam and jetsam inside the liquid body. This leads to the changes in the physical properties of the wave from Newtonian to Non-Newtonian fluid type.

The constant of proportionality between the viscous stress tensor and the velocity gradient is known as the viscosity. A simple equation to describe incompressible Newtonian fluid behavior is

$$\tau_{ij} = \mu \left(\frac{\partial v_i}{\partial x_j} + \frac{\partial v_j}{\partial x_i} - \frac{2}{3}\delta_{ij} \nabla \cdot \mathbf{v} \right) + \kappa \delta_{ij} \nabla \cdot \mathbf{v}$$

Where,

τ is the shear stress exerted by $\tau = -\mu \frac{dv}{dy}$ the fluid

μ is the fluid viscosity – constant of proportionality

$\frac{dv}{dy}$ is the velocity gradient perpendicular to the direction of shear.

If the fluid is not incompressible the general form for the viscous stress in a Newtonian fluid is where $\kappa$the second viscosity coefficient (or bulk viscosity) is. If a fluid does not obey this relation, it is termed a non-Newtonian fluid, of which there are several types. Non-Newtonian fluids can be either plastic, Bingham plastic, pseudoplastic, dilatant, thixotropic, rheopectic, viscoelastic.

In some applications another rough broad division among fluids is made: ideal and non-ideal fluids. An Ideal fluid is non-viscous and offers no resistance whatsoever to a shearing force. An ideal fluid really does not exist, but in some calculations, the assumption is justifiable. One example of this is the flow far from solid surfaces. In many cases the viscous effects are

concentrated near the solid boundaries (such as in boundary layers) while in regions of the flow field far away from the boundaries the viscous effects can be neglected and the fluid there is treated as it were inviscid (ideal flow). When the viscosity is neglected, the term containing the viscous stress tensor $\boldsymbol{\tau}$ in the Navier–Stokes equation vanishes. The equation reduced in this form is called the Euler equation.

Thusly, approvals should be directed to enhance the alignments and unwavering quality status for any torrent numerical models results. Generally, scientists like to utilize physical demonstrating method for such errand as a result of their capacity to mimic the real wonders in a controlled situation and that it would essentially lessen the arbitrary mistakes included. Then again, the utilization of field information regularly connected with their higher level of mistakes because of the numerous variables influencing the hydrodynamics parameters. Subsequently, essential relationship of interest might be hard to be gotten from such strategy and may requires much higher order of differential conditions to explain for the wave conditions. Since the extent of tidal wave is an unlimited subject to study, flow exploration will just concentrate on the impact of silt burden to the run-up, effect power and immersion at the beach front area. Further subtle elements of the issue proclamations are introduced in the accompanying sub segment.

1.2 PROBLEM STATEMENT

Tsunami waves that engender shoreward frequently connected with silt, debris and sediment either the ones existing on the shorelines or carried away by the tidal waves from afar. Hypothetically, compelling level of suspended sediment may change the rheology of tidal wave water from Newtonian to non-Newtonian liquid sort. In the end, this may modify the hydrodynamic of wave, especially the run-up. Wave run-up stature is the key parameter that decides the effects to the coastal structures. Amid the run-up stage, gliding garbage e.g. woods, compartments and boats are conveyed together.

These are not much considered which add to the seriousness of outcome auxiliary harms (FEMA, 2012; Murata et al, 2010). Study on the effect of flotsam and jetsam stacking has been led by analysts, for example, Como and Mahmoud (2013) and Haehnel and Daly (2004). In any case, little exertion was made to segregate and examine the impact of liquid properties i.e. consistency to hydrodynamics and basic effects. A snappy takeoff in the midst of tsunami is a presence and downfall circumstances. Standard codes for outline of structures to permit vertical clearings amid tidal wave had been drafted by FEMA (2012). The codes considers strengths, for example, hydrostatic and hydrodynamic forces caught up on a divider, refuse influence urge, and lift power.

The proposed conditions additionally considered the impact of dregs, which is termed as silt loaded liquid thickness (ρs). Be that as it may, FEMA (2012) just made the presumption that lone five percent (5%) of the mud focus will be transported. Already, the presumption was at ten percent (10%). This outcomes in the prescribed estimation of liquid thickness to 1100 kg/m3 or 1.1 times the thickness of freshwater. This specific suspicion should be surveyed and overhauled particularly regarding consistency.

1.3 OBJECTIVE

This report studies the characteristics of waves and types of fluids in order achieve the following objectives:

1) To characterize tsunami bore waveform and changes in the physical properties of waves with Newtonian fluid using dam-break wave generation
2) To characterize tsunami bore waveform and changes in the physical properties of waves with Non-Newtonian fluid using dam-break wave generation
3) To compare the results of using the Newtonian fluid and Non-Newtonian fluid.

1.4 SCOPE OF STUDY

The scope of the research works is summarized as follows in order to achieve the objectives within the time frame and funds allocated:

For objective one, the analysis will determines parameters related to the characteristic of tsunami bore waveform. The test will be conducted at the laboratory in Universiti Teknologi PETRONAS. In this objective, it is vital to observe and analyze the wave motion upon using Newtonian fluid. Further information on the design and experimental setup will be discussed in the Methodology section by using the Dam-Break Wave Generation.

Objective two is similar to objective one, except that, instead of using Newtonian fluid, a Non-Newtonian fluid will be used.

Objective three will be the main answer for this research as it will be the comparison of the results obtained from objective one and objective two.

1.4 HYPHOTHESIS

The changes in tidal wave liquid from Newtonian to non-Newtonian fluid may bring about change of hydrodynamic parameters. In hypothetical sense, there will be a diminishment in wave height, and wave celerity. This is a direct result of the expansion in drag coefficients came about because of the expansion in consistency may ruin the orbital movements of wave at the lower limit as it spreads from transitional and shallow water district up to the most extreme immersion limit. Opposite, the effect power by gooey wave liquid is thought to increment with the presentation of higher force vitality because of the adjustment in liquid sort. In this way, the current tidal waves run-up equation by Charvet et al. (2013) should be modified.

1.5 SIGNIFICANCE OF FEASIBILITY OF STUDY

This research aims to contribute to the current knowledge pertaining tsunami hydrodynamics especially on Non-Newtonian fluid affecting the characteristic and the loadings of tsunami waves. Many researchers neglect the fact that Non-Newtonian fluid can affect the run-up height of the waves upon impact. Should this research can prove to be a success, a great impact can occur in the engineering field such as designing the revetment, groin, and embankment. Houses or residential buildings can also be design nearer to the shoreline. Not only that, it can prolong the time for evacuation of civilian whenever there is a tsunami occurring.

CHAPTER 2

LITERATURE REVIEW

This chapter provides a short explanation on the background of the hydrodynamics, characteristics and loadings of tsunami. There will also be reviews on some of the studies related to them, including Newtonian and Non-Newtonian fluids. Not only this section will describe about the relationship between the tsunami and its properties, it can also be a benchmark for the design of dam-break generation that will be used in this study.

2.1 TSUNAMI

A tsunami, also known as the great wave in harbor (Dudley and Lee, 1988) is a series of waves in a water body caused by the displacement of a large volume of water, generally in an ocean or a large lake. Earthquakes, volcanic eruptions and other underwater explosions (including detonations of underwater nuclear devices), landslides, glacier calving, meteorite impacts and other disturbances above or below water all have the potential to generate a tsunami (Wells, 1990). Unlike normal ocean waves which are generated by wind or tides which are generated by the gravitational pull of the Moon and Sun, a tsunami is generated by the displacement of water.

Tsunami waves do not resemble normal sea waves, because their wavelength is far longer. Rather than appearing as a breaking wave, a tsunami may instead initially resemble a rapidly rising tide, and for this reason they are often referred to as tidal waves, although this usage is not favored by the scientific community because tsunamis are not tidal in nature. Tsunamis generally consist of a series of waves with periods ranging from minutes to hours, arriving in a so-called "wave train" (Fradin et al., 2008). Wave heights of tens of meters can be generated by large events. Although the impact of tsunamis is limited to coastal areas, their destructive power can be enormous and they can affect entire ocean basins; the 2004 Indian Ocean tsunami was among the deadliest natural disasters in human history with at least 230,000 people killed or missing in 14 countries bordering the Indian Ocean.

Tsunami are sometimes referred to as tidal waves. This once-popular term derives from the most common appearance of tsunami, which is that of an extraordinarily high tidal bore. Tsunami and tides both produce waves of water that move inland, but in the case of tsunami the inland movement of water may be much greater, giving the impression of an incredibly high and forceful tide. In recent years, the term "tidal wave" has fallen out of favor, especially in the scientific community, because tsunami actually have nothing to do with tides, which are produced by the gravitational pull of the moon and sun rather than the displacement of water. Although the meanings of "tidal" include "resembling"(Houghton, 2008) or "having the form or character of" the tides, use of the term tidal wave is discouraged by geologists and oceanographers.

The term seismic sea wave also is used to refer to the phenomenon, because the waves most often are generated by seismic activity such as earthquakes (Smid, 1990). Prior to the rise of the use of the term "tsunami" in English-speaking countries, scientists generally encouraged the use of the term "seismic sea wave" rather than the inaccurate term "tidal wave." However, like "tsunami," "seismic sea wave" is not a completely accurate term, as forces other than earthquakes – including underwater landslides, volcanic eruptions, underwater explosions, land or ice slumping into the ocean, meteorite impacts, or even the weather when the atmospheric pressure changes very rapidly – can generate such waves by displacing water.

2.1.1 THE MECHANISM OF TSUNAMI

The principal generation mechanism (or cause) of a tsunami is the displacement of a substantial volume of water or perturbation of the sea (Haugen et al., 2005). This displacement of water is usually attributed to either earthquakes, landslides, volcanic eruptions, glacier calving or more rarely by meteorites and nuclear tests (Margaritondo, 2005). The waves formed in this way are then sustained by gravity. Tides do not play any part in the generation of tsunamis.

2.1.2 TSUNAMI CAUSED BY SEISMIC REACTION

Tsunami can be generated when the sea floor abruptly deforms and vertically displaces the overlying water. Tectonic earthquakes are a particular kind of earthquake that are associated with the Earth's crustal deformation; when these earthquakes occur beneath the sea, the water above the deformed area is displaced from its equilibrium position. More specifically, a tsunami can be generated when thrust faults associated with convergent or destructive plate boundaries move abruptly, resulting in water displacement, owing to the vertical component of movement involved. Movement on normal (extensional) faults can also cause displacement of the seabed, but only the largest of such events (typically related to flexure in the outer trench swell) cause enough displacement to give rise to a significant tsunami, such as the 1977 Sumba and 1933 Sanriku events (Kanamori,1971).

2.1.3 TSUNAMI CAUSED BY LANDSLIDES

In the 1950s, it was discovered that larger tsunamis than had previously been believed possible could be caused by giant submarine landslides. These rapidly displace large water volumes, as energy transfers to the water at a rate faster than the water can absorb. Their existence was confirmed in 1958, when a giant landslide in Lituya Bay, Alaska, caused the highest wave ever recorded, which had a height of 524 meters (over 1700 feet) (George,1999). The wave did not travel far, as it struck land almost immediately. Two people fishing in the bay were killed, but another boat amazingly managed to ride the wave.

Another landslide-tsunami event occurred in 1963 when a massive landslide from Monte Toc entered the Vajont Dam in Italy. The resulting wave surged over the 262 m (860 ft) high dam by 250 meters (820 ft) and destroyed several towns. Around 2,000 people died (Petley, 2008). Scientists named these waves mega tsunamis.

Some geologists claim that large landslides from volcanic islands, e.g. Cumbre Vieja on La Palma in the Canary Islands, may be able to generate mega tsunamis that can cross oceans, but this is disputed by many others.

In general, landslides generate displacements mainly in the shallower parts of the coastline, and there is conjecture about the nature of large landslides that enter water. This has been shown to lead to effect water in enclosed bays and lakes, but a landslide large enough to cause a transoceanic tsunami has not occurred within recorded history.

2.2 CHARACTERISTIC OF TSUNAMI

Tsunamis cause damage by two mechanisms: the smashing force of a wall of water travelling at high speed, and the destructive power of a large volume of water draining off the land and carrying a large amount of debris with it, even with waves that do not appear to be large.

While everyday wind waves have a wavelength (from crest to crest) of about 100 metres (330 ft) and a height of roughly 2 meters (6.6 ft), a tsunami in the deep ocean has a much larger wavelength of up to 200 kilometers (120 mi). Such a wave travels at well over 800 kilometers per hour (500 mph), but owing to the enormous wavelength the wave oscillation at any given point takes 20 or 30 minutes to complete a cycle and has an amplitude of only about 1 metre (3.3 ft). This makes tsunamis difficult to detect over deep water, where ships are unable to feel their passage.

The velocity of a tsunami can be calculated by obtaining the square root of the depth of the water in meters multiplied by the acceleration due to gravity (approximated to 10 m sec2). For example, if the Pacific Ocean is considered to have a depth of 5000 meters, the velocity of a tsunami would be the square root of √5000 x 10 = √50000 = ~224 meters per second (735 feet per second), which equates to a speed of ~806 kilometers per hour or about 500 miles per hour. This formula is the same as used for calculating the velocity of shallow waves, because a tsunami behaves like a shallow wave as it peak to peak value reaches from the floor of the ocean to the surface.

The reason for the Japanese name "harbor wave" is that sometimes a village's fishermen would sail out, and encounter no unusual waves while out at sea fishing, and come back to land to find their village devastated by a huge wave.

As the tsunami approaches the coast and the waters become shallow, wave shoaling compresses the wave and its speed decreases below 80 kilometers per hour (50 mph). Its wavelength diminishes to less than 20 kilometers (12 mi) and its amplitude grows enormously. Since the wave still has the same very long period, the tsunami may take minutes to reach full height. Except for the very largest tsunamis, the approaching wave does not break, but rather appears like a fast-moving tidal bore (USGS, 2008). Open bays and coastlines adjacent to very deep water may shape the tsunami further into a step-like wave with a steep-breaking front.

When the tsunami's wave peak reaches the shore, the resulting temporary rise in sea level is termed run up. Run up is measured in meters above a reference sea level. A large tsunami may feature multiple waves arriving over a period of hours, with significant time between the wave crests. The first wave to reach the shore may not have the highest run up (Nelson, 2009).

About 80% of tsunamis occur in the Pacific Ocean, but they are possible wherever there are large bodies of water, including lakes. They are caused by earthquakes, landslides, volcanic explosions, glacier calving, and bolides.

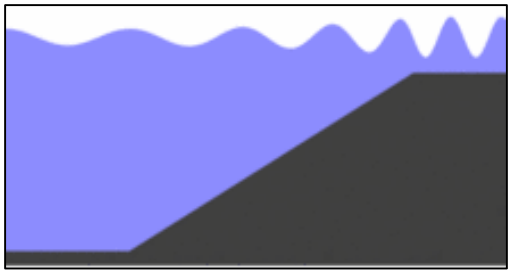

Figure 2.1: Wave Breaking

2.3 TIDAL BORE

A tidal bore, often simply given as bore in context, is a tidal phenomenon in which the leading edge of the incoming tide forms a wave (or waves) of water that travels up a river or narrow bay against the direction of the river or bay's current.

Bores occur in relatively few locations worldwide, usually in areas with a large tidal range (typically more than 6 meters (20 ft.) between high and low water) and where incoming tides are funneled into a shallow, narrowing river or lake via a broad bay. The funnel-like shape not only increases the tidal range, but it can also decrease the duration of the flood tide, down to a point where the flood appears as a sudden increase in the water level. A tidal bore takes place during the flood tide and never during the ebb tide. (Chanson, 2011)

A tidal bore may take on various forms, ranging from a single breaking wave front with a roller – somewhat like a hydraulic jump – to undular bores, comprising a smooth wave front followed by a train of secondary waves known as whelps. Large bores can be particularly unsafe for shipping but also present opportunities for river surfing. (David, 1998)

Two key features of a tidal bore are the intense turbulence and turbulent mixing generated during the bore propagation, as well as its rumbling noise. The visual observations of tidal bores highlight the turbulent nature of the surging waters. The tidal bore induces a strong turbulent mixing in the estuarine zone, and the effects may be felt along considerable distances. The velocity observations indicate a rapid deceleration of the flow associated with the passage of the bore as well as large velocity fluctuations. A tidal bore creates a powerful roar that combines the sounds caused by the turbulence in the bore front and whelps, entrained air bubbles in the bore roller, sediment erosion beneath the bore front and of the banks, scouring of shoals and bars, and impacts on obstacles. The bore rumble is heard far away because its low frequencies can travel over long distances. The low-frequency sound is a characteristic feature of the advancing roller in which the air bubbles entrapped in the large-scale eddies are acoustically active and play the dominant role in the rumble-sound generation. (Chanson, H.2009)

A research has been done by Árnason, H. (2005) on interactions between an incident bore and a free-standing coastal structure. The objective in this segment is to show a couple of subjective perceptions about the stream around the hindrances and portray the primary elements of the

stream structure. A splash up occurs on the upstream side of the column just after the bore has arrived.

After the water falls back there is a buildup of water right upstream of the column caused by the flow blockage, which then flattens out both in the upstream direction and towards the sides of the tank. When the wave coming off the column reaches the sidewalls, a wave forms over the whole width at the upstream edge of the column which then starts to propagate upstream. Smaller waves can also be seen moving at an angle from the sidewalls.

Amason (2005) also mentioned that as the bore wave propagates towards the column and upon impact, runs up to it, causing a buildup of water on the upstream face of the column. It is highest in an area, extending a distance about equal to the bore depth, upstream of the large columns with blockage ratio b/B of about 0.2 and higher, but evens out at a lower level further upstream. For the case of the large circular column and higher bores, two prominent waves travel upstream from the column.

These waves are attributable not only to the effects of flow being redirected around the obstacle in the presence of a free surface but also to the presence of the tank sidewalls, effectively making a series of columns upon which the bore impinges. In the wake of the obstacles, the convergence of the split flow at the back of the obstacle results in a turbulent rooster tail that extends downstream.

The rooster tail is highly three-dimensional and unsteady. It is usually asymmetric in the transverse direction and fluctuates from side to side. The wake behind the obstacle shows larger wake angles and more transverse velocity components for the smaller bores, while larger bores maintain more of their downstream directed momentum.

2.4 VISCOSITY

The viscosity of a fluid is a measure of its resistance to gradual deformation by shear stress or tensile stress. For liquids, it corresponds to the informal concept of "thickness"; for example, honey has a much higher viscosity than water (Symon, 1971).

Viscosity is a property emerging from impacts between neighboring particles in a liquid that are moving at various speeds. At the point when the liquid is constrained through a tube, the particles which is the liquid moves rapidly close to the tube's axis and slower closer to its dividers; hence some stress, (for example, a weight contrast between the two closures of the tube) is expected to overcome the friction between molecule layers to keep the liquid moving. For a given velocity design, the stress required is relative to the liquid's viscosity.

A liquid that has no imperviousness to shear anxiety is known as a perfect or in viscid liquid. Zero consistency is watched just at low temperatures in superfluid. Else, all liquids have positive consistency, and are actually said to be thick or viscid. In like manner speech, nonetheless, a fluid is said to be thick if its thickness is generously more prominent than that of water, and might be depicted as portable if the consistency is detectably not as much as water. A liquid with a moderately high viscosity, for example, pitch, may give off an impression of being a solid. Thickness in this way tidal wave case are partitioned into two, which are the Newtonian liquids and Non-Newtonian liquids.

2.4.1 Non-Newtonian and Newtonian Fluid

Newton's law of viscosity is a constitutive equation (like Hooke's law, Fick's law, and Ohm's law): it is not a central law of nature but rather an estimation that holds in a few materials and comes up short in others.

A liquid that carries on as indicated by Newton's law, with a viscosity of μ that is not dependent of stress, is said to be Newtonian. Gasses, water, and numerous normal fluids can be viewed as Newtonian in conventional conditions and settings. There are numerous non-Newtonian liquids that essentially differs from the lawin several way or another. For example:

- **Shear thickening liquids,** whose viscosity increases with the rate of shear strain
- **Shear thinning liquids**, whose viscosity decreases with the rate of shear strain.
- **Thixotropic liquids**, that become less viscous over time when shaken, agitated, or otherwise stressed.
- **Rheopectic liquids**, that become more viscous over time when shaken, agitated, or otherwise stressed.
- **Bingham plastics** that behave as a solid at low stresses but flow as a viscous fluid at high stresses.

Shear thinning liquids are very commonly, but misleadingly, described as thixotropic.

Even for a Newtonian fluid, the viscosity are often depends on its composition and temperature. For gases and other compressible fluids, it depends on temperature and varies very slowly with pressure.

The viscosity of some fluids may differs depending on other factors. A magneto rheological fluid, for example, becomes thicker when subjected to a magnetic field, possibly to the point of behaving like a solid.

2.4.2 NON-NEWTONIAN FLUIDS

In contrast with classical fluid mechanics developed for Newtonian fluids, the theory of non-Newtonian fluid dynamics is a very new branch of applied sciences. The increasing importance of non-Newtonian fluids has been recognized in those fields dealing with materials, whose flow behavior of stress and shear rate cannot be characterized by Newton's law of viscosity (Skelland, 1967; Bohme, 1987; Astarita and Marmcci, 1974; and Crochet et al., 1984). Therefore, non-Newtonian fluid mechanics is being developed. In a broad sense, fluids are divided into two main categories: (1) Newtonian, and (2) non-Newtonian.

Newtonian fluids follow Newton's law of viscous resistance and possess a constant viscosity. Non-Newtonian fluids deviate from Newton's law of viscosity, and exhibit variable viscosity. The behavior of non-Newtonian fluids is generally represented by a rheological model, or correlation of shear stress and shear rate. Examples of substances which exhibit non-Newtonian behavior include solutions and melts of high molecular weight polymers, suspensions of solids in liquids, emulsions, and materials possessing both viscous and elastic properties. There are many rheological models available for different non-Newtonian fluids in the literature (Skelland, 1967; Savins, 1969; Bud et al., 1960). Scheidegger (1974) gave a very comprehensive summary of rheological equations of various non-Newtonian fluids in porous media.

The present review focuses only on those non-Newtonian fluids which are commonly encountered in porous media. The major attention here is directed to relationship between viscosity and the flow of the bore waves.For a Newtonian fluid, the shear stress z is linearly related to the shear rate y by Newton's law of viscosity (Bird et al., 1960) as,

$$\tau = -\mu\gamma$$

where the coefficient p is defined as dynamic viscosity of the fluid. According to the relationships between shear stress and shear rate, non-Newtonian fluids are commonly grouped in three general classes (Skelland, 1967): (1) time independent non-Newtonian fluids; (2) time-dependent non-Newtonian fluids; and (3) viscoelastic non-Newtonian fluids.

Time-independent fluids are those for which the rate of shear y, or the velocity gradient, is a unique but non-linear function of the instantaneous shear stress z at that point. For the time-independent fluid, the relationship is

$$\gamma = f(\tau)$$

The time-independent non-Newtonian fluids can be characterized by the flow curves of z versus y, as shown in Figure 2. These are: (a) Bingham plastics, curve A; (b) pseudo plastic fluids (shear thinning), curve B; and (c) dilatant fluids (shear thickening), curve C. Time-dependent fluids have more complex shear stress and shear rate relation- ships. In these fluids, the shear rate depends not only on the shear stress, but also on shearing time, or on the previous shear stress rate history of the fluid. These materials are usually classified into two groups, thixotropic fluids and rheopectic fluids, depending upon whether the shear stress decreases or increases in time at a given shear rate and under constant temperature. Typical curves of the time-dependent behavior of non- Newtonian fluids are shown in Figure 2.4.2.1.

A viscoelastic material exhibits both elastic and viscous properties, and shows partial recovery upon the removal of the deformable shear stress. The rheological properties of such a substance at any instant will be a function of the recent history of the material and cannot be described by relationships between shear stress and shear rate alone, but will require inclusion of the time derivative of both quantities.

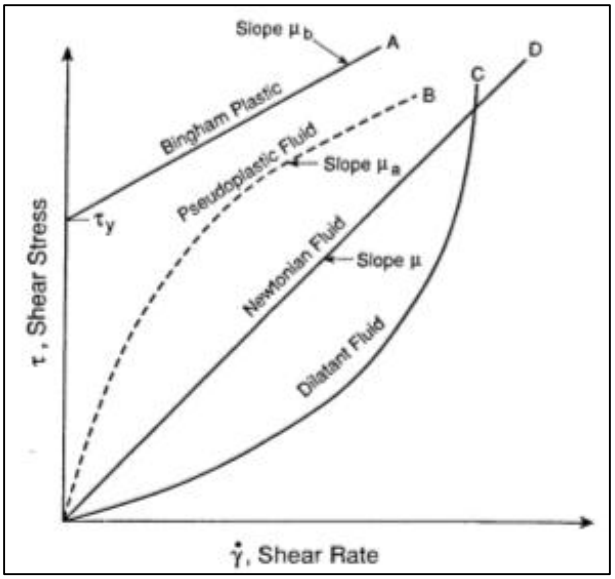

Figure 2.2: Graph of Shear Stress VS Shear Rate

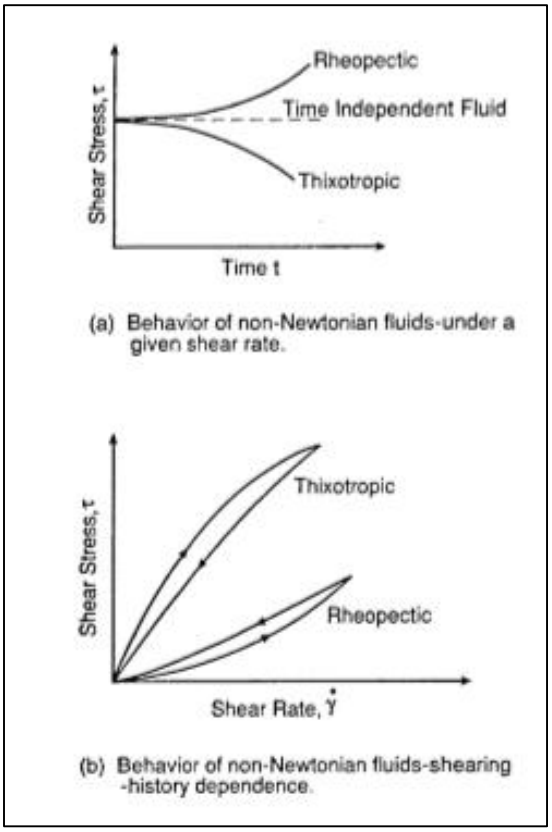

Figure 2.3: Graph showing the behavior of Non-Newtonian Fluid

One of the mechanical models, first proposed by Maxwell (Skelland, 1967) for viscoelastic fluids, is

$$\boldsymbol{\tau = \mu \frac{dy}{dt} - \frac{\mu}{\lambda} \frac{d\tau}{dt}}$$

where p is viscosity, and h is a rigidity modulus. Liquids which obey this law are known as Maxwell liquids. Another mechanical model is referred to as the Voigt model, which characterizes the rheological performance by the relationship,

$$\boldsymbol{\tau = \mu \frac{d\gamma}{dt} + \lambda \gamma}$$

The rheological behavior of real viscoelastic fluids has been represented with some success by more or less complex combinations of generalized Maxwell and Voigt models, consisting of Maxwell or Voigt model units connected in series or in parallel.

Regardless of the theories mentioned regarding non-Newtonian fluid, there are no researchers ever apprehend on performing any research on it. Therefore, it is difficult to find any research regarding non-Newtonian fluid. However, this can be the upper hand on the importance of this research. This research will be a proof on the impact of non-Newtonian fluid by comparing the result of Newtonian and Non-Newtonian fluid affecting the hydrodynamics and loadings of tsunami waves.

2.5 TSUNAMI LOADING

For the design of vertical evacuation structures, a few tsunami loading design must be considered. They are hydrostatic forces, buoyant forces, hydrodynamic forces, impulsive forces, debris impact forces, debris damming forces, uplift forces; and additional gravity loads from retained water on elevated floors. Wave-breaking forces are not considered in the design of vertical evacuation structures. In general, tsunamis break offshore, and vertical evacuation structures should be located some distance inland from the shoreline.

The term 'wave-breaking' is defined here as a plunging-type breaker in which the entire wave front overturns. When waves break in a plunging mode, the wave front becomes almost vertical, generating an extremely high pressure over an extremely short duration. Once a tsunami wave has broken, it can be considered as a bore wave due to its very long wavelength. Further justification for not considering wave-breaking forces can be found in Yeh (2008).

Wave-breaking forces could be critical for vertical evacuation structures located in the wave-breaking zone, which is beyond the scope of this document. If it is determined that a structure must be located in the wave breaking zone, ASCE/SEI 7-10 Minimum Design Loads for Buildings and Other Structures and the Coastal Engineering Manual, EM 1110-2-1100, (U.S. Army Coastal Engineering Research Center, 2008) should be consulted for additional guidance on wave-breaking forces.

2.5.1 KEY ASSUMPTIONS FOR ESTIMATING TSUNAMI LOAD EFFECTS

Tsunami load effects are determined using the following key assumptions:

- Tsunami flows consist of a mixture of sediment and seawater. Most suspended sediment transport flows do not exceed 5% sediment concentration. Based on an assumption of vertically averaged sediment volume concentration of 5% in seawater, the fluid density of tsunami flow should be taken as 1.1 times the density of freshwater, or $\rho_s = 1{,}100$ kg/m3 = 2.13 slugs/ft3.

- Tsunami flow depths vary significantly depending on the three dimensional bathymetry and topography at the location under consideration. Figure 6-2 shows three possible scenarios where topography could affect the relationship between maximum tsunami elevation, TE, at a particular location and the ultimate inland run up elevation, R. For the loading expressions presented in this chapter, it is assumed that Figure 6-2b applies, that is TE = R. These expressions may be adjusted if numerical simulations of tsunami inundation provide more appropriate estimates of TE at the location being considered.

- There is significant variability in local tsunami run up heights, based on local bathymetry and topographic effects, and uncertainty in numerical simulations of tsunami inundation. Based on empirical judgment from past tsunami survey data, it is recommended that the design run up elevation, R, be taken as 1.3 times the predicted maximum run up elevation, R*, to envelope the potential variability in the estimates of modeling. The inundation elevation from the run up point back towards the shoreline would then be scaled by the same factor. Figure 6-3 shows a typical numerical prediction (Yamazaki et al., 2011) made for the 2009 Samoa Tsunami, which demonstrates that the 1.3 safety factor for uncertainty is realistic.

2.6 HYDRODYNAMIC FORCES

When water flows around a structure, hydrodynamic forces are applied to the structure as a whole and to individual structural components. These forces are induced by the flow of water moving at moderate to high velocity, and are a function of fluid density, flow velocity and structure geometry. Also known as drag forces, they are a combination of the lateral forces caused by the pressure forces from the moving mass of water and the friction forces generated as the water flows around the structure or component. Hydrodynamic forces can be computed using the following equation:

$$F_d = \frac{1}{2}\rho_z C_d B(hu^2)_{max}$$

where ρ s is the fluid density including sediment (1100 kg/m3 = 2.13 slugs/ft3), Cd is the drag coefficient, B is the breadth of the structure in the plane normal to the direction of flow (i.e. the breadth in the direction parallel to the shore), h is flow depth, and u is flow velocity at the location of the structure. For forces on components, B is taken as the width of the component. The drag coefficient may be conservatively taken as Cd = 2.0; the actual value is shape-, orientation-, and size-dependent. The resultant hydrodynamic force is applied approximately at the centroid of the wetted surface of the component, as shown in Figure 4.

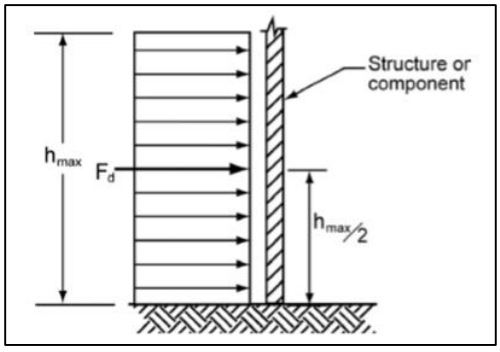

Figure 2.4: Hydrodynamic force distribution and location of resultant

The combination hu^2 represents the momentum flux per unit mass per unit width. Note that $(hu^2)_{max}$ does not equal $h_{max}\ u_{max}^2$. The maximum flow depth, h_{max}, and maximum flow velocity, u_{max}, at a particular site may not occur at the same time. The hydrodynamic forces should be based on the parameter $(hu^2)_{max}$, which is the maximum momentum flux per unit mass per unit width occurring at the site at any time during the tsunami. The maximum value of (hu^2) can be obtained by running a detailed numerical simulation model or acquiring existing simulation data. The numerical model in the run up zone must be run with a very fine grid size to ensure adequate accuracy in the prediction of (hu^2). When numerical simulation data are not available, the value $(hu^2)_{max}$ can be roughly estimated based on information in the inundation map, using Equation 6-6:

$$(hu^2)_{max} = gR^2\left(0.125\text{-}0.235\frac{z}{R} + 0.11\left(\frac{z}{R}\right)^2\right)$$

where g is the acceleration due to gravity, R is the design run up elevation taken as 1.3 times the maximum run up elevation, R*, and z is the ground elevation at the base of the structure. To use this formula, the sea level datum must be consistent with that used in the inundation maps.

Although this classical analytical solution is based on one-dimensional nonlinear shallow water theory for a uniformly sloping beach, with no lateral topographical variation and no friction, the maximum value of (hu^2) obtained from Equation 6-6 can be used for: (1) preliminary design; (2) approximate design in the absence of other modeling information; and (3) to evaluate the reasonableness of numerical simulation results.

2.7 REVIEW OF WAVE GENERATION TECHNIQUE

The physical modelling of long waves in laboratory environments has been frequently reported in literature. Depending on their generation source such as landslides, earthquakes, meteor impacts, pyroclastic or even volcano eruption, these waves were generated differently at laboratory scales (Hughes, 1993). In physical modelling, the choice of length and time-scales is very crucial. Because the global effects of tsunami, the choice is not easy; models focusing either on the source on target region often break down.

A comprehensive review of advances in physical long wave modeling is reported in Liu et al, (1991), Yet et al, (1995) and Liu (2008). Detailed technical information on physical modelling techniques is provided in Yalin (1971) and Hughes (1993). Different approaches on wave generation could be determined from literature. The different wave generation technique, which are described in the following sections are mostly sorted according to the generation mechanism.

2.7.1 PISTON-TYPE WAVE GENERATION

Scientist conduct lab oratory experiments on the basic of piston-type wave makers, which release wave energy to the water column by horizontally moving a wave paddle generating waves in first or second order (e.g. Dean and Dalrymple, 1992; Schaffer, 1996). Early experiments were conducted that addressed the run-up solitary waves as a probable representation of long waves. For details of the applied facility (Synolakis, 1987), T3.1). In this study, solitary waves were generated using the wave maker theory of Goring (1979), Synolakis (1990) also reports on the generation of long waves. Similarly, Briggs et al. (1993) studied solitary wave run-up on a milder slope of a 1 vertical to 30 horizontal beach for a range of nonlinearities (cp. also M.J. Briggs et al., 1995). Later, Liu et al. (1995); M. Briggs et al. (1995) and Yeh et al. (1994) reported tsunami run-up experiments on a conical island. In terms of the absolute stroke and attainable maximum wavelength, a significant improvement was reported by Moronkeji (2007) who conducted experimental studies on the run-up and draw-down of solitary and cnoidal waves over a movable bed at two different beach slopes. At the O.H. Hinsdale Wave Research Laboratory, University of Oregon, (Moronkeji, 2007) the experiments were conducted using electrically driven wave boards. A variation of the commonly used piston-type wave maker principle had been reported by Teng et al. (2000).

Solitary waves were generated using a vertical plate fastened to a carriage driven with a motor of adjustable speed. By varying the speed and distance between the carriage and plate, solitary waves of different amplitude were generated. As a unique advantage, this method resolved the problem related to limiting the stroke length of commercial and custom-made piston-type wave makers. This is because the path of the carriage could be specified independently. This marks a step forward in the generation of arbitrary long waves, though his test arrangement was just partially capable of generating wave troughs, and typical wavelengths could not be obtained because of the limited length of the wave flume. In another investigation, Schmidt-Koppenhagen et al. (2007) reported a set of hydraulic experiments in an exceptionally large-wave flume in Hanover, Germany, which investigated solitary waves. The aim of the experiments was to model the full propagation distance from a source region in deep water into the shallow water. Other large-wave flume experiments looking at solitary and cnoidal wave types in other large-wave tanks can be found in literature but are not listed here.

2.7.2 DAM-BREAK ANALOGY

Another approach to generate long waves and surge flow in the laboratory incorporates the analogy between dam-break-induced bores and surge flow resulting from a tsunami near- and on-shore (Hughes, 1993; Ippen, 1966; Lauber and Hager, 1998). Yeh et al. (1989) were among the first who presented an experimental procedure where a single bore was generated by lifting an aluminum plate gate. The gate, which initially separated the quiescent water on the beach from the higher water level behind the gate, was triggered by a pneumatic cylinder. The instantaneous opening of the gate generated bores in a remarkably repeatable manner.

Chanson et al. (2003) presented a technique where water was released from an overhead water tank at the beginning of the wave flume by an orifice gate. By this means, turbulence is introduced into the physical model even before any wave propagation or breaking took place in the prototype. Further details are provided in Table 1. Likewise, Gomez-Gesteira and Dalrymple (2004) cited a small-scale experiment performed by Yeh and Petroff at the University of Washington referred to as a "bore in a box", in which a dam-break wave impacted a free-standing rectangular structure. A complementary wave generation technique in which a hinged gate releases a body of water to flow into the physical model domain was then reported by Nistor et al. (2009). Furthermore, this technique additionally benefited from the fact that the tail of the dam-break-induced bore was supported and maintained by two pumps discharging into the back of the collapsing water volume.

2.7.3 VERTICAL WAVE BOARD MOTION

Another means of generating long wave motion in a laboratory was described by Monaghan and Kos (2000), who used Scott Russell's idea of a sinking box (Russell, 1844) to illustrate the formation of a solitary wave in a long rectangular tank. Since then, numerical models had been validated (cp. also Abadie et al., 2008) with the help of the results obtained from Russell's early laboratory findings. In general, the presented generation methodology was capable of generating a solitary wave. However, in the region near the vertical wave board motion, vortexes and turbulent and undirected fluxes are generated in the water body. These effects are supposed to adversely alter the wave propagation and run-up in the laboratory.

Apart from generating waves through the downward directed wave maker motion Raichlen (1970) first mentioned wave generation by upward/ downward moving wave flume bottom, which aimed at generating long waves in accordance to the source motion from tectonic movements of a sea floor at plate boundaries. A description of a study taking advantage of a vertically moving piston was presented by Hammack (1973) and Segur (2007). Both authors distinguished between a generation section and downstream section of the wave evolution in their experiment. This implies that the utilization of the 'moving bottom' generation technique resembles an earthquake stimulation and can be used in deep water conditions.

2.7.4 VOLUME-DRIVEN WAVE GENERATION

A novel modeling approach in tsunami wave generation has been reported (Reynolds, 1887; Wilkie and Young, 1992). The pneumatic wave generator was successful in its developmental stages, and, at that time, it was depicted as versatile equipment for a wide range of purposes and model scales. The tidal wave generation is functioned by means of an inverted box at the seaward end of the physical model fixed to the flume floor. The flumeward facing box side ended at a distance above the bottom, forming an outflow gap and allowing water to leave or enter the box chamber, which resulted in a time-dependent water level change (see also Allen et al., 1992). Thus, a modified version of the old principle of storing water in a tank and releasing it under the control of a valve–pump system had been constructed (Rossetto et al., 2011). The controller scheme and hardware of the tidal wave generator had been optimized in order to adapt to a tsunami. Additional facility demands due to shorter wavelength were met using a quieter, high-capacity vacuum pump, faster controller algorithms, optimized valves, and servo motors

CHAPTER 3

METHODOLOGY

This chapter deliberates the development of Dam-Break wave generator and its properties. The equipment and instrument that are used to test the model are also presented. The material used for the Dam-Break Wave Generator construction as well as the experimental set-up will be thoroughly discussed. Not only have that, this chapter also delivered the project activities and Gantt chart for the overall study of Dam-Break Wave Generator.

3.1 DAM-BREAK WAVE GENERATOR

The dam-break wave generator is used to produce a single bore by lifting gate which is wood coated with waterproof paint at a certain height. The fluid will be stored at the rear area of the wave flume at specified level. The optimum gate height and upstream water level will be determine during preliminary experimentation in which the flow velocity should reach 9m/s representing the actual onshore tsunami flow. The dam break is shown in figure 3.1.

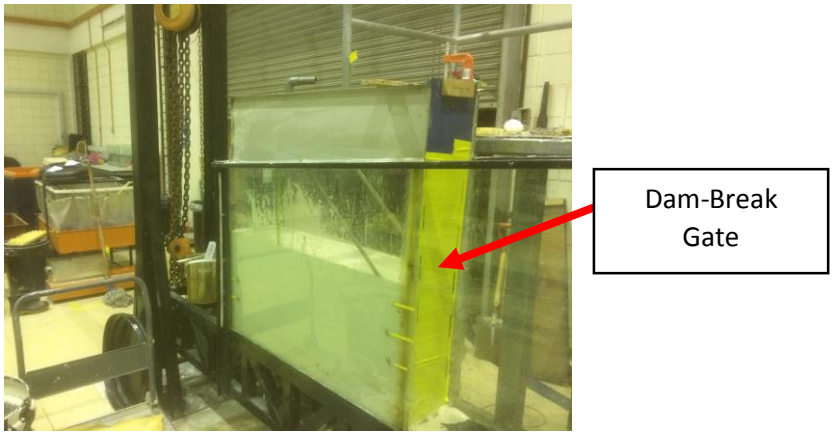

Figure 3.1: Dam-Break gate

3.2 LABORATORY EQUIPMENT AND EQUIPMENTS

3.2.1 Wave Flume

The experiment takes place in a 8.65m long, 0.24m width and (0.8m and 1.3m) high trapezoidal wave flume as shown in figure 3.1.1. The maximum water level permitted by the flume is 0.7m with a maximum allowable wave height of 0.2m. The walls of the flume were constructed with glass panels to ease the observation and monitoring on the experiments that are being conducted inside the wave flume.

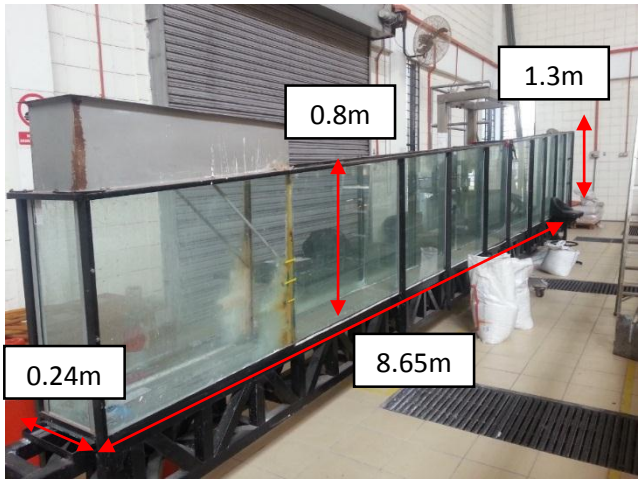

Figure 3.2: Sediment Flume

3.2.2 Wave Probe

The wave probes will be used to measure the incident wave height values before the structure and the transmitted wave height values after the structure, throughout the testing. In this study, the focus will be more on the different types of fluid that can affect the height of the wave upon impact. Which also means how it can affect the run-off height. In this experiment, the wave probe is be called as wire probe, since copper wire will be used as the wave probe. Figure 3.2.2.1 shows a wave probe used for the experiment.

Figure 3.3: Wire Probe to measure wave height

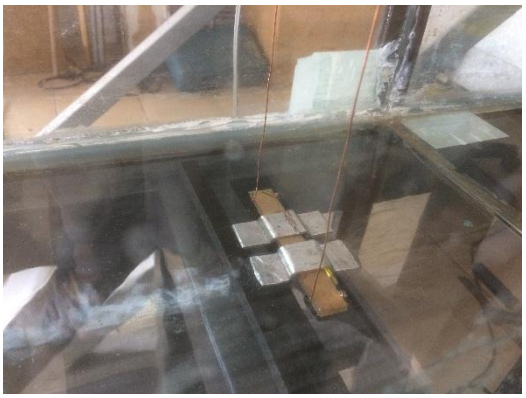

Figure 3.4: Installed Wire Probe

3.2.4: Video Recorder

A video recorder will be used to record the movement of the wave upon impact against the vertical rectangular structure. It is also used to see the flow of the waves passing through the structure having different types of physical properties. The Go Pro Hero 4 will be used as the video recorder as it has special features such as slow-motion and able to record high speed movement of any object. Figure 3.2.4.1 shows the Go Pro hero 4 that will be used as the video recorder.

Figure 3.5: Go Pro Hero 4

3.2.5: Pressure Transducer

Three pressure transducer will be used to measure the dynamic pressure upon wave impact. The transducer will be attached to the vertical rectangular structure facing the wave. Upon impact the pressure transducer will send the data to the computer for interpretation. Figure 3.2.5.1 and figure 3.2.5.2 shows the pressure transducer used and the vertical rectangular structure respectively.

Figure 3.6: Pressure Transducer

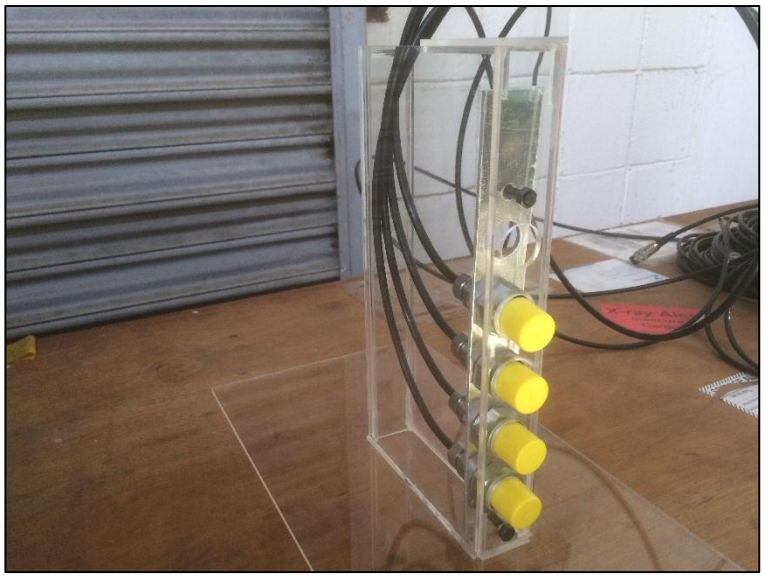

Figure 3.7: Vertical Rectangular Structure

3.2.6 Data Logger and Transducer Output & Power Supply Unit

A data logger (also data recorder) is an electronic device that records data over time or in relation to location either with a built in instrument or sensor or via external instruments and sensors. Increasingly, but not entirely, they are based on a digital processor (or computer).

The Transducer Output & Power Supply Unit is a self-contained interface box feeds up to eight separate voltage inputs in the range of -10V to +10V to a host PC for data acquisition via a USB link. It has 8 input sockets each able to supply 24V DC at approximately 100mA to any compatible sensor or transducer. Power is from an external desktop-style PSU and two panel-mounted LEDs provide power-on and USB activity indication. Power lead, USB lead and USB driver software are also supplied. This unit can accommodate up to 8 compatible transducers.

Figure 3.8: Data Logger

Figure 3.9: Transducer Output & Power Supply Unit

3.3 EXPERIMENTAL SET-UP

A systematic test program is established to study the hydrodynamics waves and wave loading having different types of fluids. Figure 3.3.1 shows the setup for this experiment. A wave probe will be placed near the vertical rectangular structure to measure the height of the wave upon impact. An ADV will be placed in the middle of the wave flume to measure the velocity of the wave for both types of fluids. The video recorder will be placed near the vertical rectangular structure to record the movement of the wave. The three pressure transducer will be attached to the vertical rectangular structure to measure the dynamic pressure upon impact. Table 3.3-1 lists all the fixed and manipulated parameters for the existing experimental study.

Table 3.1: Summary of Experiment Conditions

Parameters	Fixed	Manipulated
Types of fluid		x
Volume of fluid	x	
Wave Steepness	x	
Wave type	x	
Model Scale	x	
Model Orientation	x	

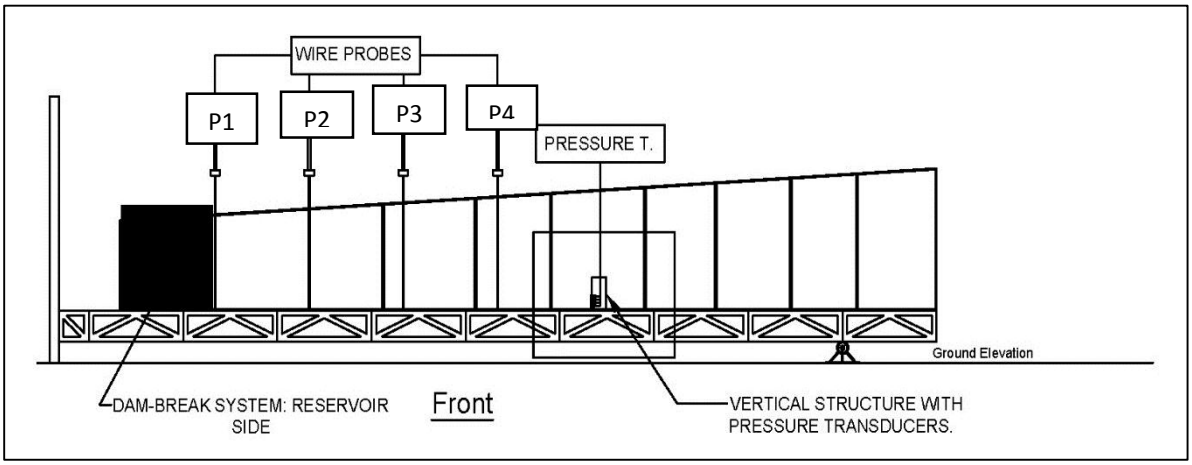

Figure 3.10: Experimental Set-up

Before conducting a run, the wire probes must be calibrated first due to the copper wires used for this experiment are subjected to tension or compression after in contact with the water. The calibration were executed for every repetition for each water level to ensure accurate reading of the wire probes. After calibration is done, the reservoir tank is then filled with the desired water depth. Before the dam-break gate is released, the video recorders will be turned on to record the movement of water hitting the rectangular structure holding the pressure transducers. After the water passes the rectangular structure, the video recorder will be stopped and the video recorder will be reviewed immediately. Wave height data recorded by the wire probes through the data logger and the data from the Transducer Output & Power Supply Unit will be analyzed. All these steps are to be repeated for every test run.

3.3.1 TEST MATRIX

Table 3.2: Test Matrix

Fluid Type	Vol. Concentration (%)	Water Depth(com)	Structure Type	No.of Rep
Newtonian	-	45	Vertical	3
non-Newtonian	20			

3.4 KEY MILESTONE

A Progression of report usually illustrated by using Gantt chart. In the Gantt chart, every work needs to be completed from the start to finish are listed and the time proposed is set up to make sure the project is done within the time given. Key milestone is used as a project checkpoint to certify how the project is progressing. Table 3.4-1 shows a summarization of the important events throughout the Final year Project 2 (FYP 2).

Table 3.3: Key Milestone

No.	Key Milestone	Proposed Week
1	Submission of Progress report	Week 7
2	Submission of Technical Report	Week 13
3	Submission of Final report	Week 14

3.5 GANTT CHART

In the first half of the study, the focus is more on the introduction and preparation towards the further study of the test model. Thus, it is important to have a Gantt chart in which will help in keeping track of the progress and proceed accordingly. The Gantt chart will give a clear indication on the task that will be done and to ensure the feasibility of the study as it is initially planned in the beginning of the study. The table 3.6-1 shows the progress of works need to be done within time given according to the guideline for Final Year Project.

Table 3.4: Key Milestone

RESEARCH	2016							
	MEI	JUN	JULY	AUG	SEP	OCT	NOV	DEC
LITERATURE REVIEW								
DESK STUDY ON WAVE GENERATOR								
FABRICATION TEST MODEL								
SAMPLE PREPARATION OF NON-NEWTONIAN FLUID								
EXPERIMENTAL SET UP								
SIMULATION OF TSUNAMI ON NEWTONIAN FLUID								
SIMULATION OF TSUNAMI ON NON-NEWTONIAN FLUID								
COMPARING THE RESULTS FOR BOTH TYPE OF FLUID								
ANALYSIS OF RESULTS								
SUBMISSION & PRESENTATION								

3.6 FLOW CHART OF RESEARCH ACTIVITIES

In completing the studies, a series of activities need to be done in order to ensure the feasibility of the study. These set of task will be done in a number of stages in order to ensure the clear flow of study. The flow chart of the research activities is given in Figure 3.7.1.

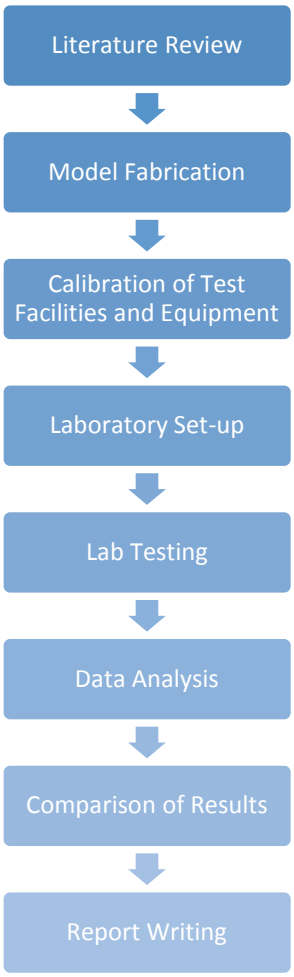

Figure 3.11: Flow Chart of Research Activities

CHAPTER 4

RESULTS AND DISCUSSION

This chapter deliberates the current achieved results and several small discussion based on the current status of experimental work. The data acquired are mainly recorded and analyzed by using HR DAQ Data Logger and the Pressure Transducer Receiver.

4.1 Selection of Wave Probe

There are two types of probes available to be used for this experiment. However, in order to find out the best wave probe that can produce a higher accuracy and efficiency, both will be tested by using 4 different water level in the reservoir tank which are 15cm, 30cm, 45cm and 60cm. The sampling rate is 1000 Hz and the time taken per flow repetition is 60s. However the time will be cut to 4s only due to the reading of reflected wave. Below are the two types of the mentioned probes.

4.1.1 Stainless Steel probe

Figure 4.1: Stainless Steel Wave Probe

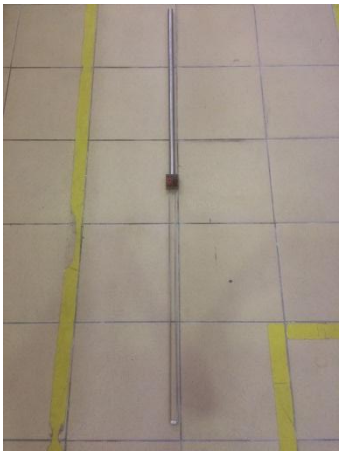

Figure 4.2: Stainless Steel Wave Probe

4.1.2 Wired Probe

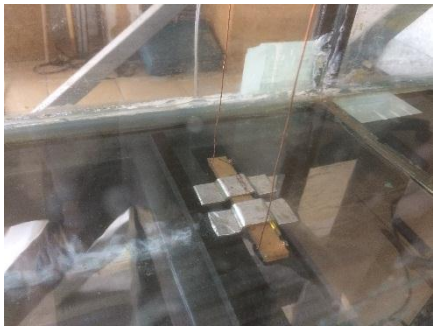

Figure 4.3: Stainless Steel Wave Probe

Figure 4.4: Stainless Steel Wave Probe

All of the waves were located at 1m from each other and the height of the wave probe is about 1m from the bed of the flume tank to the top. Before starting the experiment, all of the waves were calibrated for each repetition for each water level at the reservoir tank. This is due to the spontaneous tension difference of the copper wire when in contact with the waves.

4.2 Stainless Steel Wave Probe Reading

4.2.1 Repetition 1 for all probes

- **Water Level = 15cm**

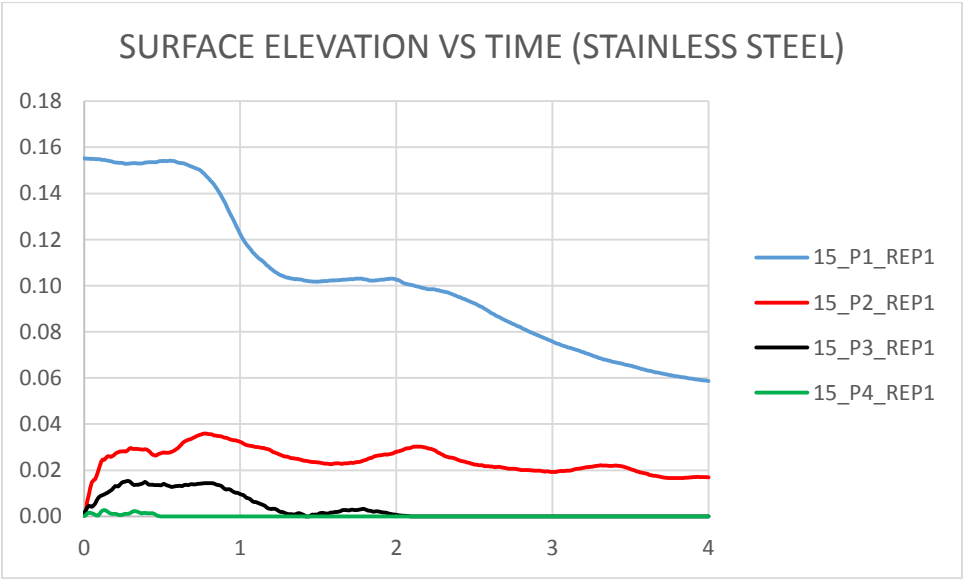

Figure 4.5: Surface elevation vs Time (Stainless Steel Wave Probe)

- **Water level = 30cm**

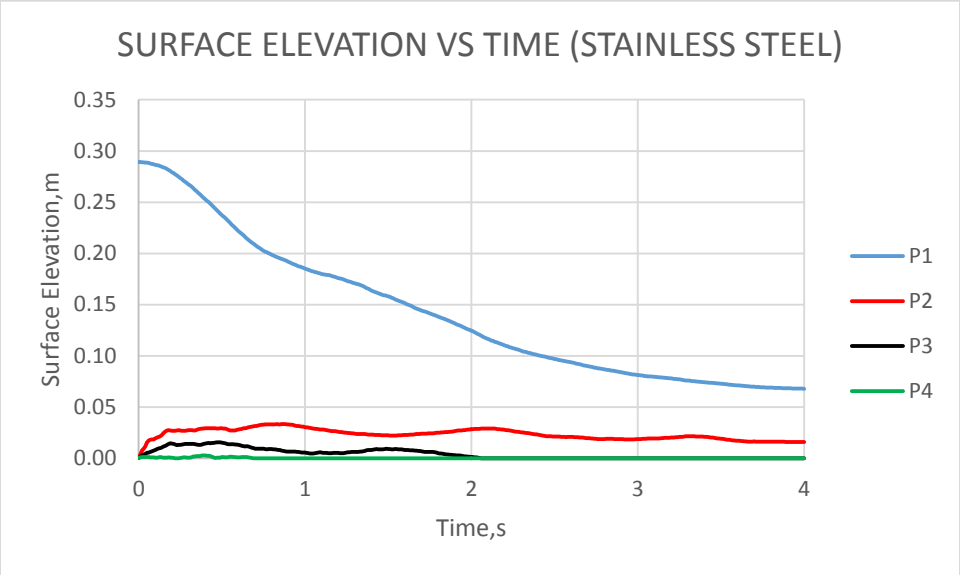

Figure 4.6: Surface elevation vs Time (Stainless Steel Wave Probe)

4.3 Wire Wave Probe

4.3.1 Repetition 1 for all

- **Water level = 15cm**

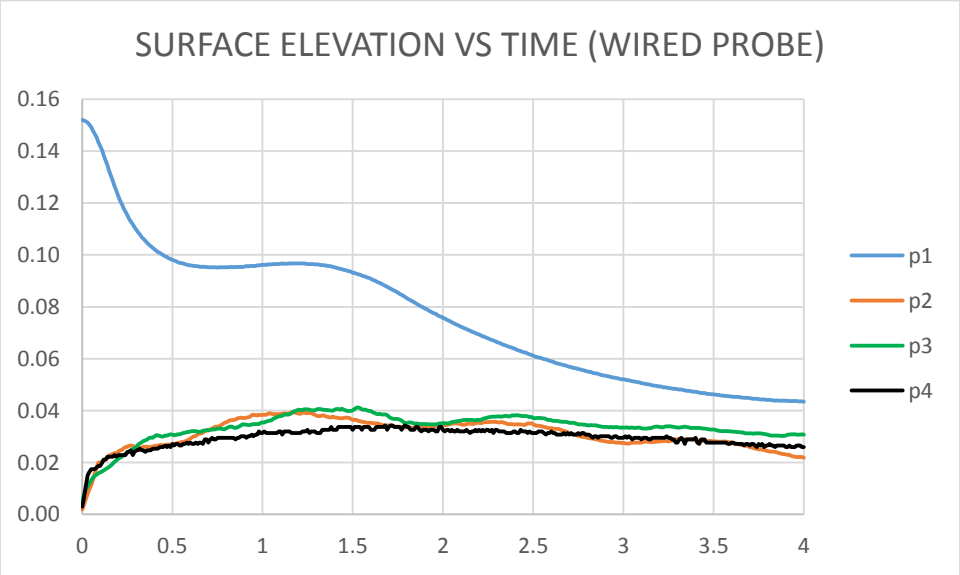

Figure 4.7: Surface elevation vs Time (Wired Wave Probe)

- **Water level = 30cm**

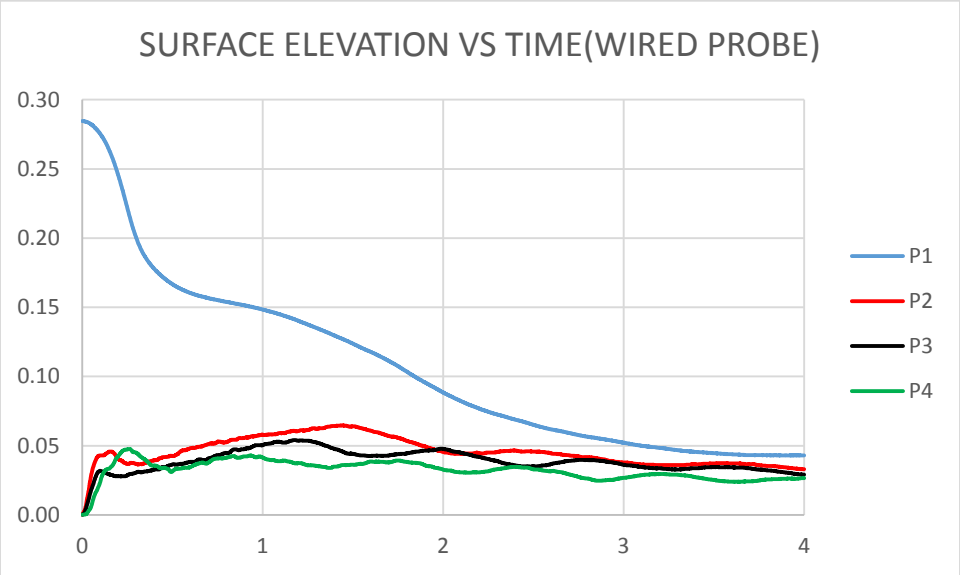

Figure 4.8: Surface elevation vs Time (Wired Wave Probe)

Based on the graph representing both wired probe and stainless steel probe, it shows that when using wave probes, the data shows a better and more stable bore height reading.

However, for stainless steel probe, it shows that the readings are quite inaccurate and illogical. Judging by its readings, it shows that the bore height at probe 4 seems to be at 0 cm even though the time is less than 4 seconds. After careful observation and analysis, it shows that the small silicon at the end of the stainless steel probe could not read the water level below it. This causes the bore height to be zero as shown in the graph.

Therefore, wired wave probe is chosen for this experiment clearly due to its ability to be able to detect the bore height at any level.

4.4 FLOW VALIDATION

In this section, the flow is validated by using different water level in the reservoir tank. This is to validate which water level in the tank will produce the desired bore height for this project, which is at a minimum of 7 to 10 cm. The velocity deliberated by the water levels will also be taken into consideration. The minimum velocity required is 2.5ms^{-1} to 5.0ms^{-1}.The water level used in this experiment are 15cm, 30cm, 45cm and 60cm.

4.4.1 All repetition for 15cm water level

- **Probe 1**

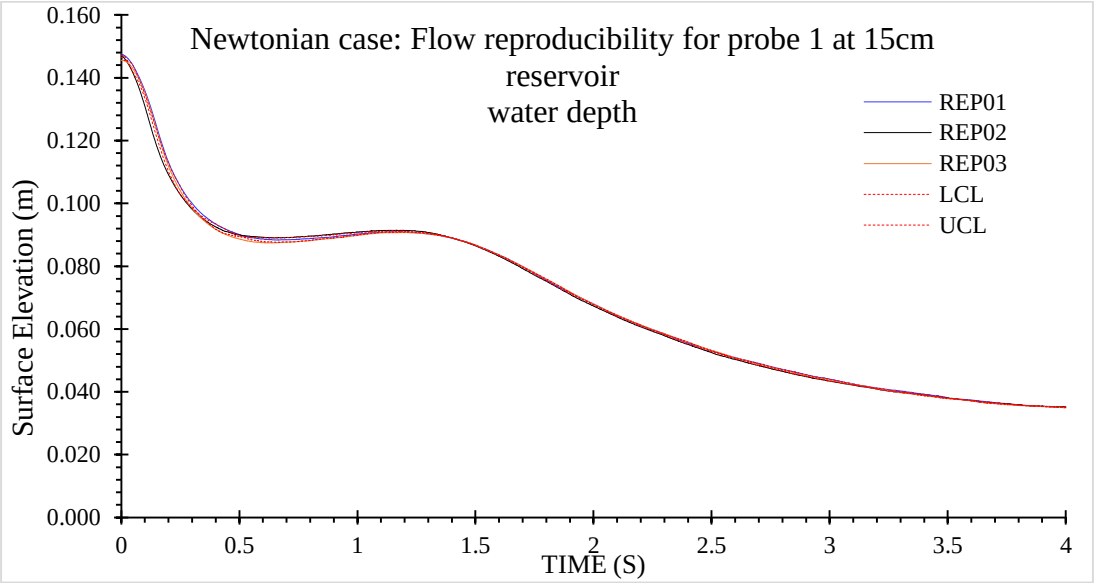

Figure 4.9: Surface Elevation VS Time for 15cm depth at Reservoir Tank

- **Probe 2**

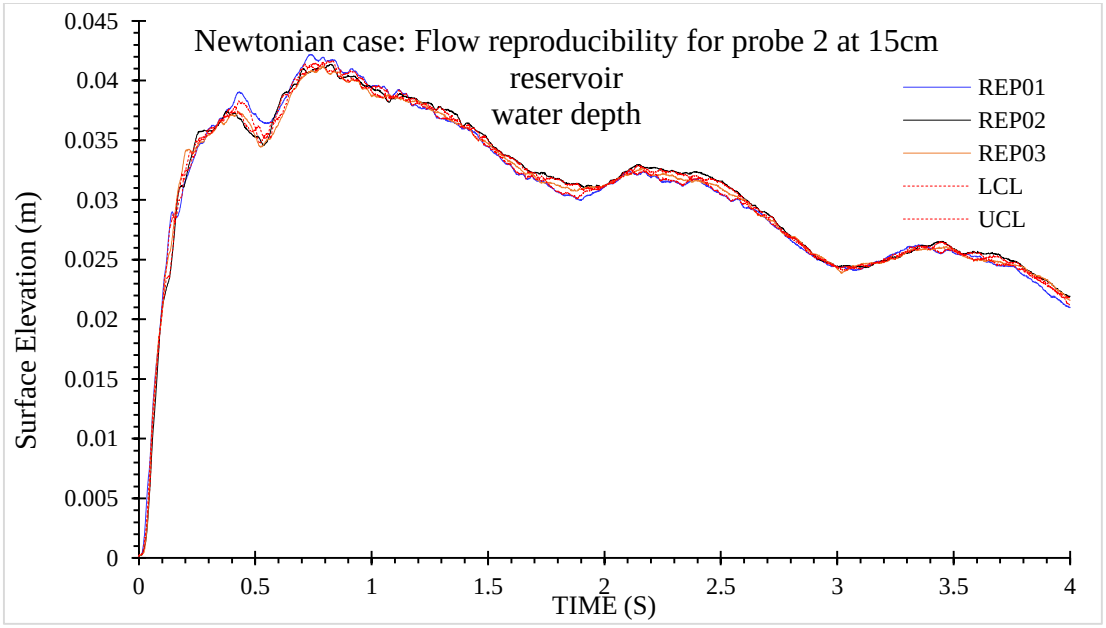

Figure 4.10: Surface Elevation VS Time for 15cm depth at Reservoir Tank

- **Probe 3**

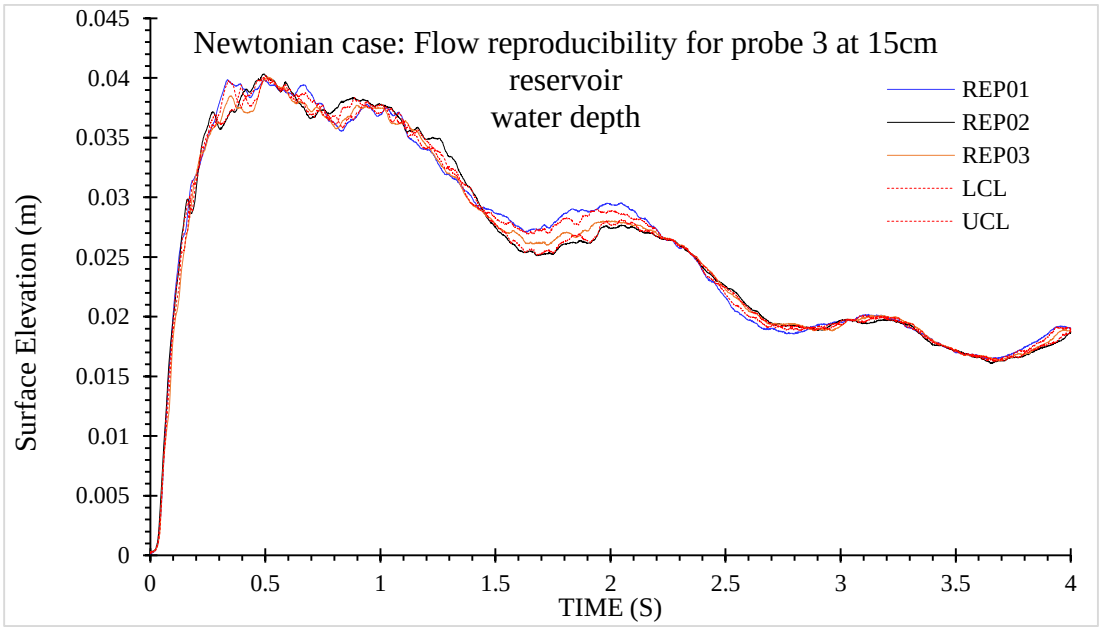

Figure 4.11: Surface Elevation VS Time for 15cm depth at Reservoir Tank

- **Probe 4**

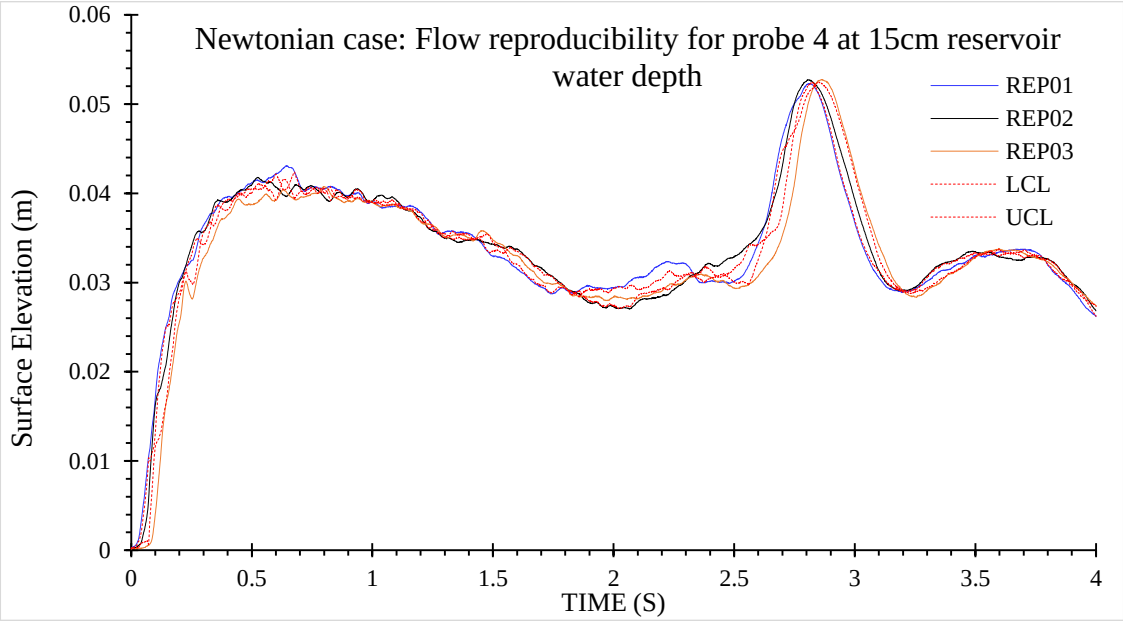

Figure 4.12: Surface Elevation VS Time for 15cm depth at Reservoir Tank

Based on all of the readings received from the probes for water level of 15cm, the average readings for surface elevation given by all of the probes is 0.04m, which is low than the required surface elevation. The summarized velocity produced for 15cm water level is as below.

Table 4.1: Summary of Velocity for 15cm Water Level

	SEC1	SEC2	SEC3
REP1	1.531394	1.236094	1.194743
REP2	1.477105	1.25	1.197605
REP3	1.519757	1.254705	1.111111

Section 1(SEC1) represent the velocity between Probe 1 to probe 2. Whereas Section 2(SEC2) represents the velocity between probe 2 to probe 3. Lastly, Section 3(SEC3) represents the velocity from probe 3 to Probe 4. The velocity produced by the flow is less than $2.5ms^{-1}$. Therefore, 15cm water level does not produce the required criteria for this experiment.

4.4.2 All repetition for 30cm water level

- **Probe 1**

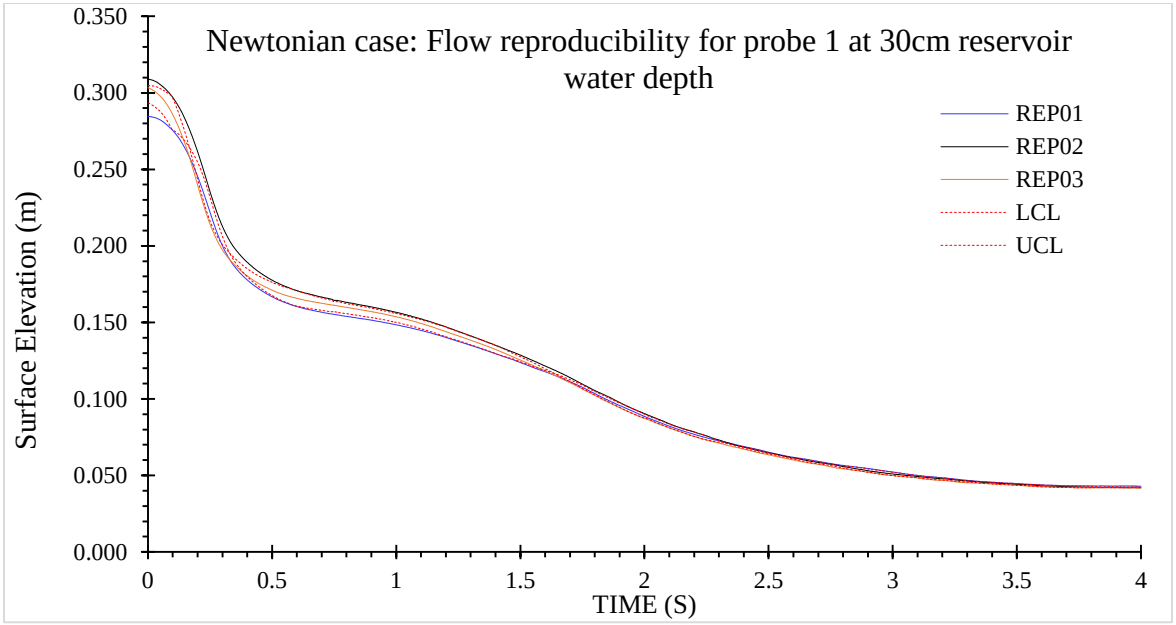

Figure 4.13: Surface Elevation VS Time for 30cm depth at Reservoir Tank

- **Probe 2**

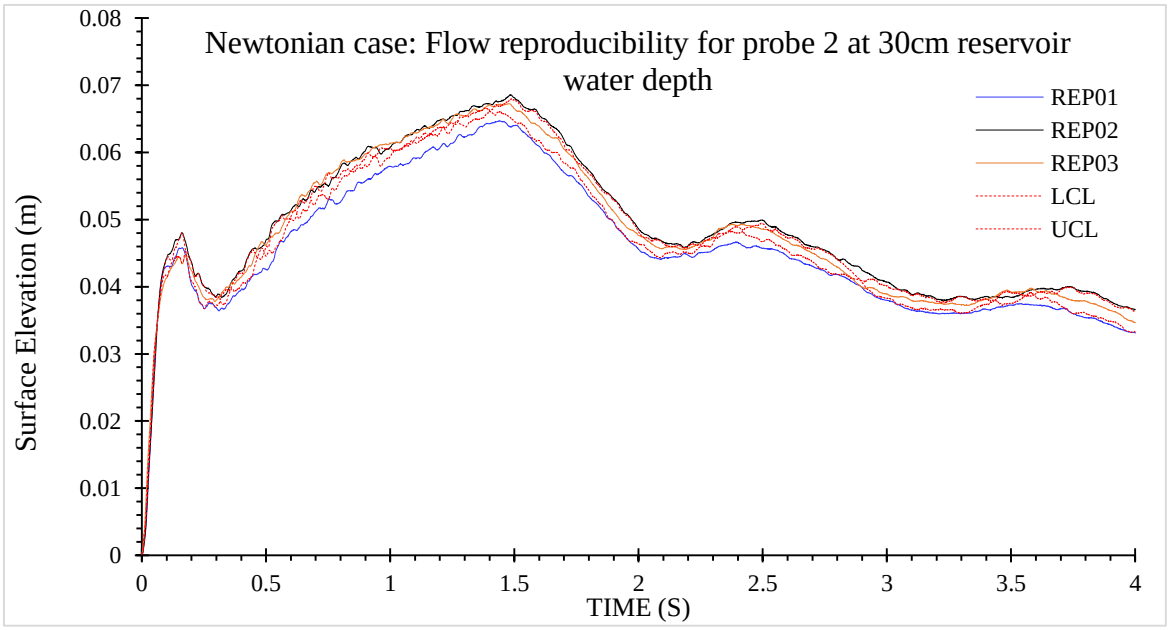

Figure 4.14: Surface Elevation VS Time for 30cm depth at Reservoir Tank

- **Probe 3**

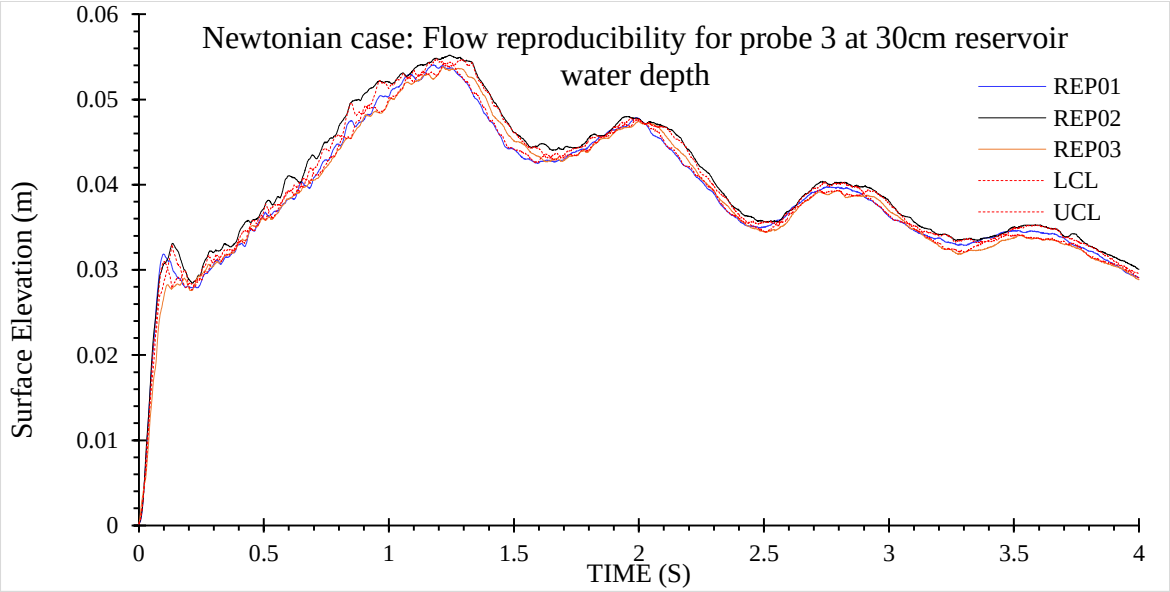

Figure 4.15: Surface Elevation VS Time for 30cm depth at Reservoir Tank

- **Probe 4**

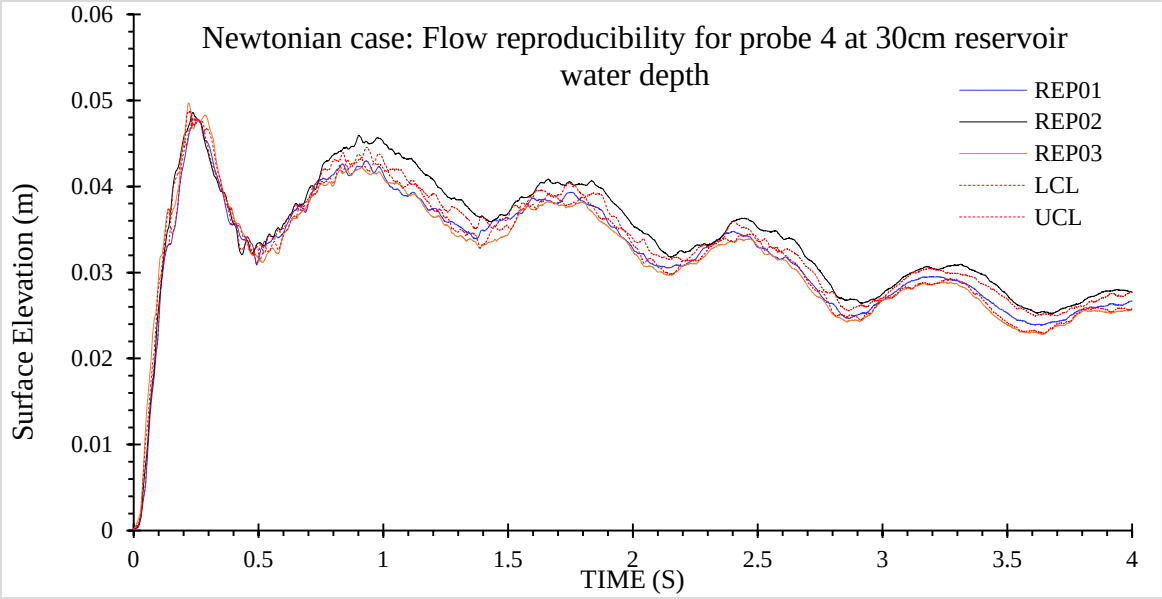

Figure 4.16: Surface Elevation VS Time for 30cm depth at Reservoir Tank

Based on all of the readings received from the probes for water level of 30cm, the average readings for surface elevation given by all of the probes is 0.05m, which is low than the required surface elevation. The summarized velocity produced for 30cm water level is as below.

Table 4.2: Summary of Velocity for 30cm Water Level

	SEC1	SEC2	SEC3
REP1	2.03252	2.469136	2.136752
REP2	2.074689	2.506266	2.252252
REP3	1.179245	2.590674	2.020202

The velocity produced around SEC2 shows a value of 2.5ms^{-1} or less. However the rest of the Sections were not able to produce the desired velocity. Therefore, since both criteria were not met, water level of 30cm is rejected.

4.4.3 All repetition for 45cm water level

- **Probe 1**

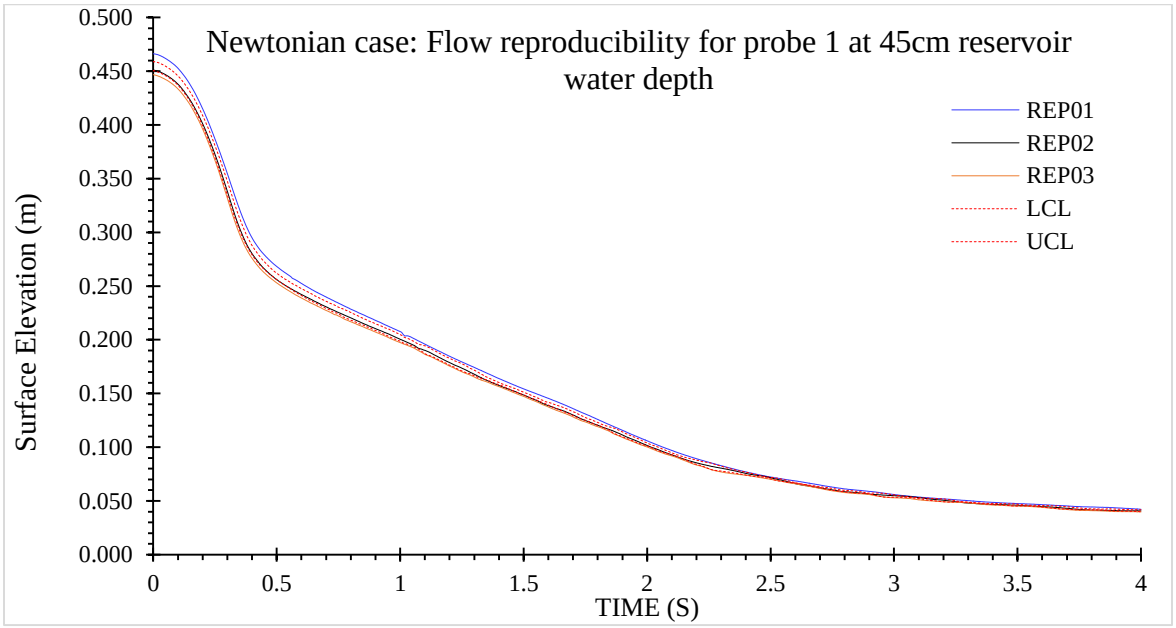

Figure 4.17: Surface Elevation VS Time for 45cm depth at Reservoir Tank

- **Probe 2**

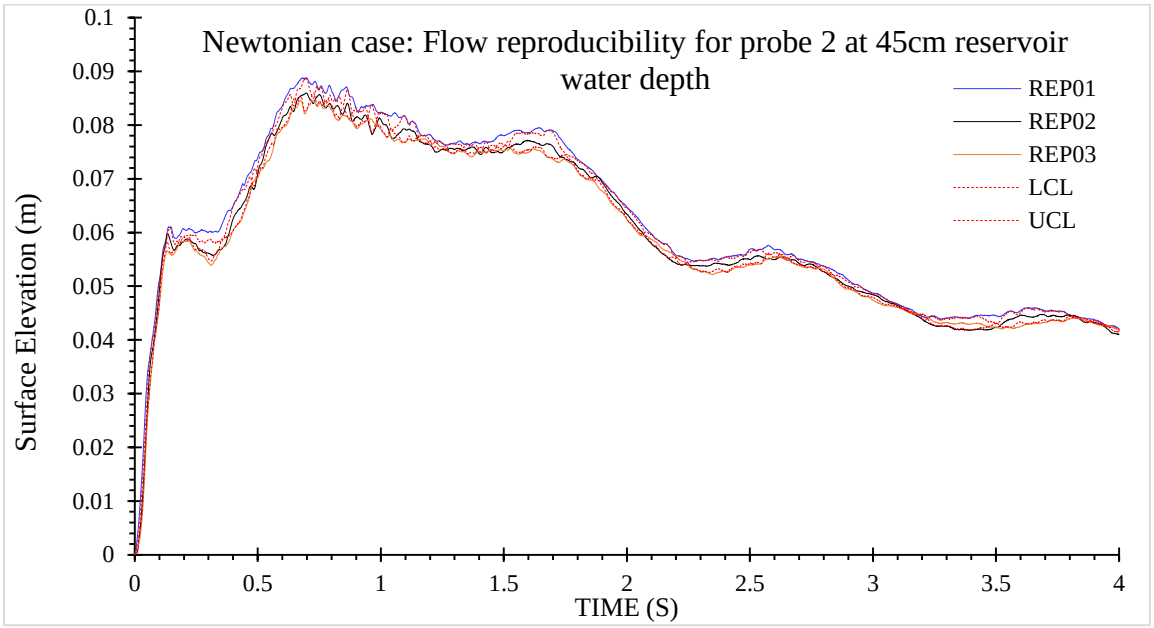

Figure 4.18: Surface Elevation VS Time for 45cm depth at Reservoir Tank

- **Probe 3**

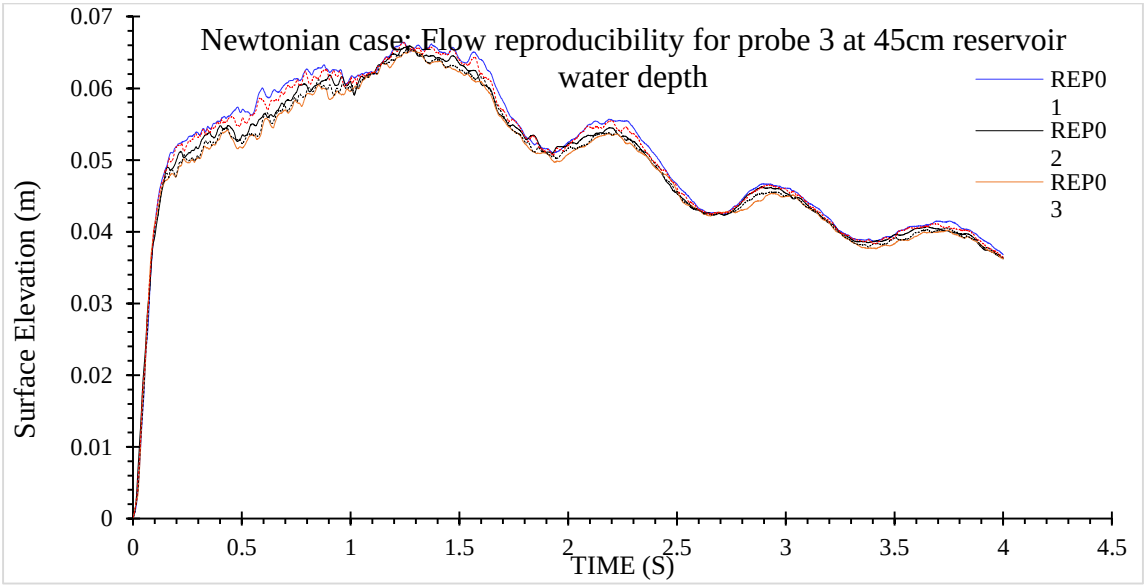

Figure 4.19: Surface Elevation VS Time for 45cm depth at Reservoir Tank

- **Probe 4**

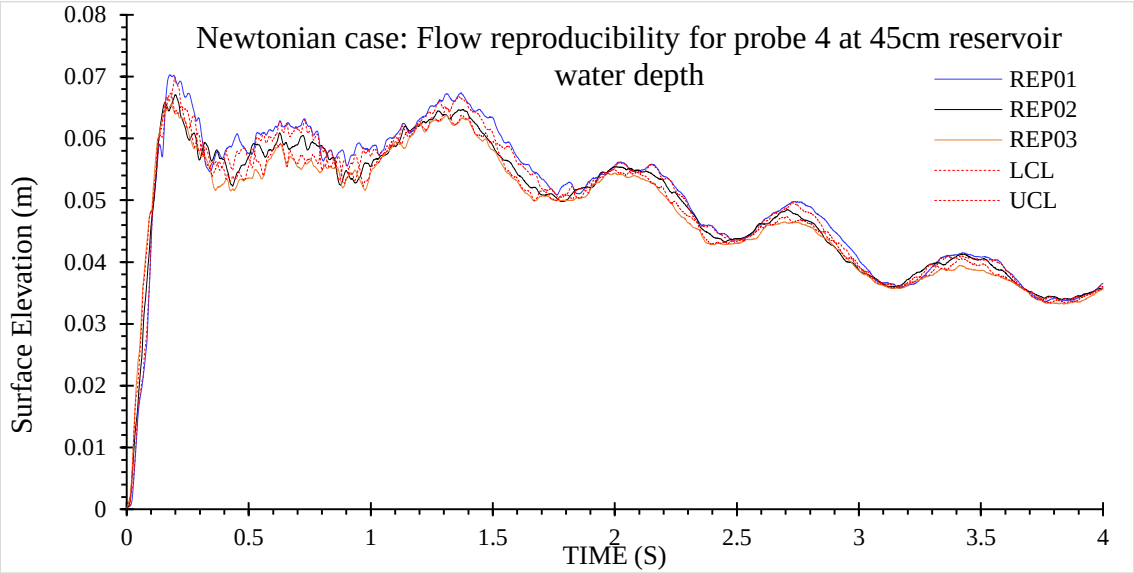

Figure 4.20: Surface Elevation VS Time for 45cm depth at Reservoir Tank

Based on all of the readings received from the probes for water level of 45cm, the average readings for surface elevation given by all of the probes is 0.07m, which achieves the required surface elevation. The summarized velocity produced for 45cm water level is as below.

Table 4.3: Summary of Velocity for 45cm Water Level

	Sec1	Sec2	Sec3
Rep1	2.544529	2.923977	3.571429
Rep 2	2.463054	2.832861	2.873563
Rep 3	2.475248	2.849003	2.793296

The velocity produced for all sections meet the required velocity. Since both of the criteria were met, water level of 45cm passes the required bore height and velocity.

4.4.4 All repetition for 60cm water level

- **Probe 1**

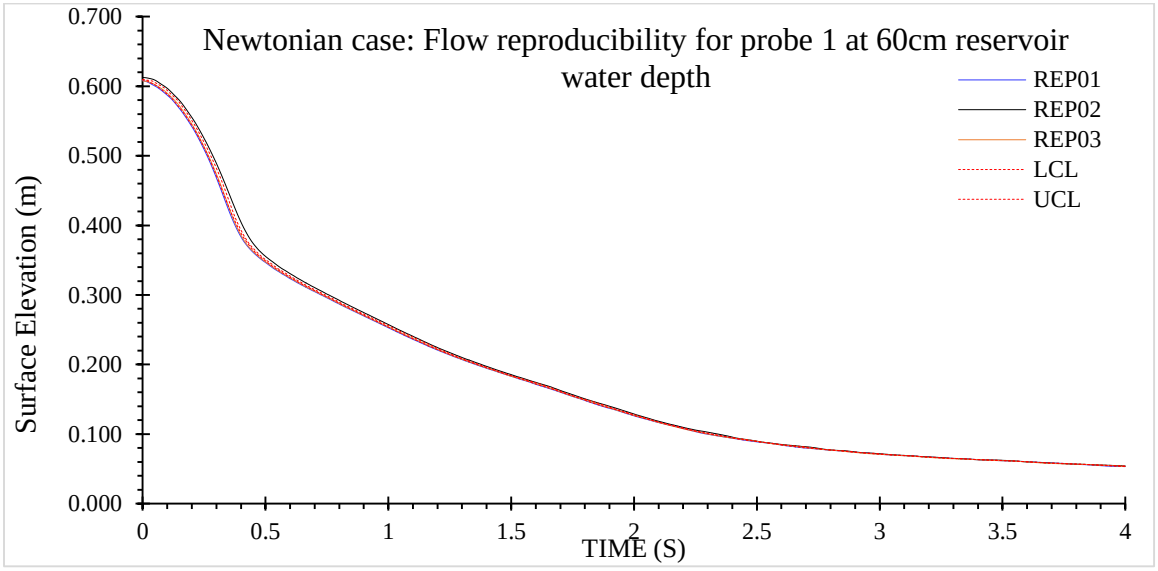

Figure 4.21: Surface Elevation VS Time for 60cm depth at Reservoir Tank

- **Probe 2**

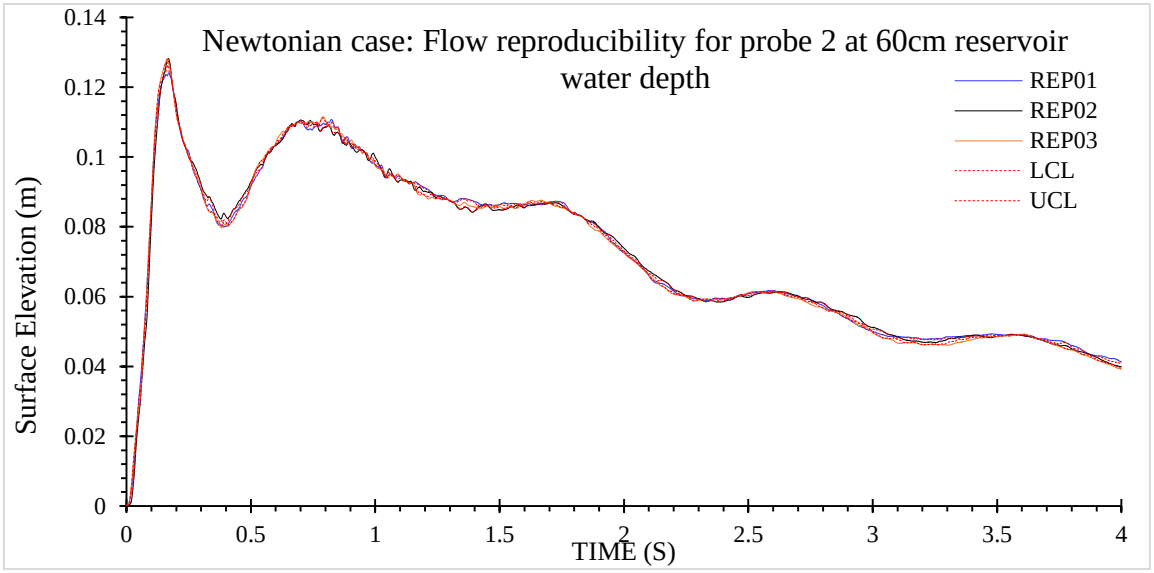

Figure 4.22: Surface Elevation VS Time for 60cm depth at Reservoir Tank

- **Probe 3**

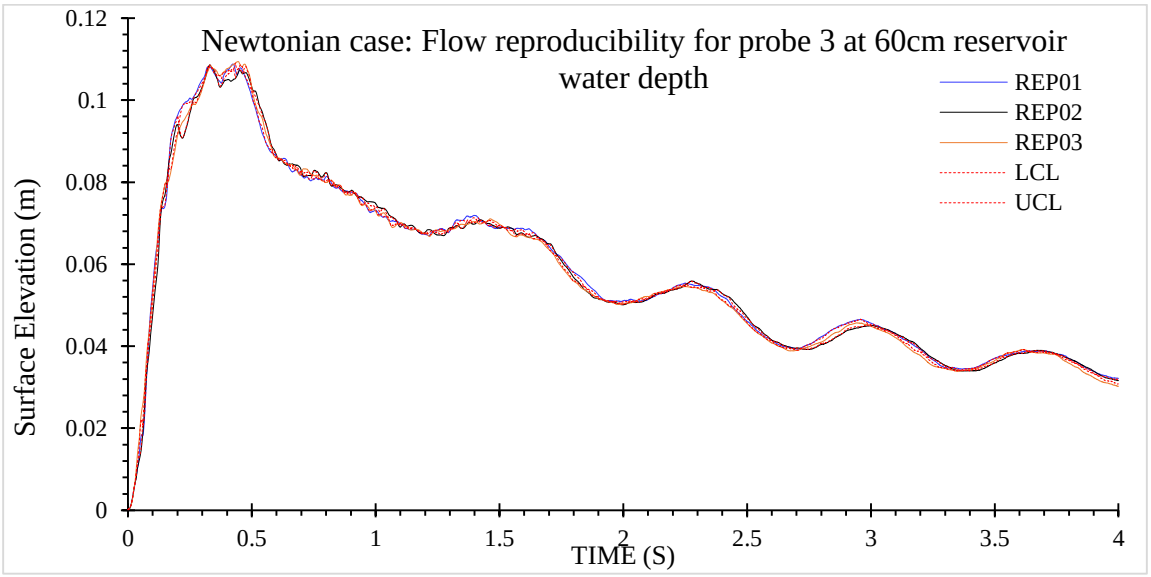

Figure 4.23: Surface Elevation VS Time for 60cm depth at Reservoir Tank

- **Probe 4**

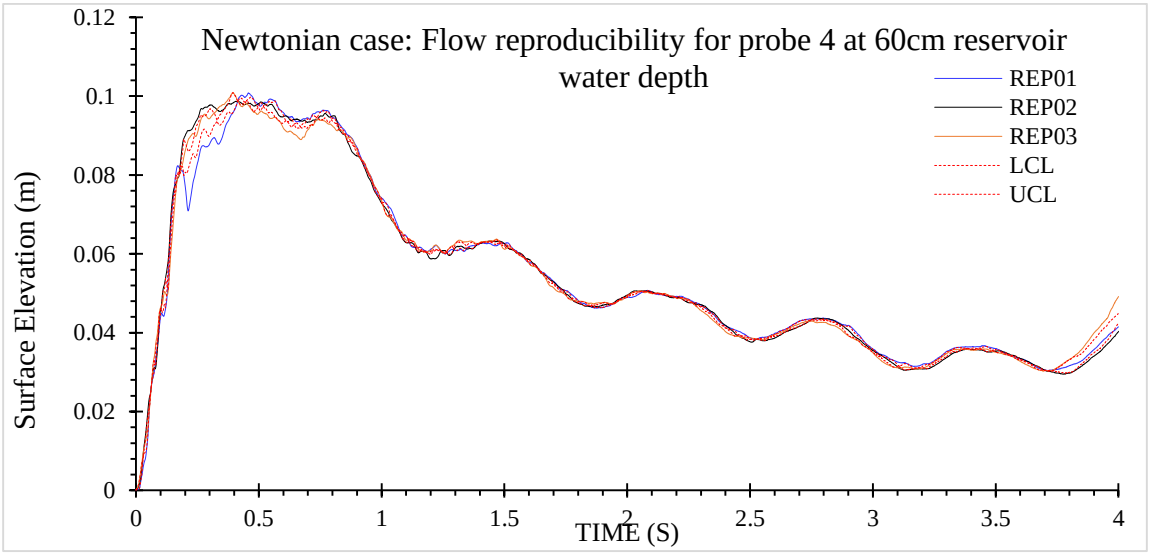

Figure 4.24: Surface Elevation VS Time for 60cm depth at Reservoir Tank

Based on all of the readings received from the probes for water level of 45cm, the average readings for surface elevation given by all of the probes is 0.1m, which achieves the required surface elevation. The summarized velocity produced for 60cm water level is as below.

Table 4.3: Summary of Velocity for 60cm Water Level

	Sec1	Sec2	Sec3
Rep1	2.544529	2.923977	3.571429
Rep 2	2.463054	2.832861	2.873563
Rep 3	2.475248	2.849003	2.793296

The velocity produced for all sections meet the required velocity. Since both of the criteria were met, water level of 60cm also passes the required bore height and velocity.

As a conclusion, water level of 15cm and 30cm were disqualified. Even though water level of 45cm and 60cm both met the minimum requirements for velocity and bore height, in this experiment, water level of 45cm is chosen over the water level of 60cm. This is due to the limitations of the size of the flume tank and also due to its overpowered velocity and impact.

4.4.5 Newtonian Bore Characteristics

Table 4.4: Summary of data for all Water Level

WATER LEVEL	ID	Bore Height (m)	Velocity (m/s)
15CM W.L	P2	0.049811	1.519756839
	P3	0.051532	1.254705144
	P4	0.04654	1.111111111
30CM W.L	P2	0.059382532	2.074688797
	P3	0.047853299	2.506265664
	P4	0.037996832	2.252252252
45CM W.L	P2	0.079347948	2.463054187
	P3	0.061092737	2.83286119
	P4	0.058088622	2.8735632
60CM W.L	P2	0.101429939	2.624671916
	P3	0.093388366	3.134796238
	P4	0.093912434	3.048780488

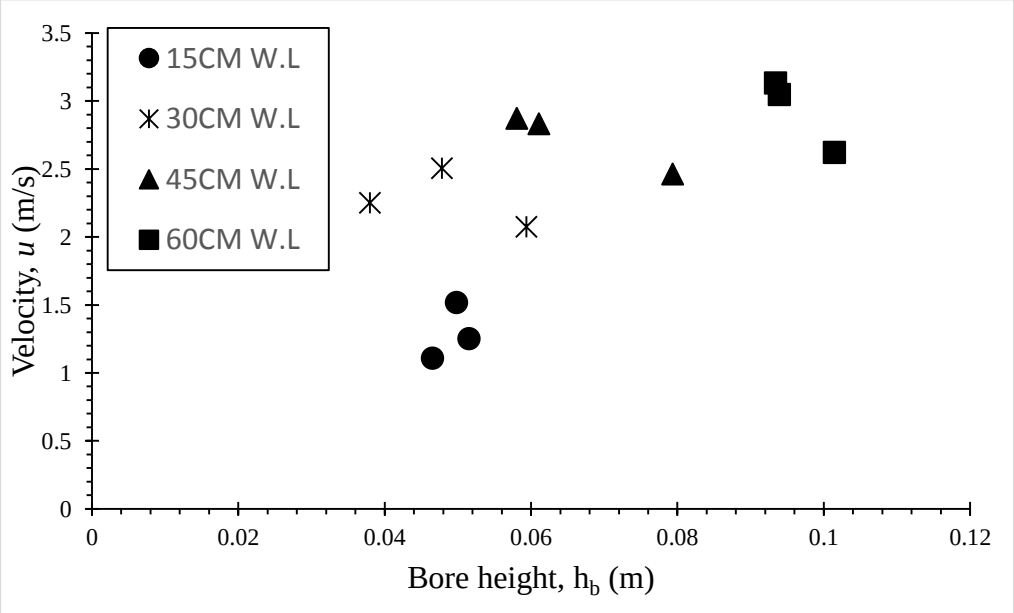

Figure 4.25: Velocity, *u* VS Bore height, h_b for all water levels

4.4.6 Comparison of Alpha Constant, a_u between FEMA (2012) and Shafiei et. Al (2016)

- **Alpha Constant value from FEMA (2012) and Shafiei et. Al (2016)**

Table 4.5: Alpha Constant value, a_u from FEMA and Shafiei

	Alpha Constant
Shafiei et. Al (2016)	1.7
FEMA (2012)	2

Based on the value of a_u above for each flow depth, their respective bore height is tabulated below:

Table 4.6: Valueobtained from the Alpha value, a_u

Flow Depth (M)	Shafiei et. Al (2016)	FEMA (2012)
0.02	0.753005976	0.885889384
0.04	1.064911264	1.252836781
0.06	1.304244609	1.534405422
0.08	1.506011952	1.771778767
0.1	1.68377255	1.980908882
0.12	1.844480415	2.169976958

The bore height, Hb and velocity, V obtained from the water levels is shown in the graph below:

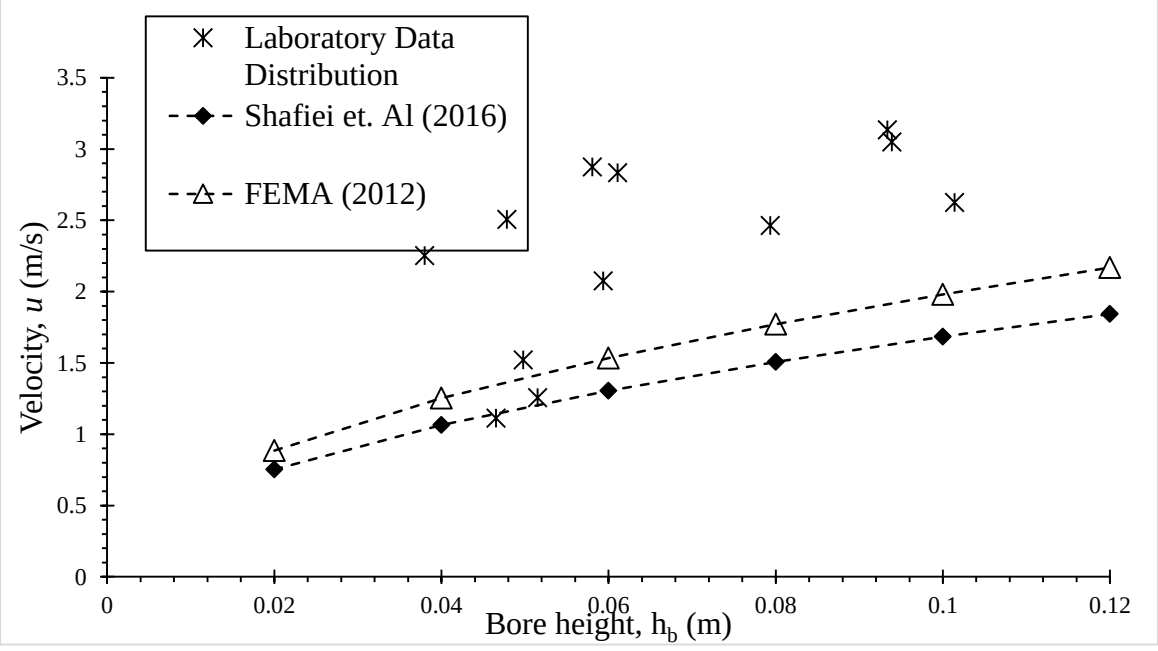

Figure 4.26: Velocity, *u* VS Bore height, h_b from conducted experiments

Once the best fit line is obtained from the laboratory data distribution, an Alpha value, $\boldsymbol{a_u}$ will be assigned to match the best fit line. The value for $\boldsymbol{a_u}$ is 3.0 which is shown in the graph below.

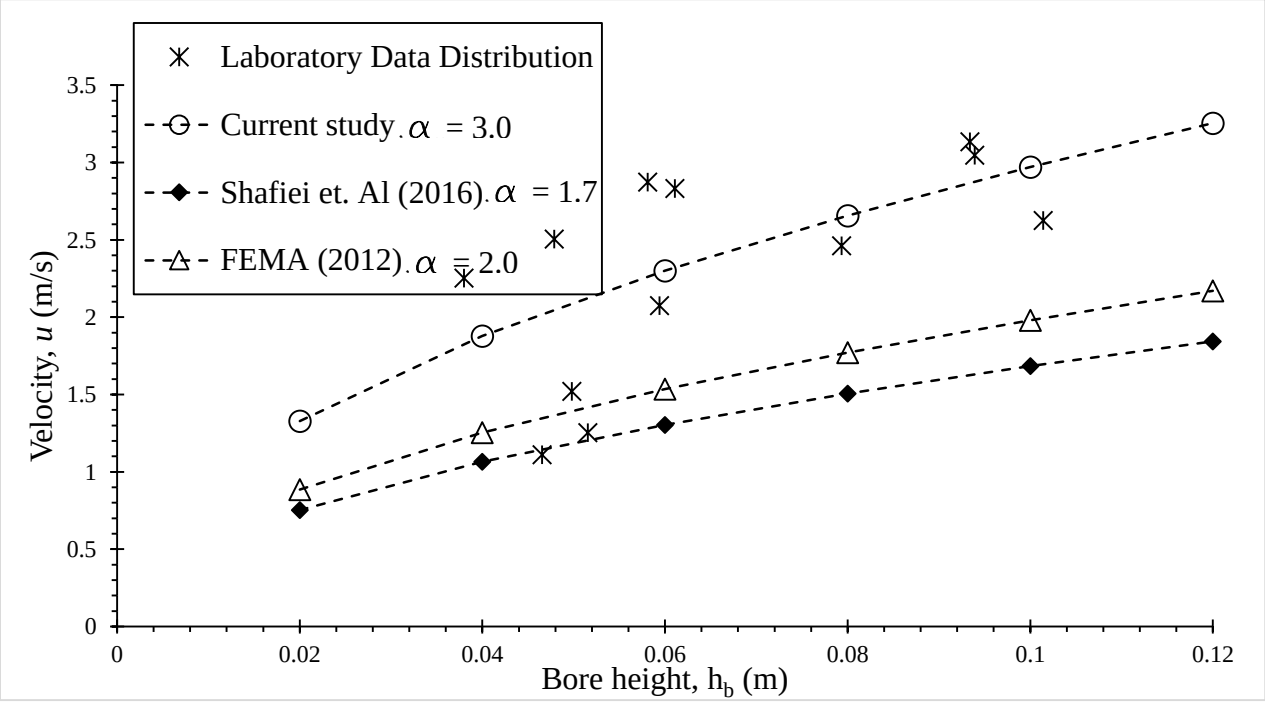

Figure 4.27: Velocity, *u* VS Bore height, h_b of the current study with value $\boldsymbol{a_u}$=3.0

4.5 Hydrodynamics and Wave loading of Newtonian fluid

In this section, 3 repetition were conducted in order to select the best repetition.

- **Newtonian flow at Probe 1**

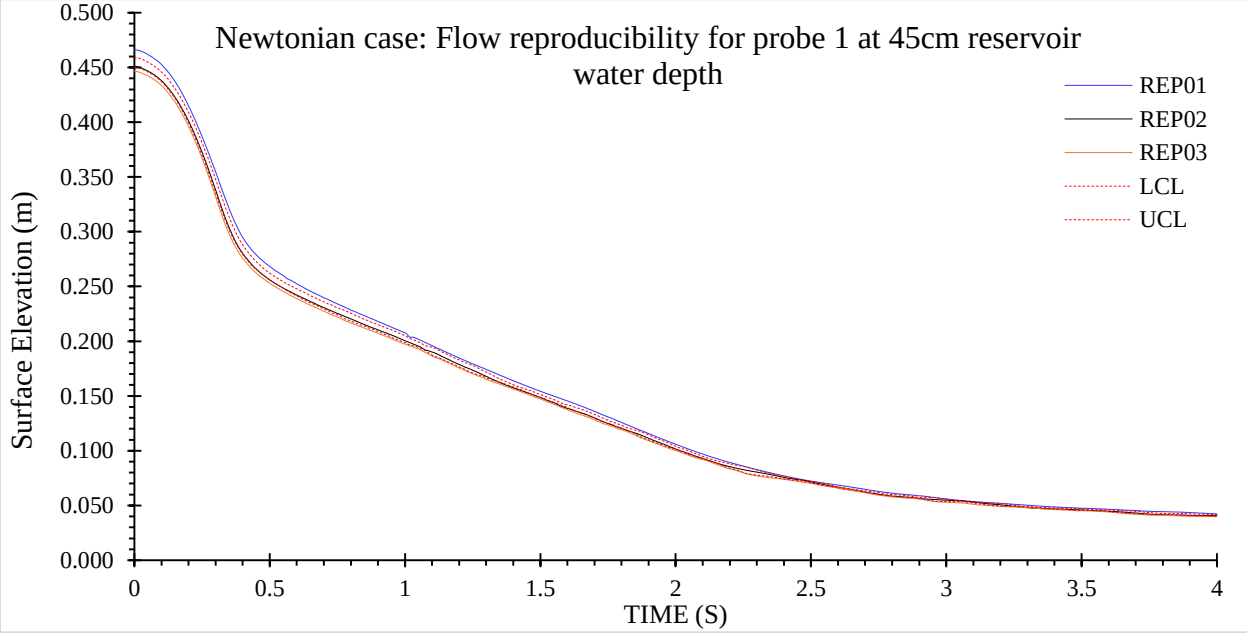

Figure 4.28: Surface Elevation VS Time for Newtonian Fluid at Probe 1

- **Newtonian flow at Probe 2**

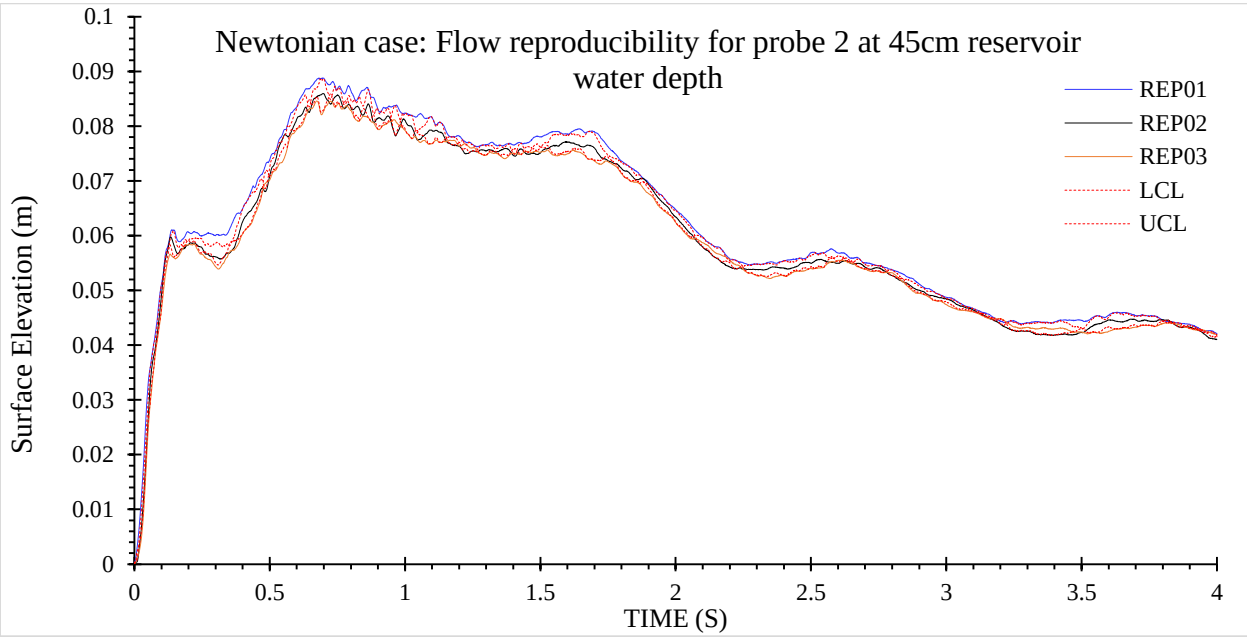

Figure 4.29: Surface Elevation VS Time for Newtonian Fluid at Probe 2

- **Newtonian flow at Probe 3**

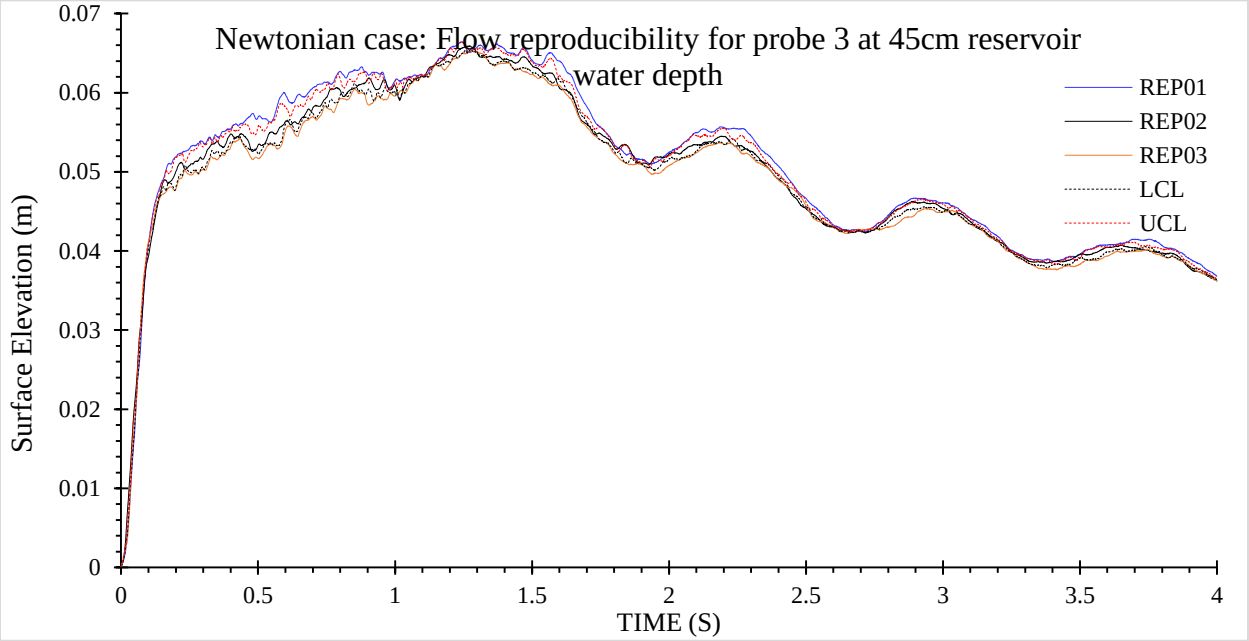

Figure 4.30: Surface Elevation VS Time for Newtonian Fluid at Probe 3

- **Newtonian flow at Probe 4**

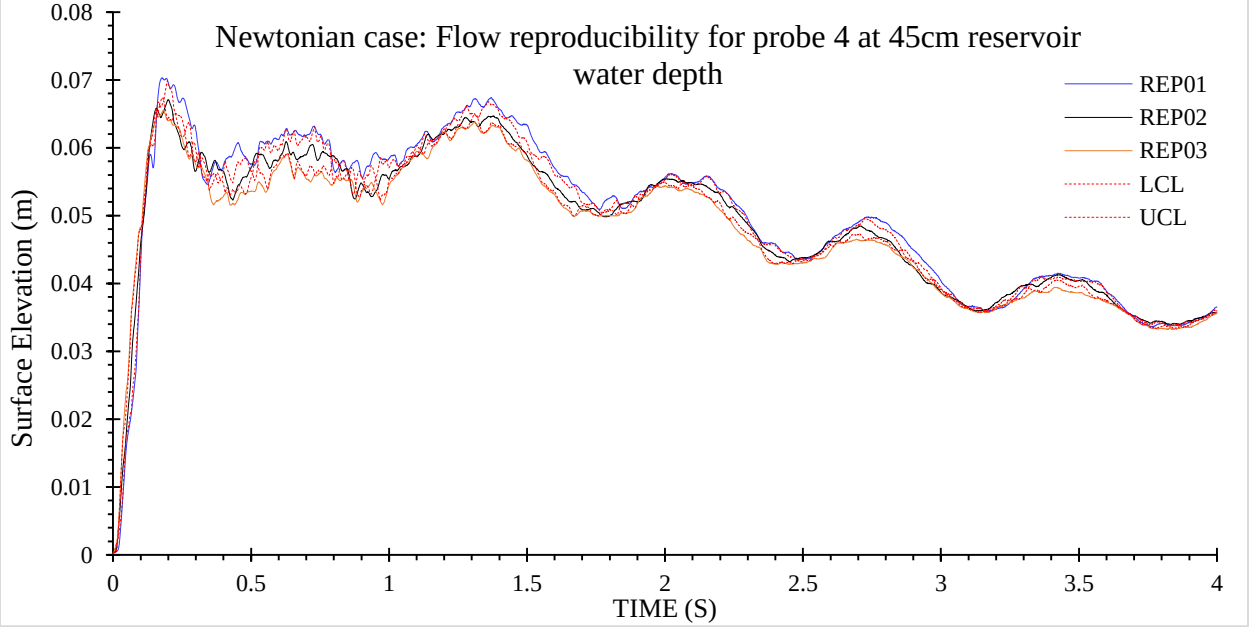

Figure 4.31: Surface Elevation VS Time for Newtonian Fluid at Probe 4

To identify the best repetition among the three repetition, the method of Upper Control Limit (UCL) and Lower Control Limit (LCL) is used. Whichever repetition lines that is able to maintain or stays inside the limit lines will be considered as the best repetition. In this case, the best repetition will be repetition 2 (REP02). Below are the graphs representing REP02 for all wired probes.

- Probe 1

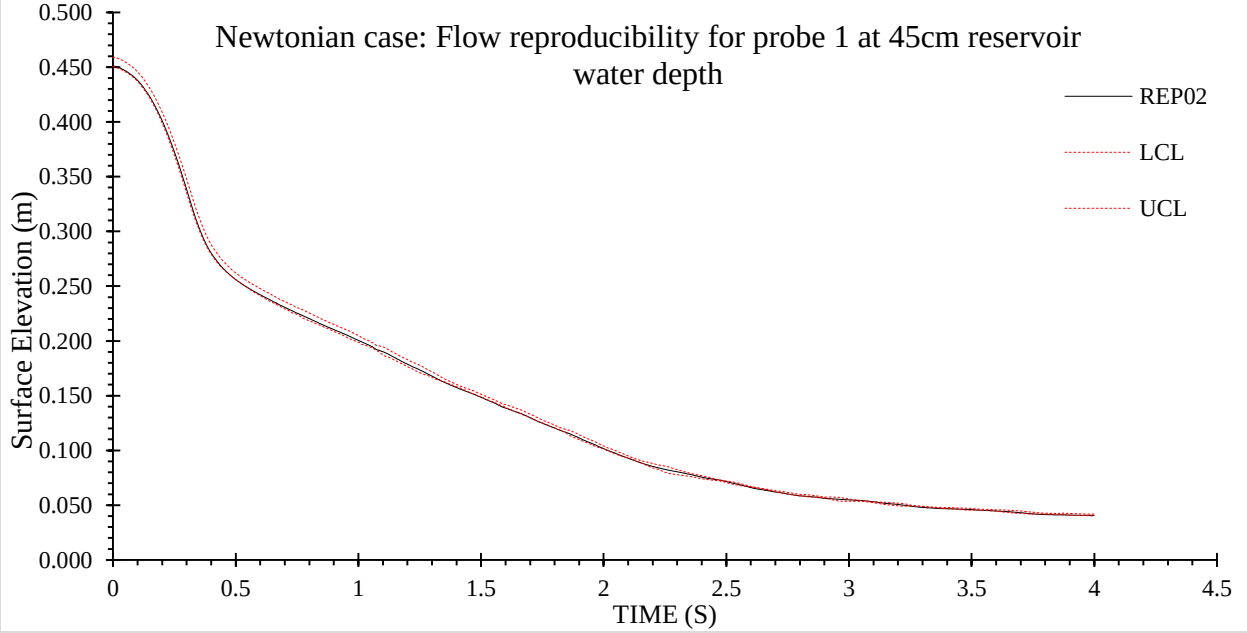

Figure 4.32: Surface Elevation VS Time for Newtonian Fluid at Probe 1 (REP02)

- Probe 2

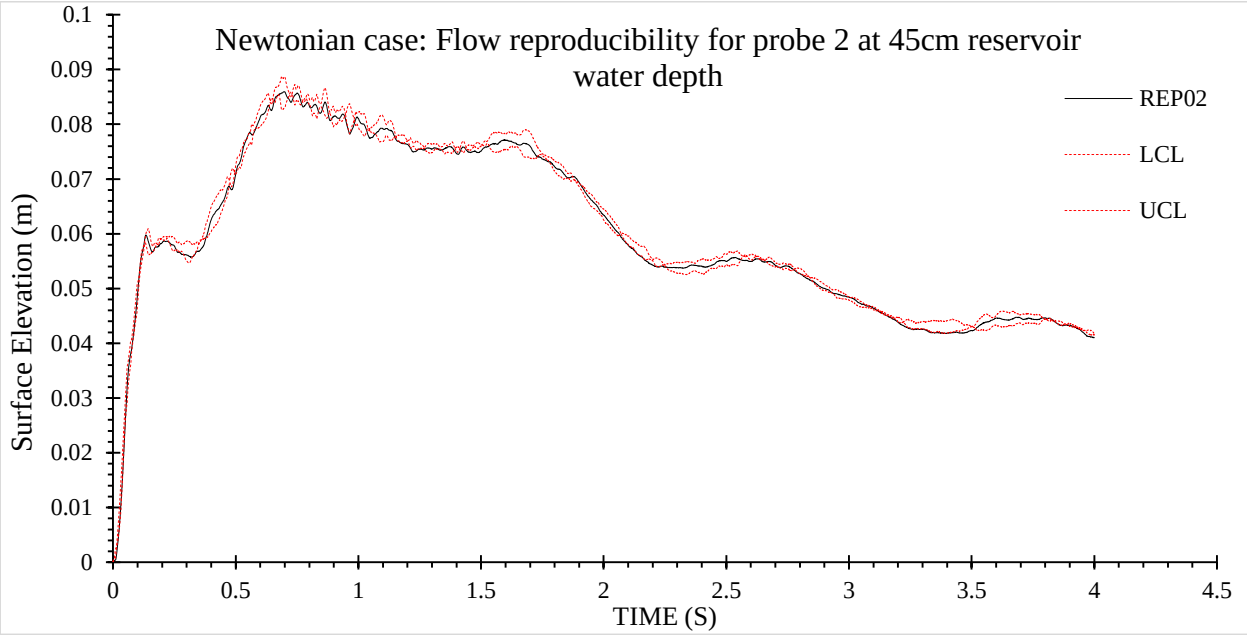

Figure 4.33: Surface Elevation VS Time for Newtonian Fluid at Probe 2 (REP02)

- Probe 3

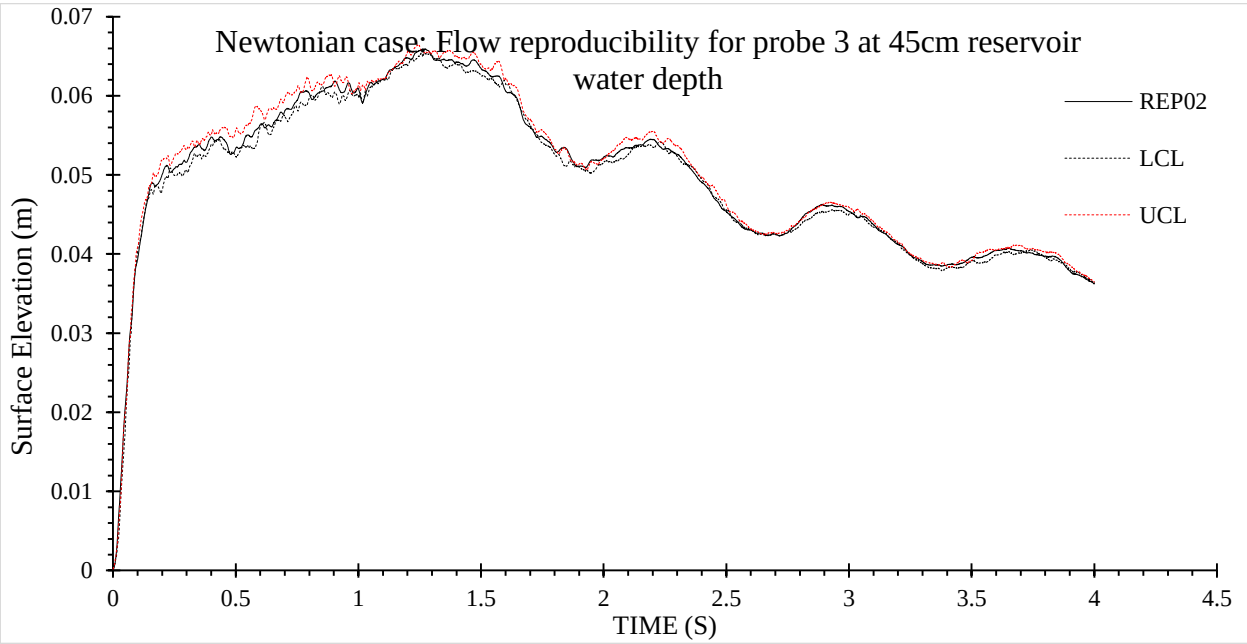

Figure 4.34: Surface Elevation VS Time for Newtonian Fluid at Probe 3 (REP02)

- Probe 4

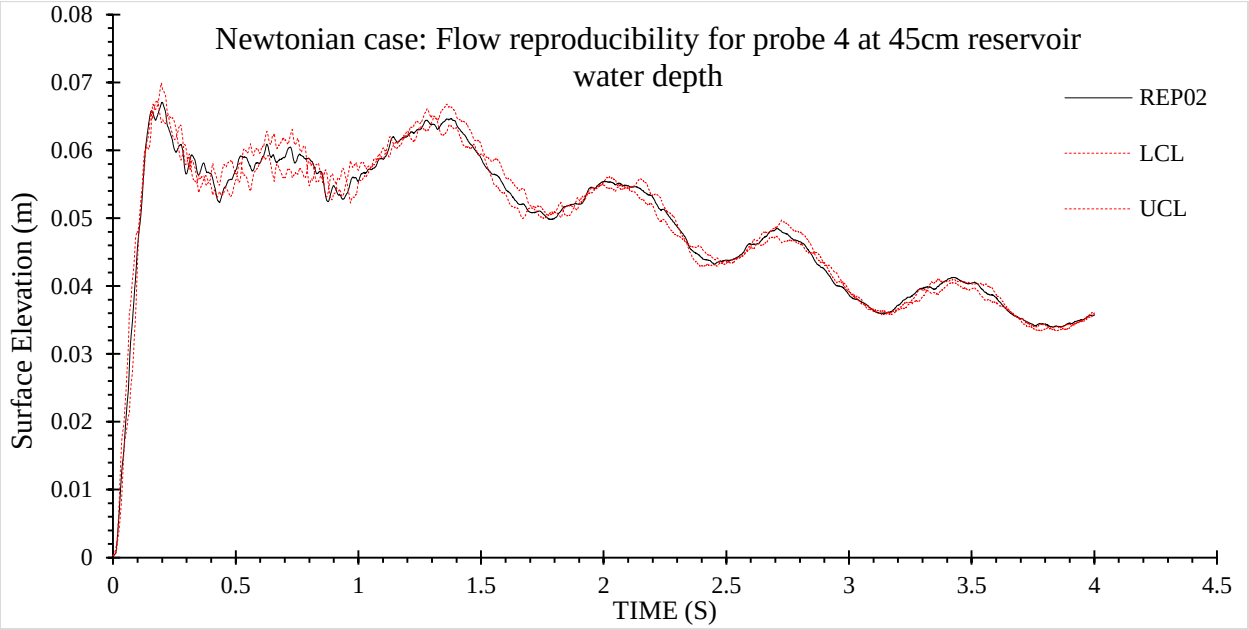

Figure 4.35: Surface Elevation VS Time for Newtonian Fluid at Probe 4 (REP02)

Velocity for this flow is tabulated as below:

Table 4.7: Velocity for Newtonian flow

	Sec1	Sec2	Sec3
Rep1	2.544529	2.923977	3.571429
Rep 2	2.463054	2.832861	2.873563
Rep 3	2.475248	2.849003	2.793296

4.5.1 Wave loading for Newtonian

- **Pressure Transducer 1**

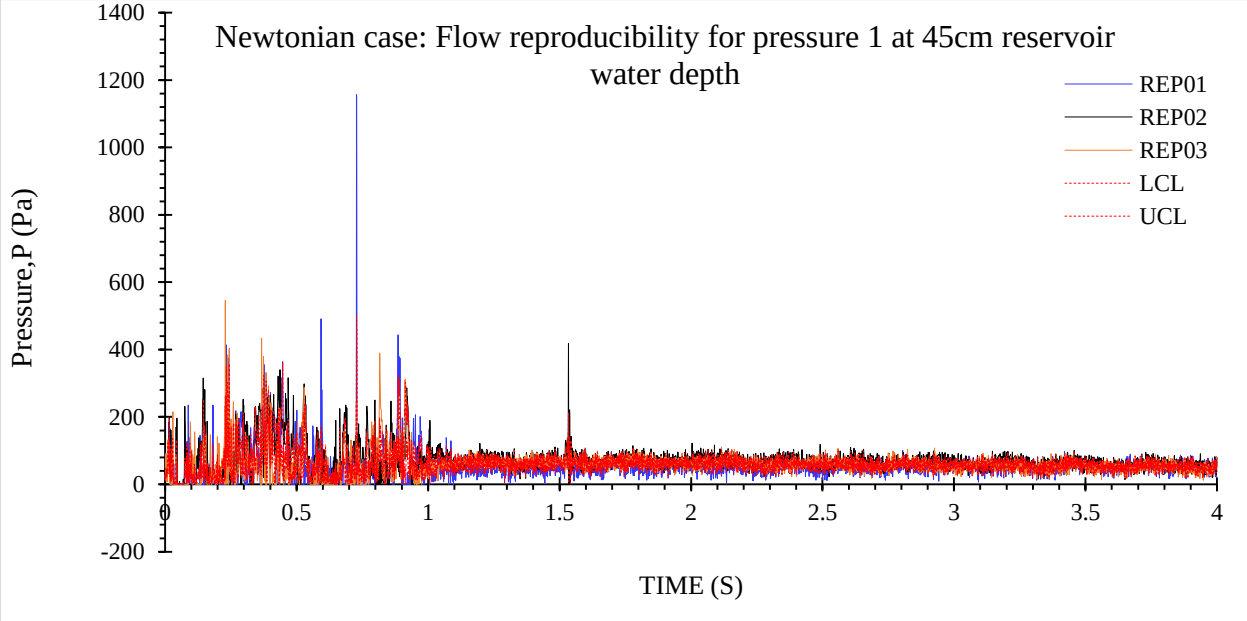

Figure 4.36: Pressure VS Time for Newtonian Fluid at PR-1

- **Pressure Transducer 2**

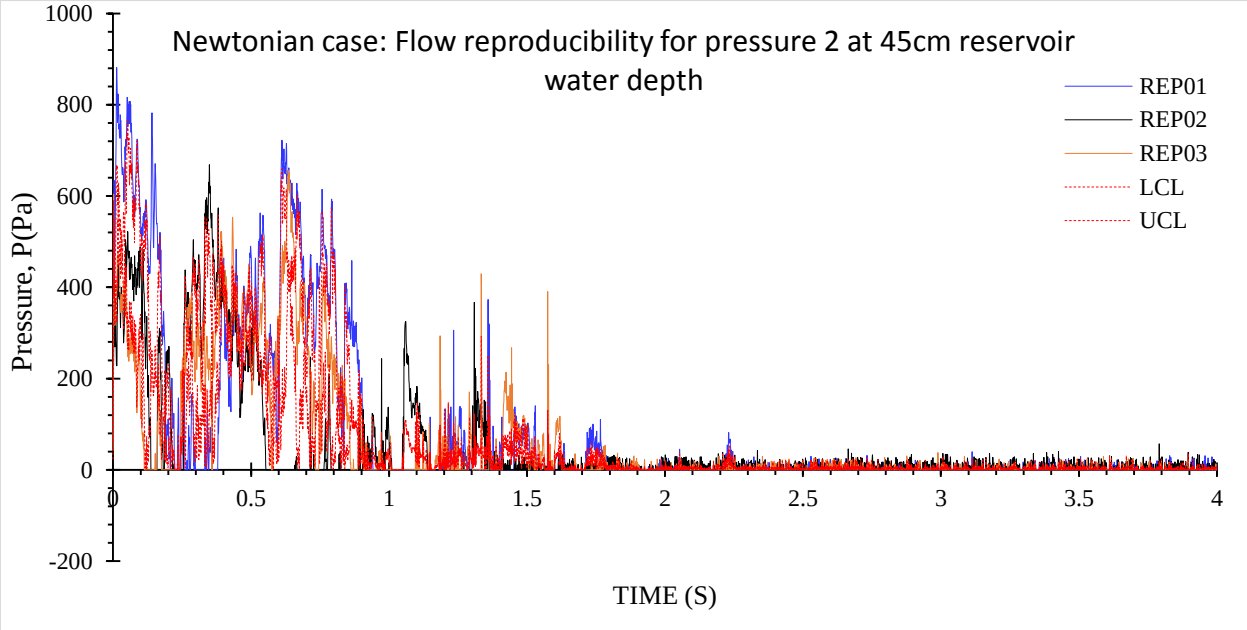

Figure 4.37: Pressure VS Time for Newtonian Fluid at PR-2

- **Pressure Transducer 3**

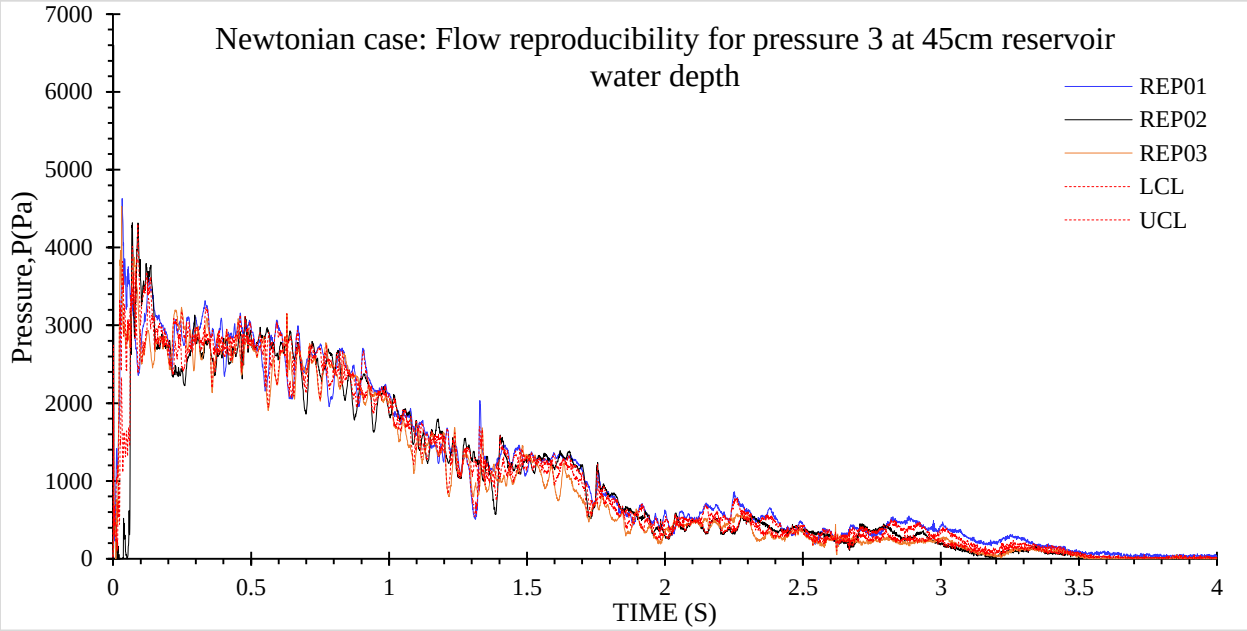

Figure 4.38: Pressure VS Time for Newtonian Fluid at PR-3

- **Pressure Transducer 4**

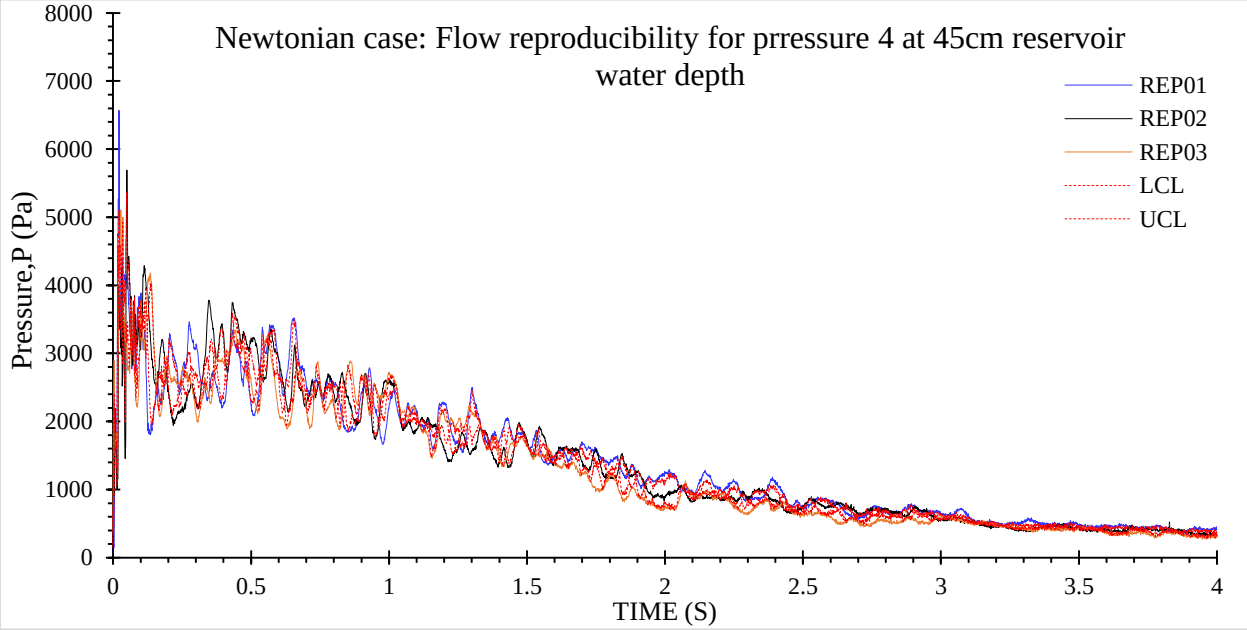

Figure 4.39: Pressure VS Time for Newtonian Fluid at PR-4

Since repetition 2 (REP02) was chosen for the Newtonian surface elevation, therefore for pressure against time, repetition 2 will also need to be used.

- Pressure Transducer 1

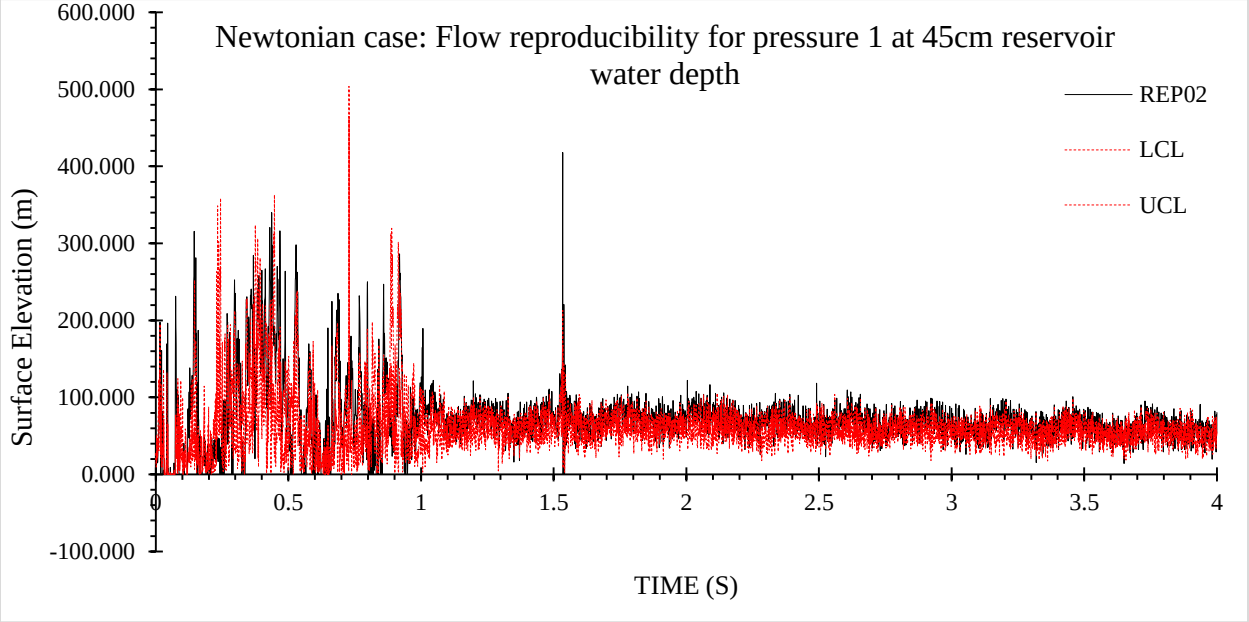

Figure 4.40: Pressure VS Time for Newtonian Fluid at PR-1 (REP02)

- Pressure Transducer 2

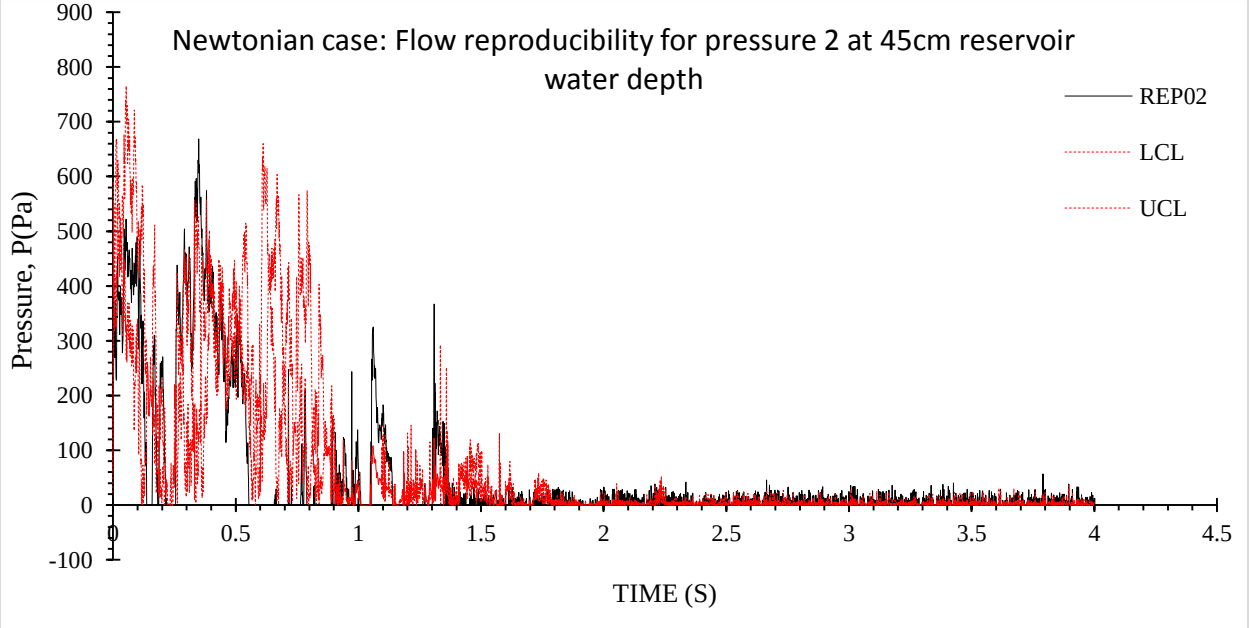

Figure 4.41: Pressure VS Time for Newtonian Fluid at PR-2 (REP02)

- Pressure Transducer 3

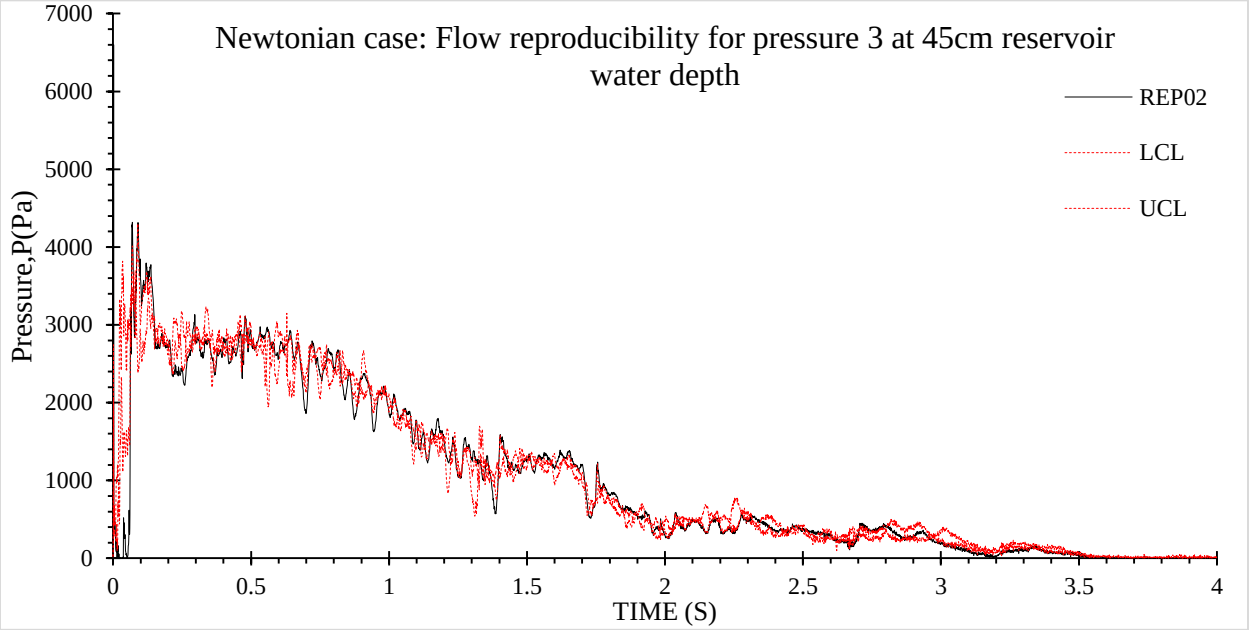

Figure 4.42: Pressure VS Time for Newtonian Fluid at PR-3 (REP02)

- Pressure Transducer 4

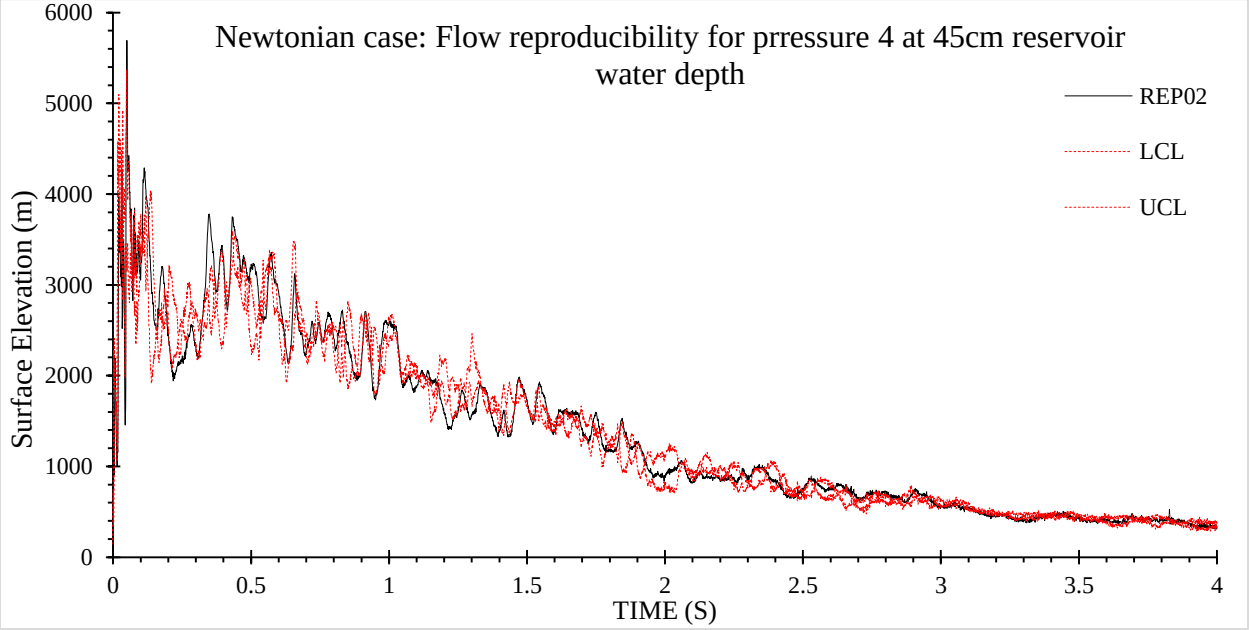

Figure 4.43: Pressure VS Time for Newtonian Fluid at PR-4 (REP02)

4.6 Hydrodynamics and Wave loading of non-Newtonian fluid

In this section, 3 repetition were conducted in order to select the best repetition.

- **Non-Newtonian flow at Probe 1**

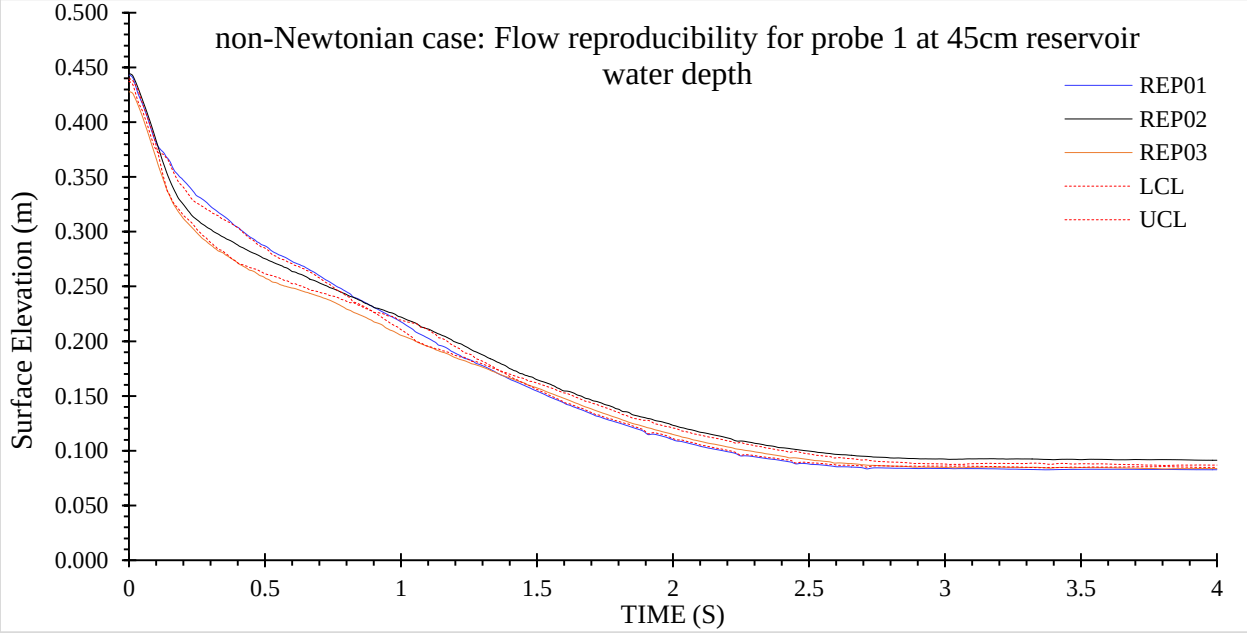

Figure 4.44: Surface Elevation VS Time for non-Newtonian Fluid at Probe 1

- **Non-Newtonian flow at Probe 2**

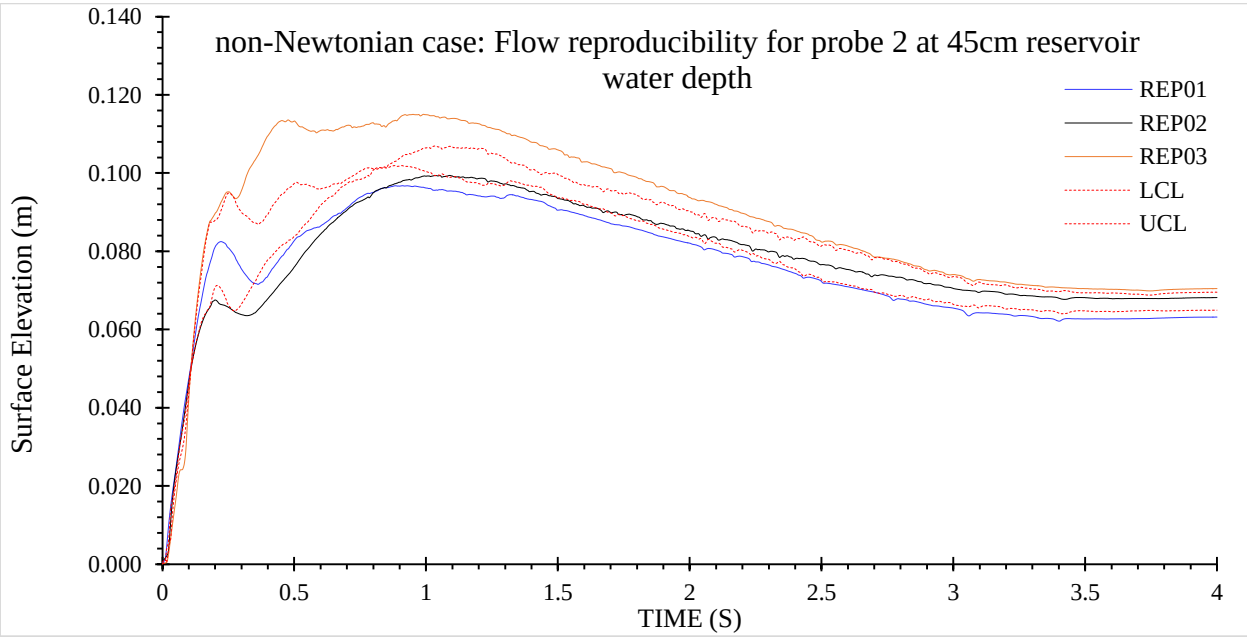

Figure 4.45: Surface Elevation VS Time for non-Newtonian Fluid at Probe 2

- **Non-Newtonian flow at Probe 3**

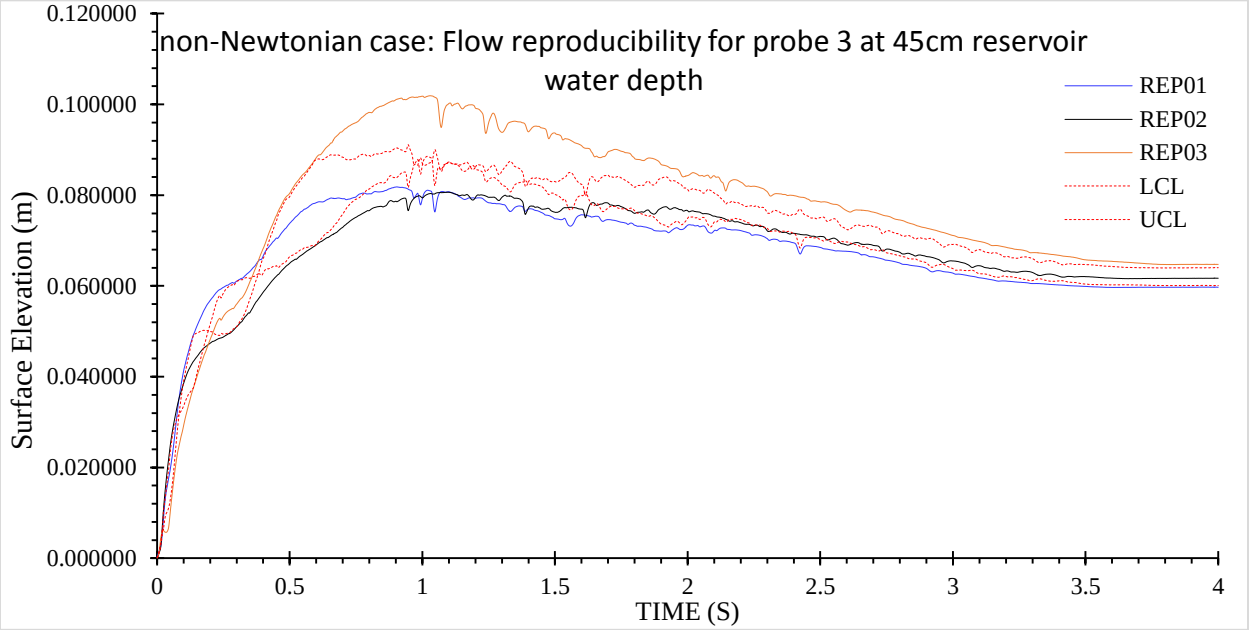

Figure 4.46: Surface Elevation VS Time for non-Newtonian Fluid at Probe 3

- **Non-Newtonian flow at Probe 4**

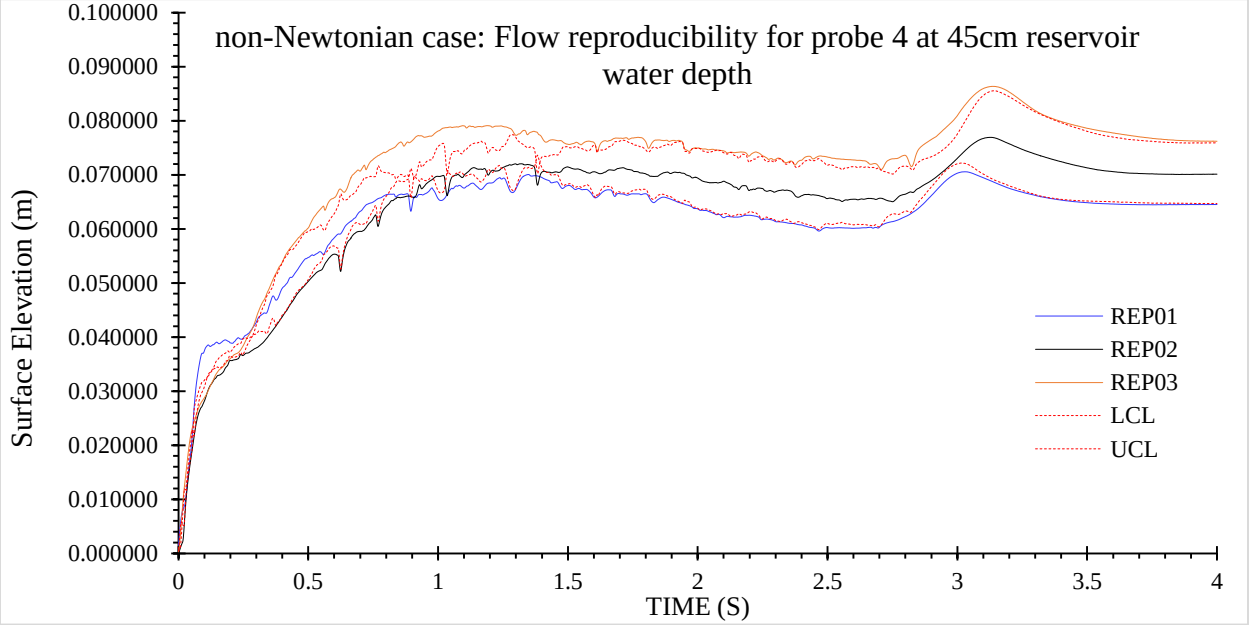

Figure 4.47: Surface Elevation VS Time for non-Newtonian Fluid at Probe 4

After careful observation and analysis of the graphs, repetition 1 (**REP01**) is the best repetition.

- Probe 1

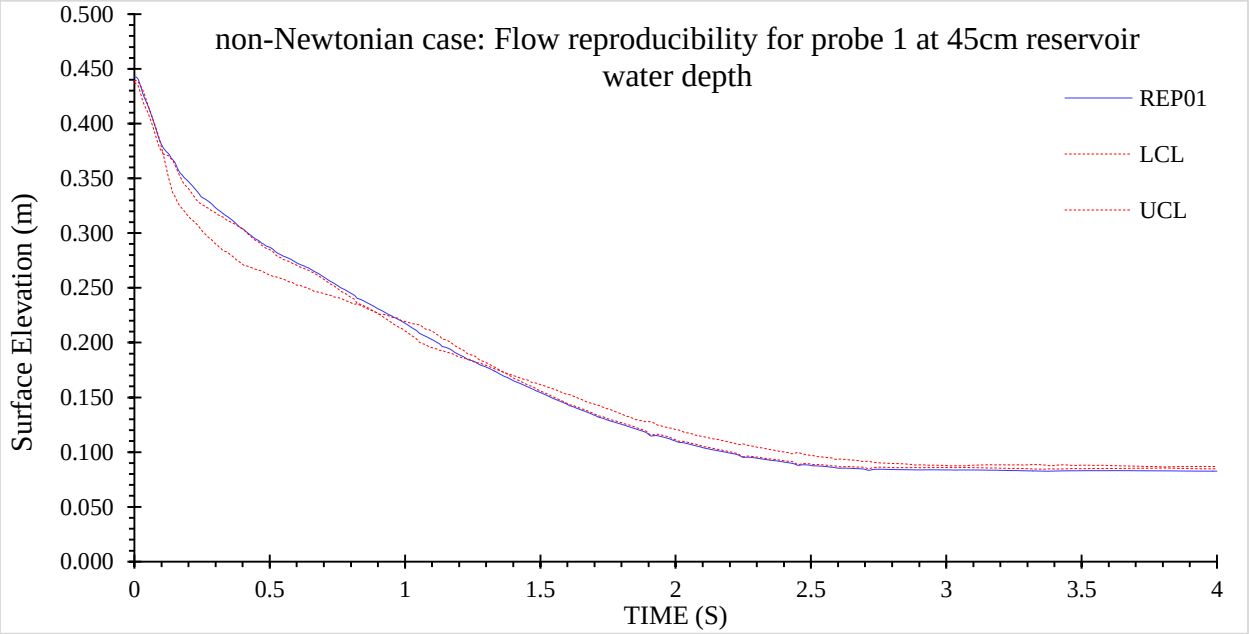

Figure 4.48: Surface Elevation VS Time for non-Newtonian Fluid at Probe 1 (REP01)

- Probe 2

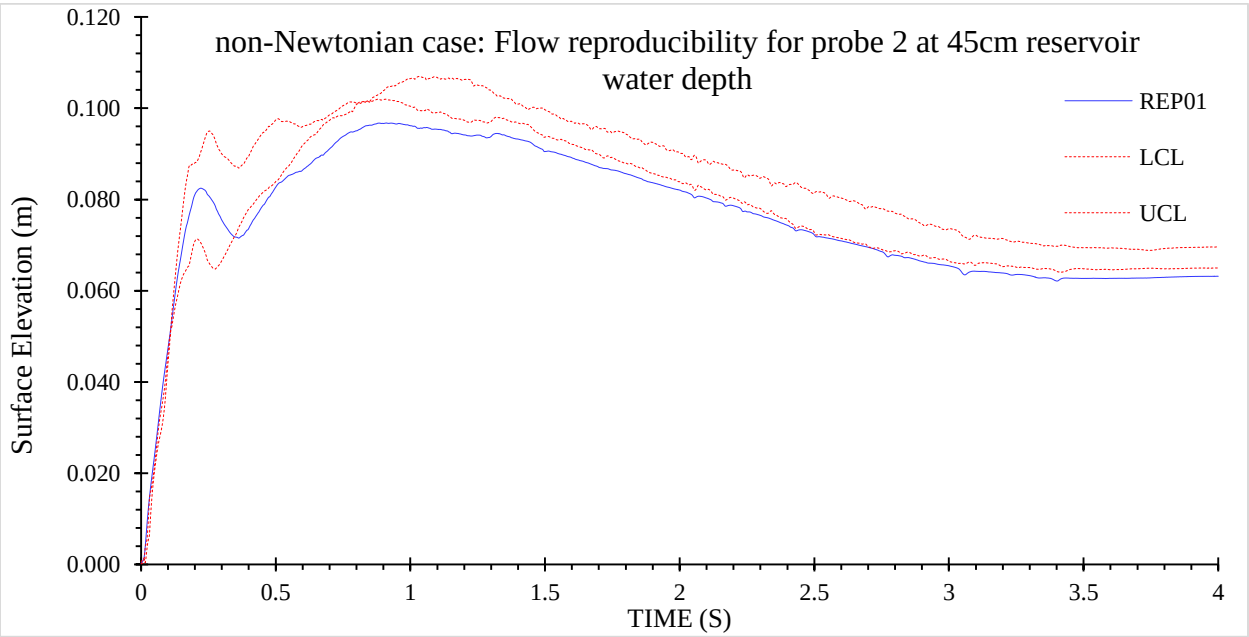

Figure 4.49: Surface Elevation VS Time for non-Newtonian Fluid at Probe 2 (REP01)

- Probe 3

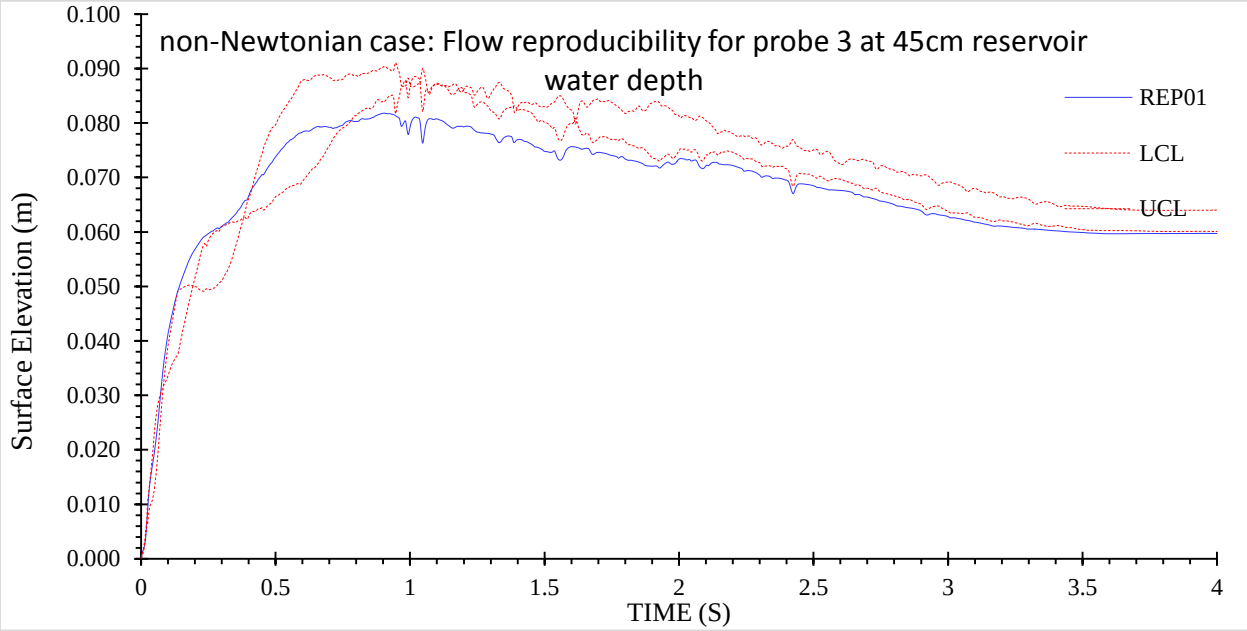

Figure 4.50: Surface Elevation VS Time for non-Newtonian Fluid at Probe 3 (REP01)

- Probe 4

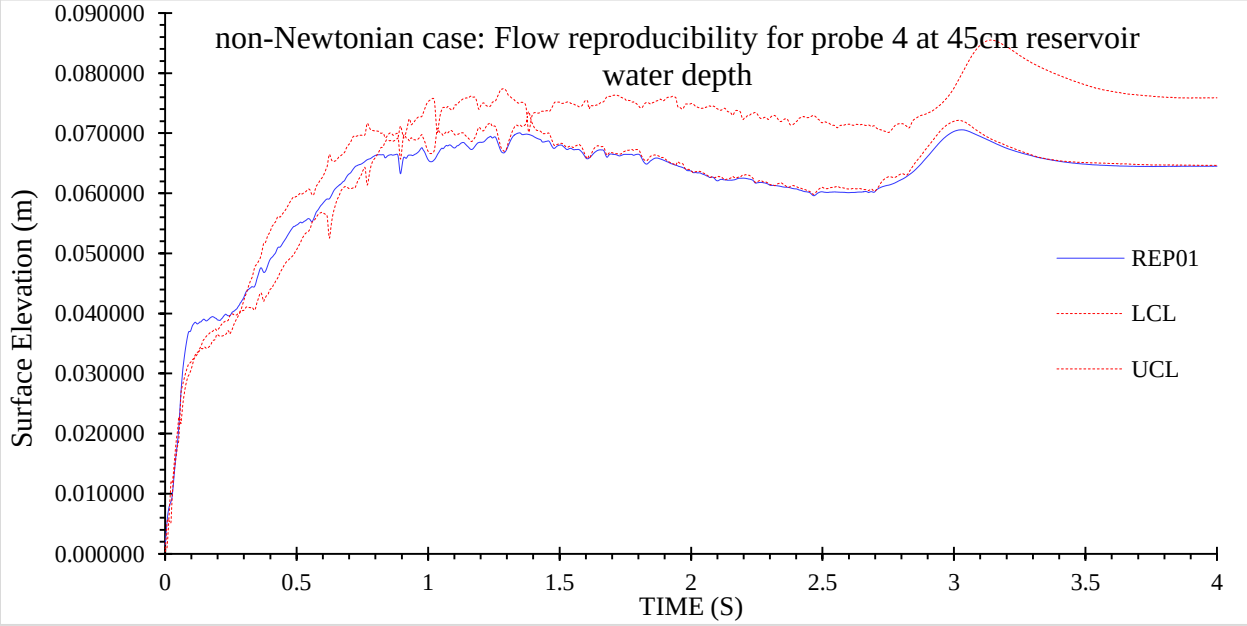

Figure 4.51: Surface Elevation VS Time for non-Newtonian Fluid at Probe 4 (REP01)

4.6.1 Wave loading of non-Newtonian fluid

- **Pressure Transducer 1**

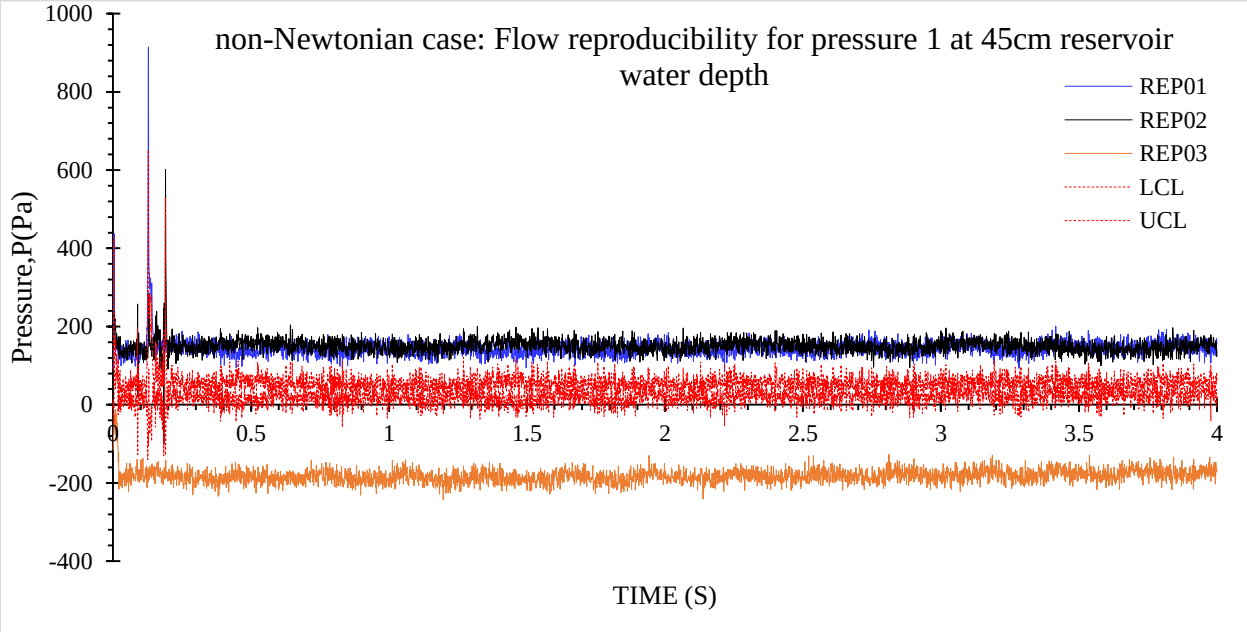

Figure 4.52: Pressure VS Time for non-Newtonian Fluid at PR-1

- **Pressure Transducer 2**

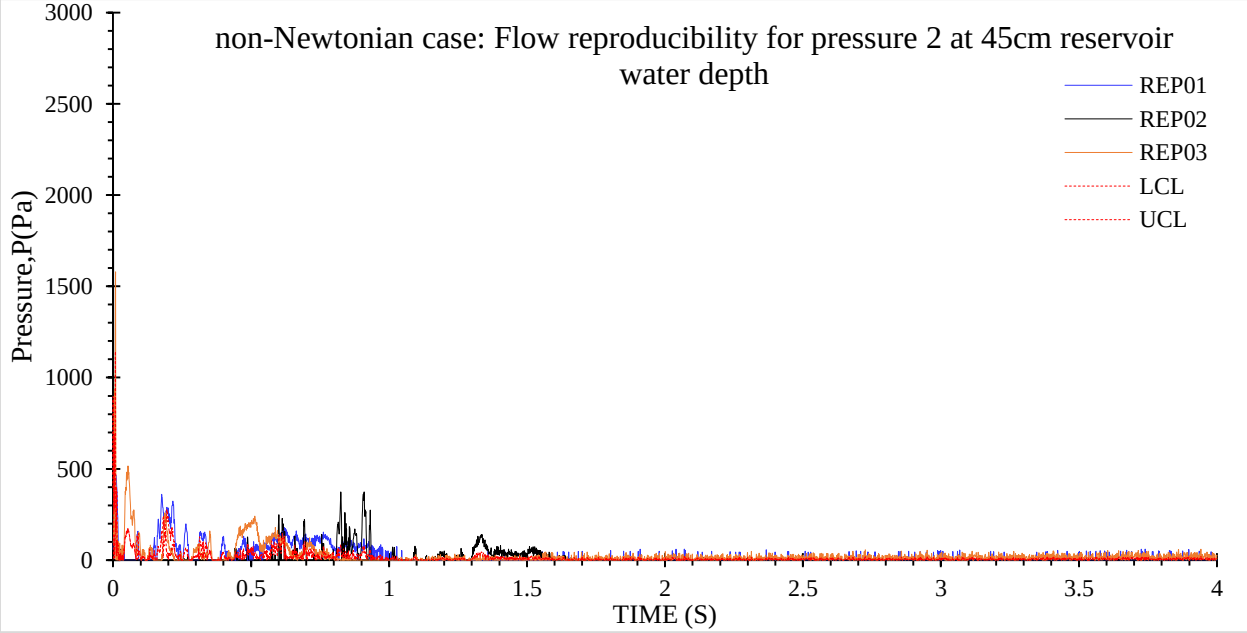

Figure 4.53: Pressure VS Time for non-Newtonian Fluid at PR-2

- **Pressure Transducer 3**

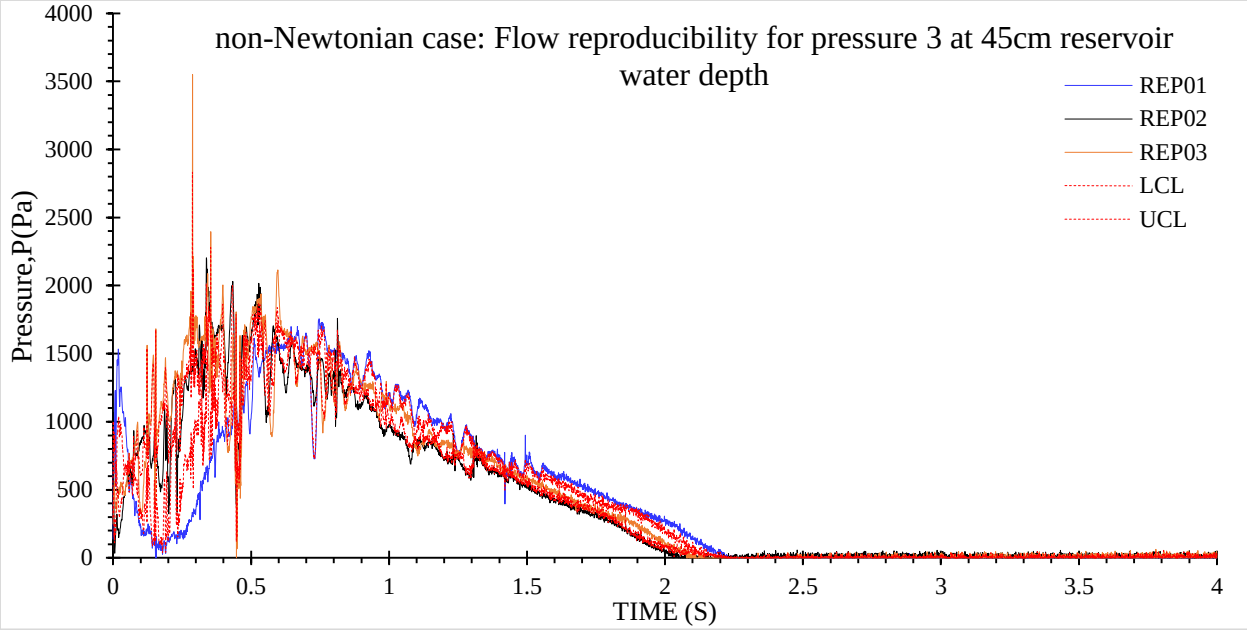

Figure 4.54: Pressure VS Time for non-Newtonian Fluid at PR-3

- **Pressure Transducer 4**

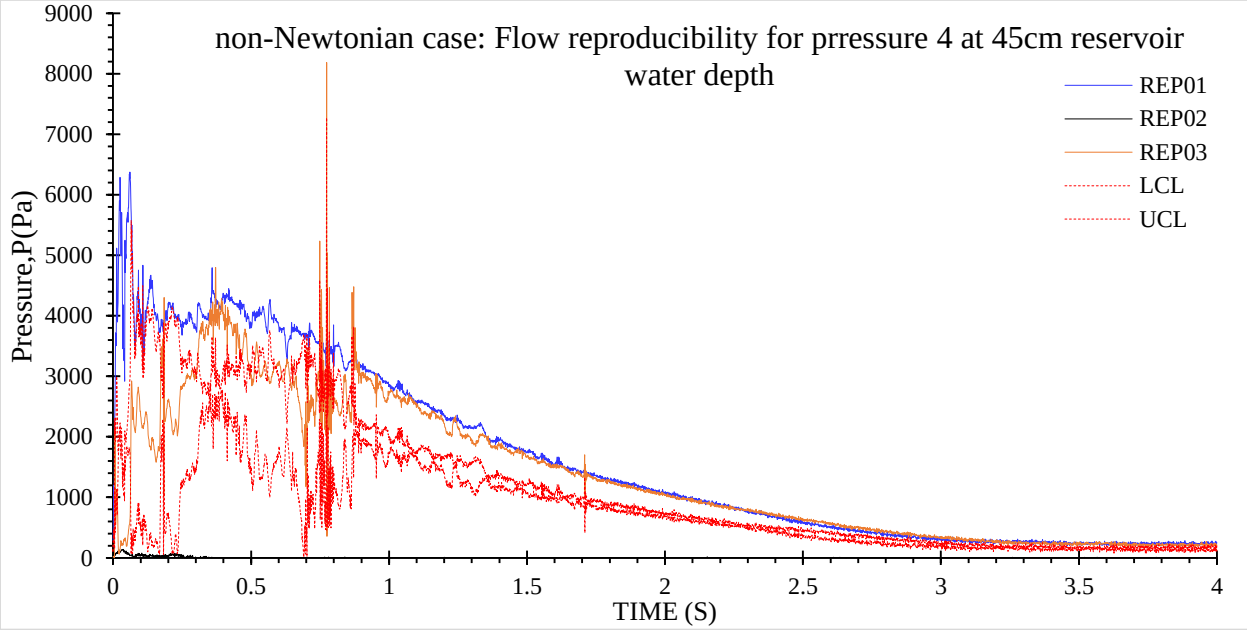

Figure 4.55: Pressure VS Time for non-Newtonian Fluid at PR-4

Since repetition 1 is selected from the non-Newtonian flow, therefore, repetition 1 from pressure will be also be chosen as well.

- Pressure Transducer 1

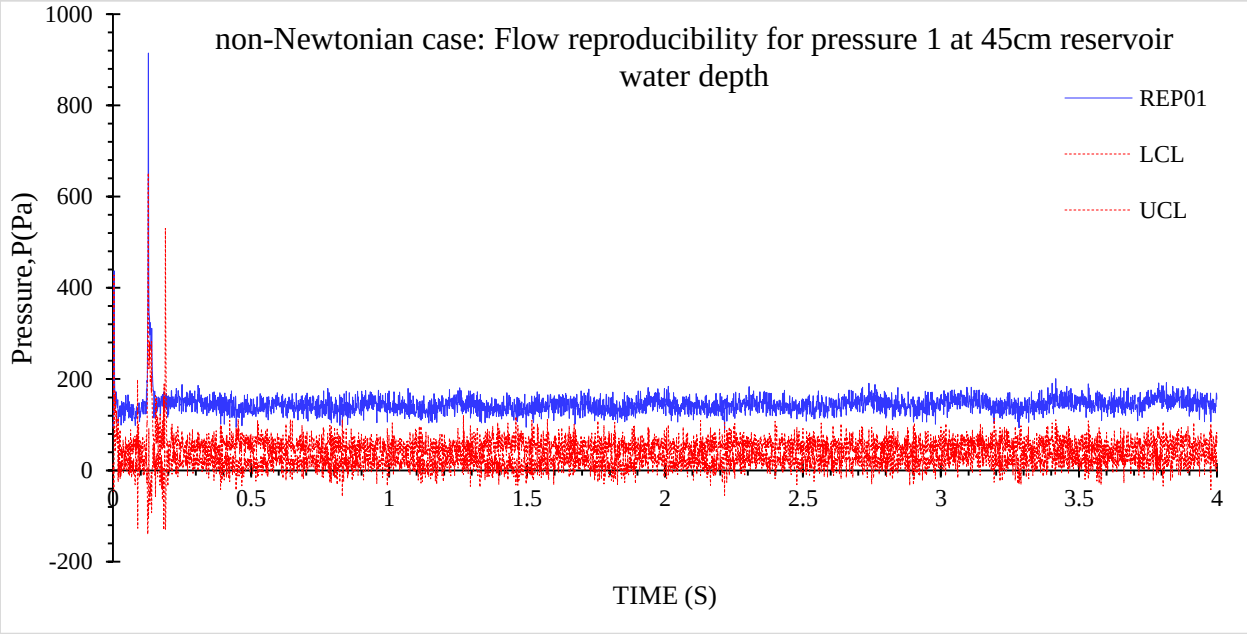

Figure 4.56: Surface Elevation VS Time for non-Newtonian Fluid at Probe 1 (REP01)

- Pressure Transducer 2

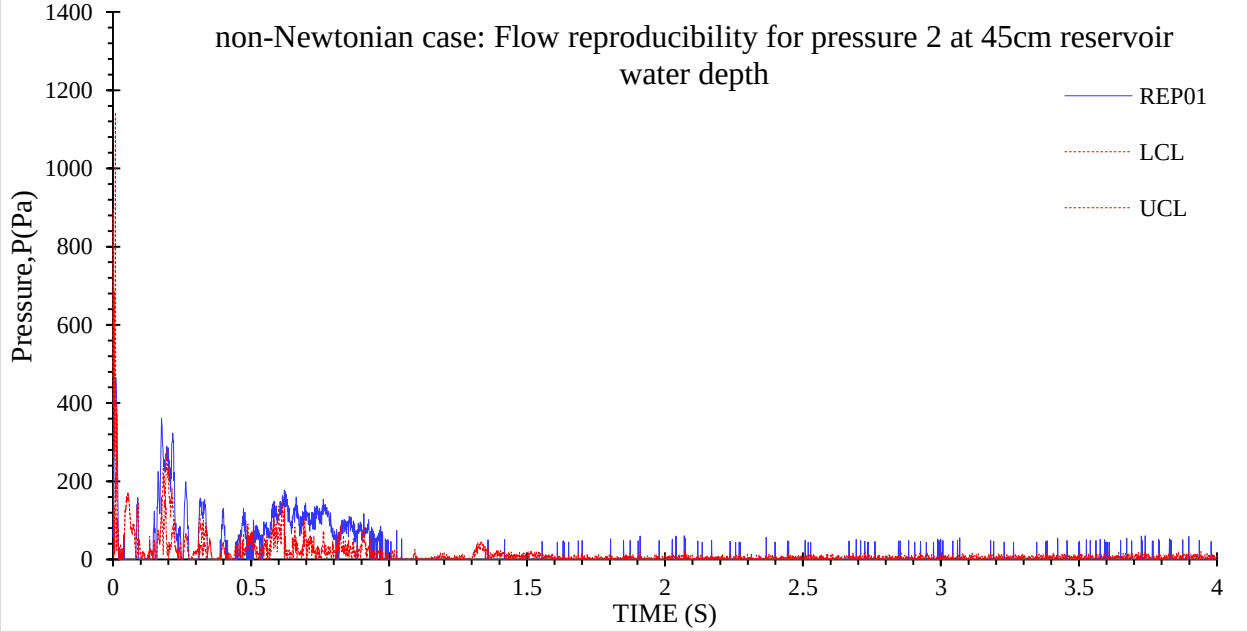

Figure 4.57: Surface Elevation VS Time for non-Newtonian Fluid at Probe 2 (REP01)

- Pressure Transducer 3

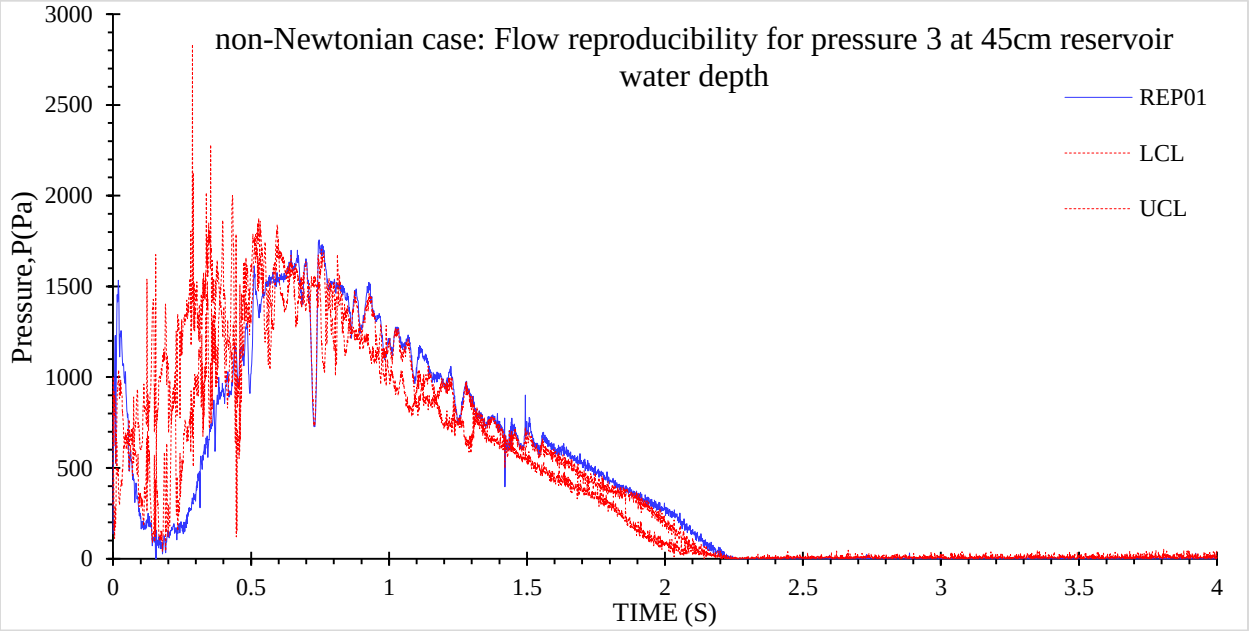

Figure 4.58: Surface Elevation VS Time for non-Newtonian Fluid at Probe 3 (REP01)

- Pressure Transducer 4

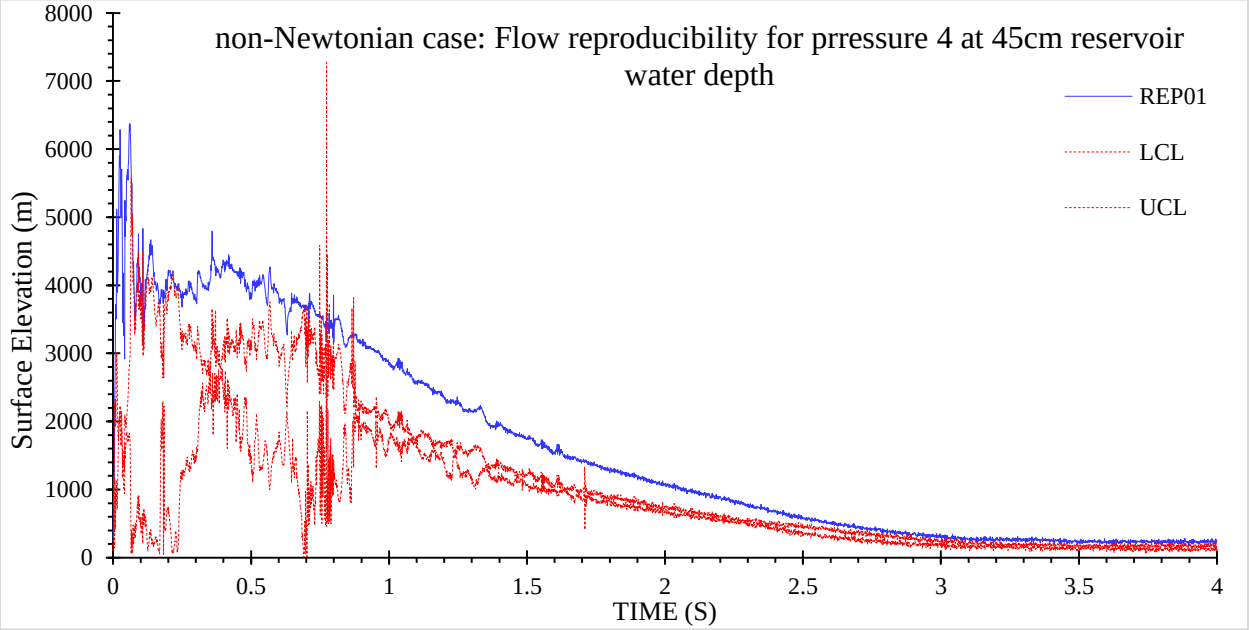

Figure 4.59: Surface Elevation VS Time for non-Newtonian Fluid at Probe 4 (REP01)

4.7 NEWTONIAN AND NON-NEWTONIAN COMPARISON

- **Flow Comparison**

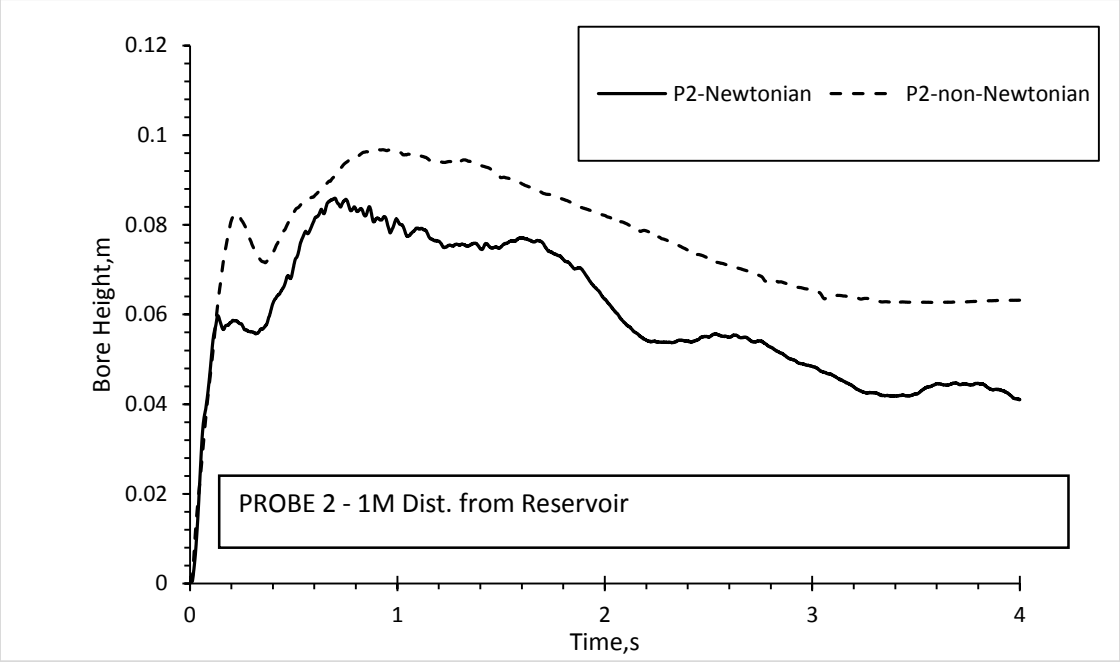

Figure 4.60: Flow comparison between Newtonian and non-Newtonian at Probe 2

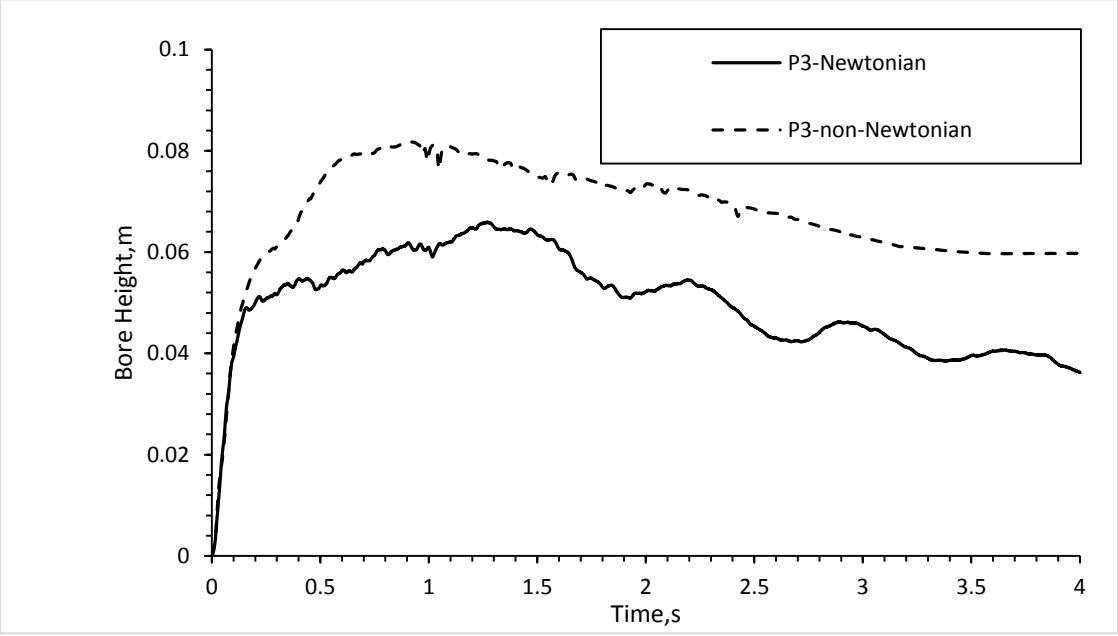

Figure 4.61: Flow comparison between Newtonian and non-Newtonian at Probe 3

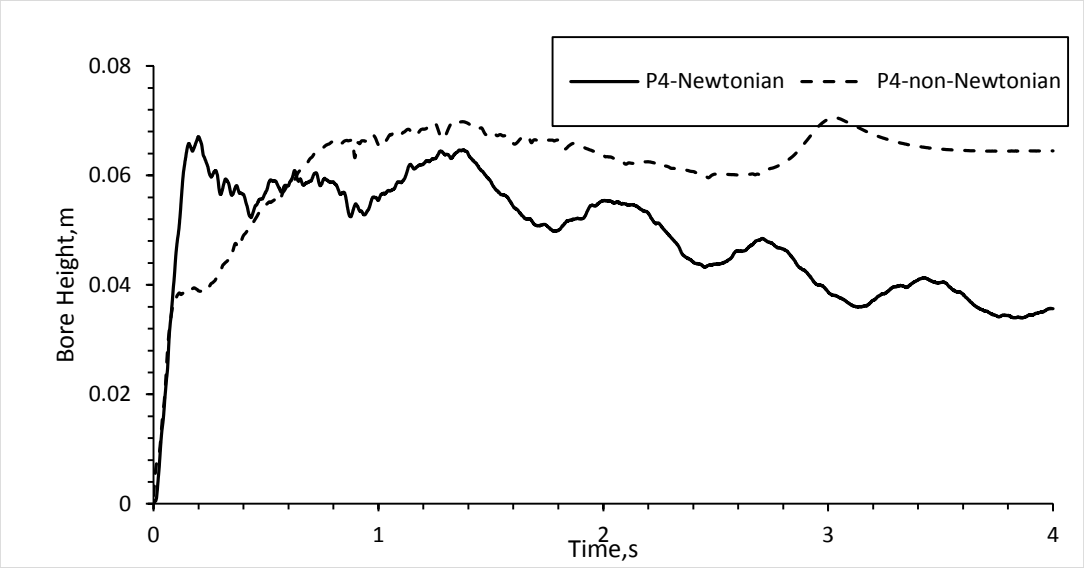

Figure 4.62: Flow comparison between Newtonian and non-Newtonian at Probe 4

By observing the pattern of the graph shown by Newtonian and non-Newtonian, both of them decreases throughout the time period. However, Newtonian graph decreases more drastically compared to non-Newtonian fluid. This is due to non-Newtonian being able to maintain its propagating body throughout the flume tank. Newtonian fluid shown to be experiencing wave breaking at the front part, therefore as soon as it passes the wave probe, the front part was at its highest height, then decreases greatly. Meanwhile for non-Newtonian, the height seems to be slightly maintained before and after it passes the wave probe. Which explains the small decreasing compared to Newtonian.

- Pressure Comparison

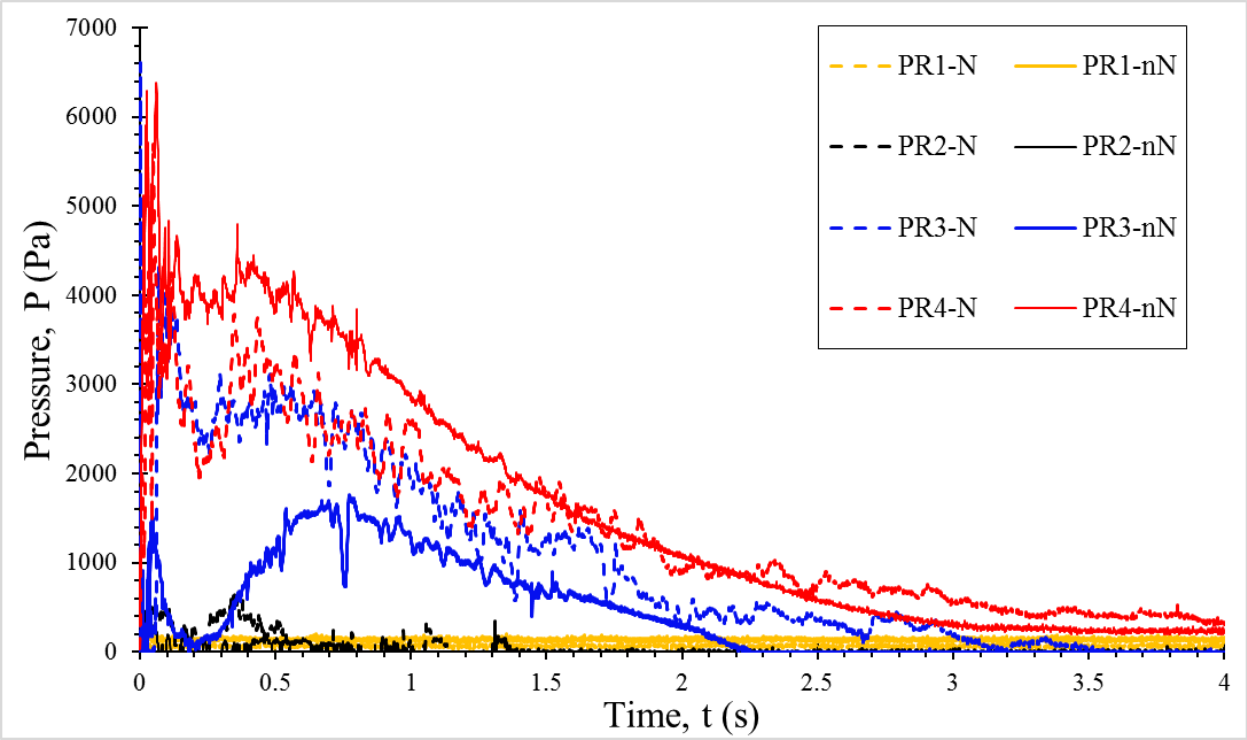

Figure 4.63: Pressure comparison between Newtonian and non-Newtonian fluid

Based on the graph, it is shown that non-Newtonian fluid produces a higher amount of pressure at PR-4 compared to Newtonian fluid. The differences between the pressure caused by non-Newtonian fluid at PR-3 and PR-4 is quite significant. This might be due to non-Newtonian fluid did not caused higher wave run-up and hits only the bottom part of the structure the most. Compared to Newtonian, PR-3 and PR-4 shows a little similarity on the pressure. This means that the wave probably caused a high wave run-up and hits both of the two transducers.

- Velocity Comparison

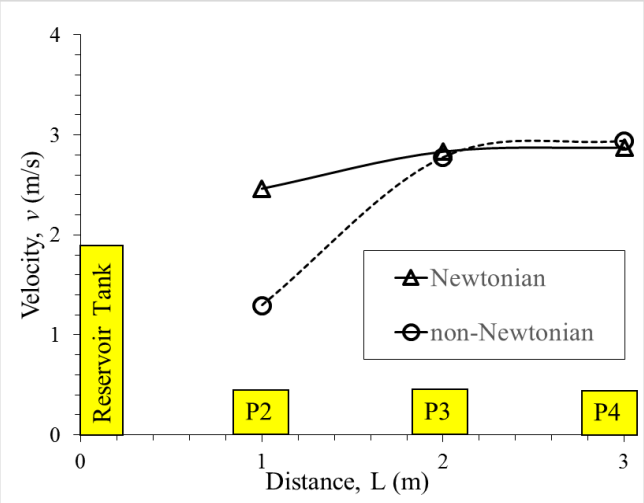

Figure 4.64: Velocity comparison between Newtonian and non-Newtonian

At L=1m, the velocity of non-Newtonian fluid at probe 2 seems to be more slowly compared to the velocity produced by Newtonian fluid. However, both fluid starts to be almost at the same pace once it reaches probe 3 and probe 4 which is at L=2m and L=3m respectively. The velocity produced by non-Newtonian at the end of the probe is just slightly lower than Newtonian fluid.

- Impulsive Pressure Comparison

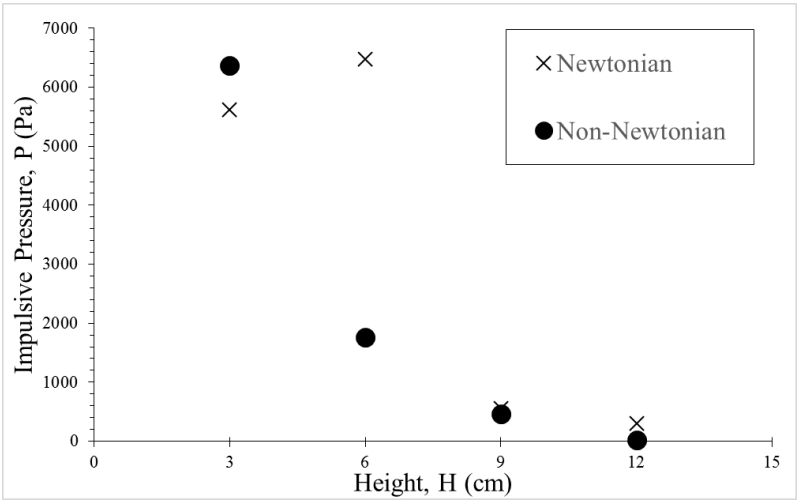

Figure 4.65: Comparison of Impulsive Pressure between Newtonian fluid and non-Newtonian fluid

By referring to figure 4.64, non-Newtonian fluid produced a high reading of pressure compared to Newtonian fluid at a height of H=3cm. The impulsive pressure decreases greatly as the height increases. For Newtonian, despite its ability to produce a lower impulsive pressure at the height of 3cm, it produces the highest impulsive force at the height of H=6cm. Which then decreases drastically, the higher the height goes.

CHAPTER 5

CONCLUSION & RECOMMENDATION

This section focuses on the conclusion that can be made from the results retrieved from the experiment. Recommendations is also included in this chapter aiming to produce a better performance of the experiment into producing a more proficient results.

5.1 Conclusion

As a result of conducting this research, it has proven that non-Newtonian produced a significant difference of outcome when comparing to Newtonian fluid. The bore height for both fluid decreases with respect to time. However the bore height produced by the non-Newtonian fluid decreases lesser compared to Newtonian fluid. For velocity, despite the fact that non-Newtonian fluid started off with a slower velocity at first, both in the end achieved the same velocity with respect to distance.

The wave impact produced from both of the fluid is the main criteria which highlights the differences between the two different fluids. Non-Newtonian fluid produced a significant amount of pressure upon impact compared to Newtonian fluid. The same goes for impulsive pressure as well.

Therefore, it is proven that non-Newtonian fluid indeed shows a significant difference in the hydrodynamics of the bore and the wave loadings upon impact on a vertical rectangular structure. Since the current design of coastal structures are all based solely on tsunami waves in a form of Newtonian fluid, another desk study on apprehending a new design based on non-Newtonian fluid should be considered in order to help reinforcing the current structural design against tsunami attack.

This research is meant to contribute to the existing knowledge and guidelines for designing in coastal engineering. With all of the results obtained from this research, hopefully the engineers and designers will make good use of this information to form a more robust design and contribute additional guidelines in the design of coastal structures or breakwaters to minimize the massive destruction that can be caused by tsunami.

5.2Recommendation

For this section, recommendations are highlighted in order to improve the current equipment and provided laboratory facilities in order to retrieve more efficient data collection and also reduce time consumption for conducting experiment.

1) Width of the flume tank should me more widened in order to avoid fluid reflected to the walls of the flume tank. During the experiment, the flow of the water seems to be reflected towards the wall which compromises the person's view as the non-Newtonian fluid covers up the wall of the flume tank.

2) Wired probe should be a recommended choice to be used to record the reading of the wave height due to its small thickness that reduces the surface run-up of the probe and also avoid the formation of the void surrounding the probe. Due to the narrow width of the flume tank, the typical design of the wave probe would disrupt the flow with its thickness.

3) A larger mixer is more recommended in order to mix and produce a larger amount of non-Newtonian fluid to be used in the experiment. The current size of the mixer causes the mixing activity to be prolonged which causes delay on the milestones.

REFERENCES

Jet Propulsion Laboratory, (2005)
http://www.jpl.nasa.gov/spaceimages/details.php?id=PIA04373

Barbara Ferreira (April 17, 2011). "When icebergs capsize, tsunamis may ensue". Nature. Retrieved 2011-04-27.

Jet Propulsion Laboratory, (2011) http://www.jpl.nasa.gov/news/news.php?release=2011-374

Fradin, Judith Bloom and Dennis Brindell (2008). Witness to Disaster: Tsunamis. Witness to Disaster. Washington, D.C.: National Geographic Society. pp. 42, 43.

Merriam Webster, (1851)
http://www.merriam-webster.com/dictionary/tidal%20wave

"Tidal", the American Heritage Stedman's Medical Dictionary. Houghton Mifflin Company. 11 November 2008.Dictionary.reference.com

-al. (n.d.). Dictionary.com Unabridged (v 1.1). Retrieved November 11, 2008, Dictionary.reference.com

The Caribbean Disaster Emergency Management Agency: Tsunami Smart: Glossary

Tsunamis,1992 http://earthsci.org/education/teacher/basicgeol/tsumami/tsunami.html

Haugen, K; Lovholt, F; Harbitz, C (2005). "Fundamental mechanisms for tsunami generation by submarine mass flows in idealised geometries". Marine and Petroleum Geology 22 (1–2): 209–217. doi:10.1016/j.marpetgeo.2004.10.016.

Margaritondo, G (2005). "Explaining the physics of tsunamis to undergraduate and non-physics students". European Journal of Physics 26 (3): 401. Bibcode: 2005EJPh...26..401M. doi:10.1088/0143-0807/26/3/007.

Lynnes, C. S.; Lay, T. (1988), "Source Process of the Great 1977 Sumba Earthquake" (PDF), Geophysical Research Letters (American Geophysical Union) 93 (B11): 13,407–13,420, Bibcode: 1988JGR....9313407L, doi: 10.1029/JB093iB11p13407

George Pararas-Carayannis (1999). "The Mega-Tsunami of July 9, 1958 in Lituya Bay, Alaska". Retrieved 2014-02-27.

Petley, Dave (Professor) (2008-12-11). "The Vaiont (Vajont) landslide of 1963". The Landslide Blog. Retrieved 2014-02-26.

Pararas-Carayannis, George (2002). "Evaluation of the threat of mega tsunami generation from postulated massive slope failures of the island volcanoes on La Palma, Canary Islands, and on the island of Hawaii". Science of Tsunami Hazards 20 (5): 251–277. Retrieved 7 September 2014.

"Life of a Tsunami". Western Coastal & Marine Geology. United States Geographical Survey. 22 October 2008. Retrieved 2009-09-09.

Prof. Stephen A. Nelson (28 January 2009). "Tsunami". Tulane University. Retrieved 2009-09-09.

Merriam-Webster, (1828) http://www.merriam-webster.com/dictionary/viscosity

Symon, Keith (1971). Mechanics (Third ed.). Addison-Wesley. ISBN 0-201-07392-7.

Briggs, M.J., Synolakis, C.E., Hughes, S.A., 1993. Laboratory measurements of tsunami runup.Tsunami '93 Proceedings. Wakayama, Japan, pp. 585–598.

Briggs, M., Synolakis, C., Harkins, G., Green, D., 1995. Laboratory experiments of tsunami runup on a circular island. Pure and Applied Geophysics 144(3–4), 569–593.

Chanson, H., Aoki, S.-I., Maruyama, M., 2003. An experimental study of tsunami runup on dry and wet horizontal coastlines. Science of Tsunami Hazards 20 (5), 278–293. Dean, R., Dalrymple, R., 1991. Water Wave Mechanics for Engineers and Scientists. World Scientific.

Goseberg, N., 2013. Reduction of maximum tsunami run-up due to the interaction with beachfront development - application of single sinusoidal waves. Natural Hazards and Earth System Sciences Discussions 1, 1119–1171. http://dx.doi.org/10.5194/ nhessd-1-1119-2013.

Hughes, S.A., 1993. Physical models and laboratory techniques in coastal engineering. Vol. 7 of Advances in Ocean Engineering.World Scientific, Scientific Publishing Co. Pte. Ltd., Singapore (November).

Schäffer, H., 1996. Second-order wavemaker theory for irregular waves. Ocean Engineering 23 (1), 47–88.

Schaffer, H., Stolborg, T., Hyllested, P., 1994. Simultaneous generation and active absorption of waves in flumes. Proc. Waves - Physical and numerical modelling. Vancouver, B.C., Canada, pp. 90–99.

Synolakis, C.E., 1987. The runup of long waves. (Dissertation) W. M. Keck Laboratory of Hydraulics and Water Resources, California Institute of Technology (December).

Synolakis, C.E., 1990. Generation of long waves in laboratory. Journal of Waterway, Port, Coastal, and Ocean Engineering 116 (2), 252–266.

Synolakis, C.E., Kanoglu, U., 2009. Nonlinear Wave Dynamics. World Scientific Publishing Co. Pte. Ltd., Singapore.

Yeh, H., Ghazali, A., Marton, I., 1989. Experimental study of bore run-up. Journal of Fluid Mechanics 206, 563–578.

Yeh, H., Liu, P., Briggs, M., Synolakis, C., 1994. Propagation and amplification of tsunamis at coastal boundaries. Nature 372 (6504), 353–355.

Yeh, H., Liu, P.L.F., Synolakis, C., 1995. Long-wave Runup Models. World Scientific, Singapore, River Edge, New York.

APPENDIX

Figure a: Flume Tank

Figure b: Go Pro view from side

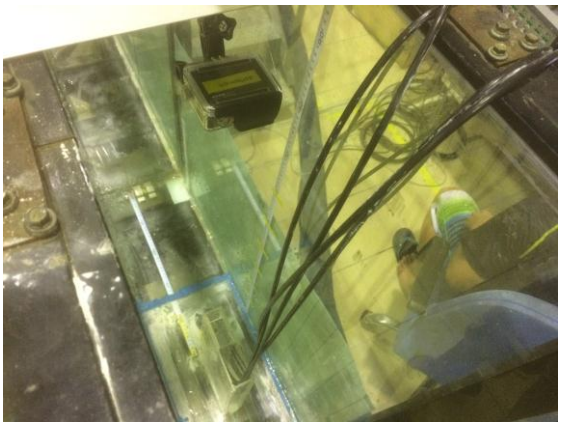

Figure c: Go Pro View from Top

Figure d: Rheometer

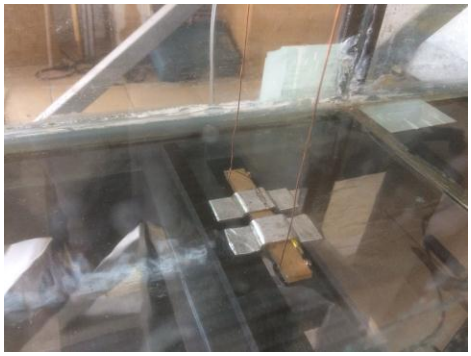

Figure e: Wired Probe

Figure f: Wired probe

Figure g: mixer

Figure h: mixer component

Figure i: mixing non-Newtonian fluid